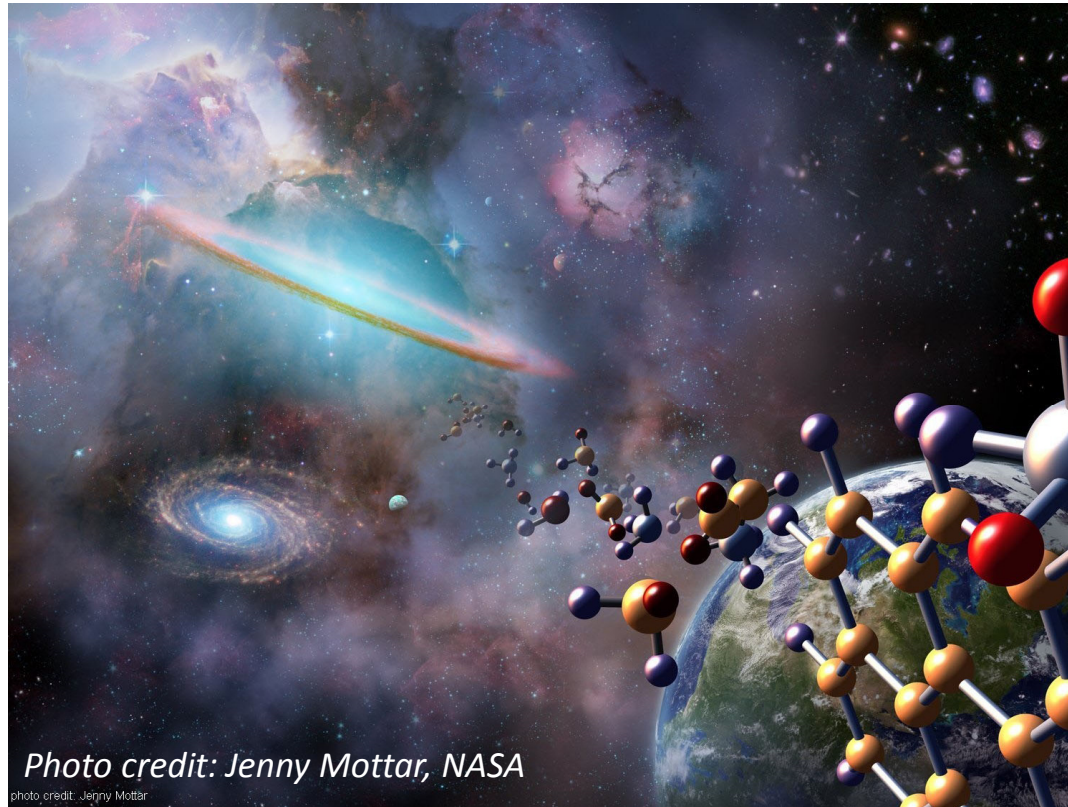


The molecular origins of life

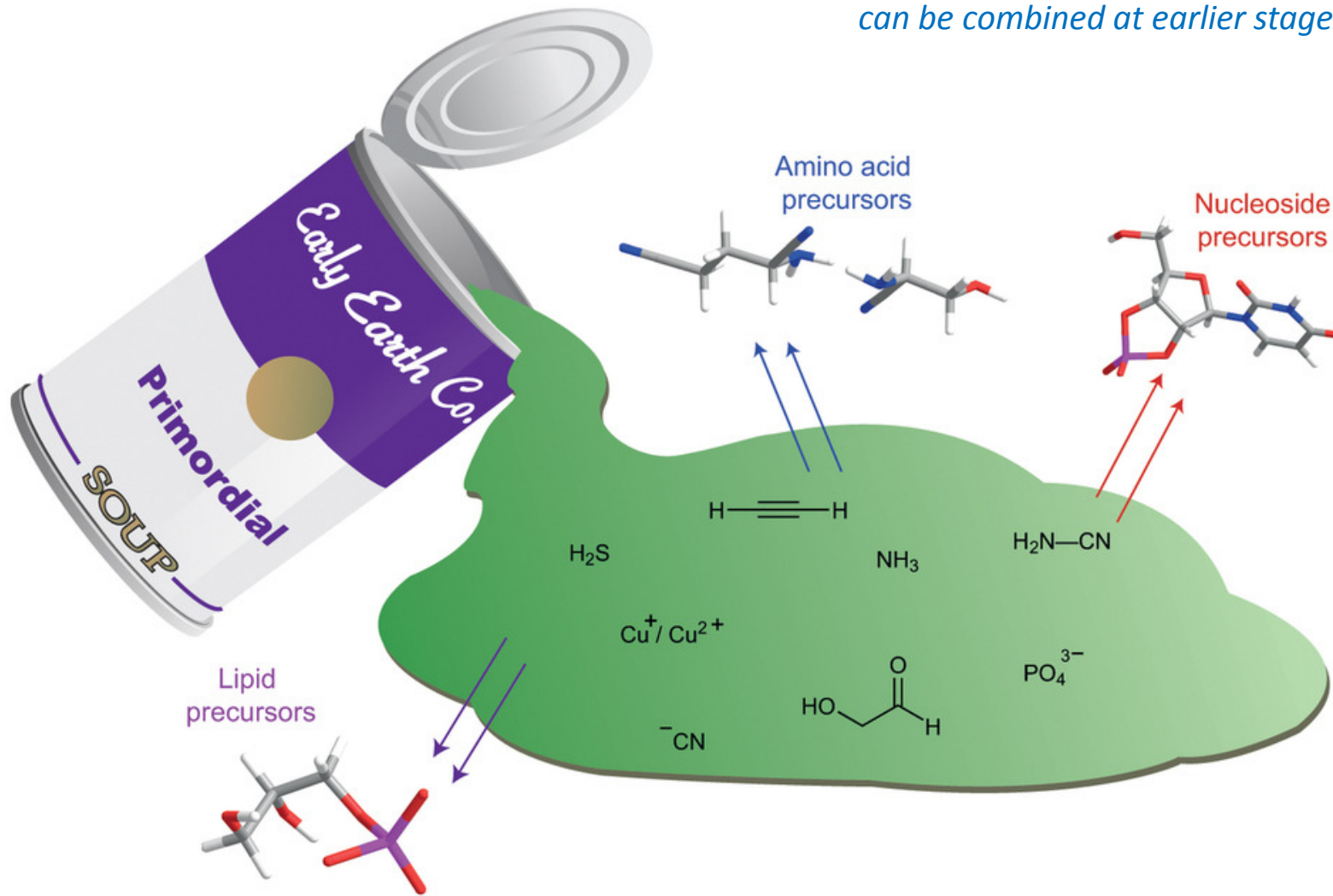


L5 SoSe 2020

Zbigniew Pianowski

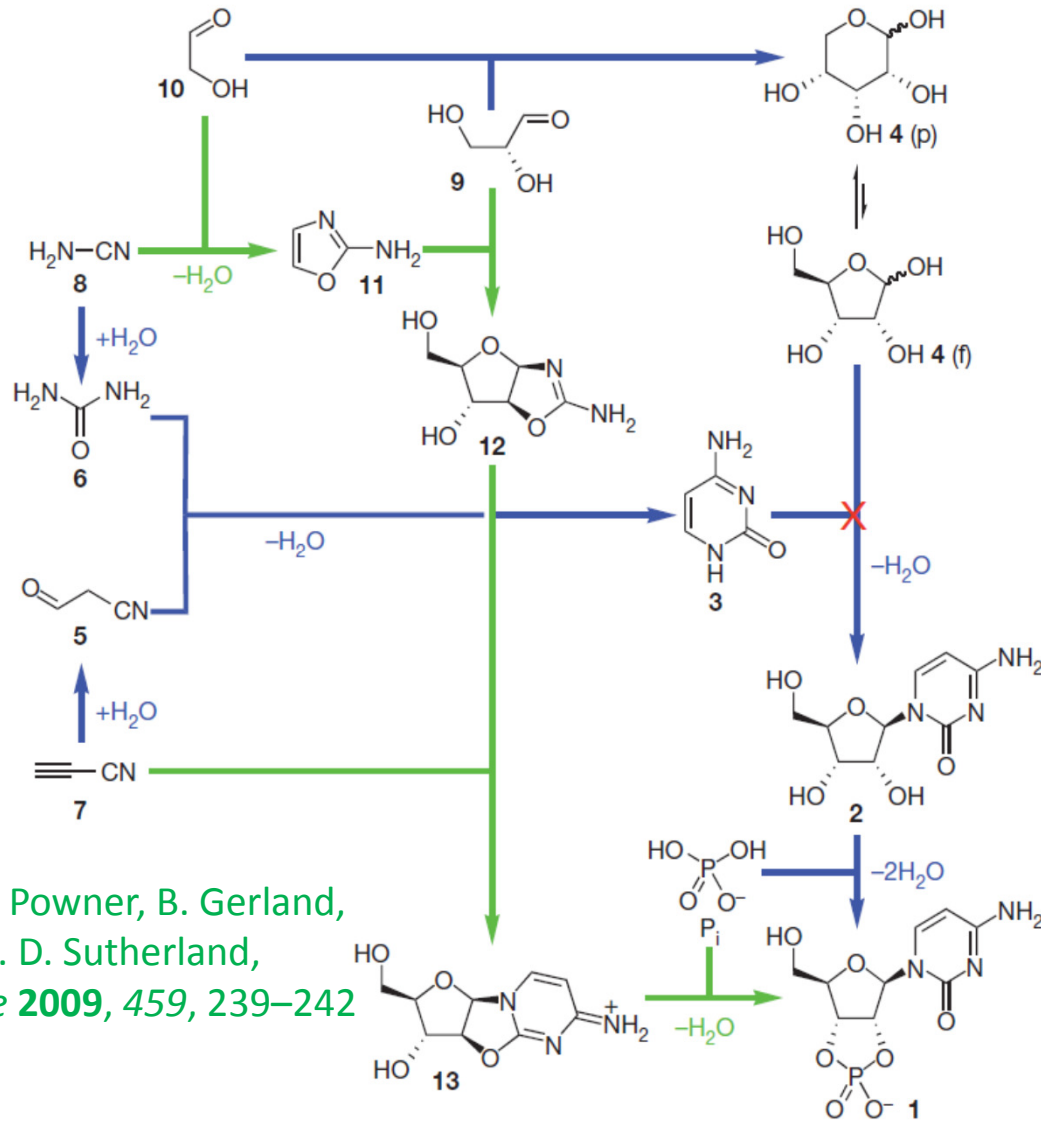
Cyanosulfidic chemistry

The aldol chemistry of sugars and cyanide chemistry of nucleobases can be combined at earlier stages than glycosylation.



- Aminoacids
- Lipids
- Carbohydrates (sugars)
- Nucleobase
- **Nucleosides (sugar+nucleobase)**

Prebiotic route to pyrimidine nucleotides



M. W. Powner, B. Gerland,
J. D. Sutherland,
Nature **2009**, *459*, 239–242



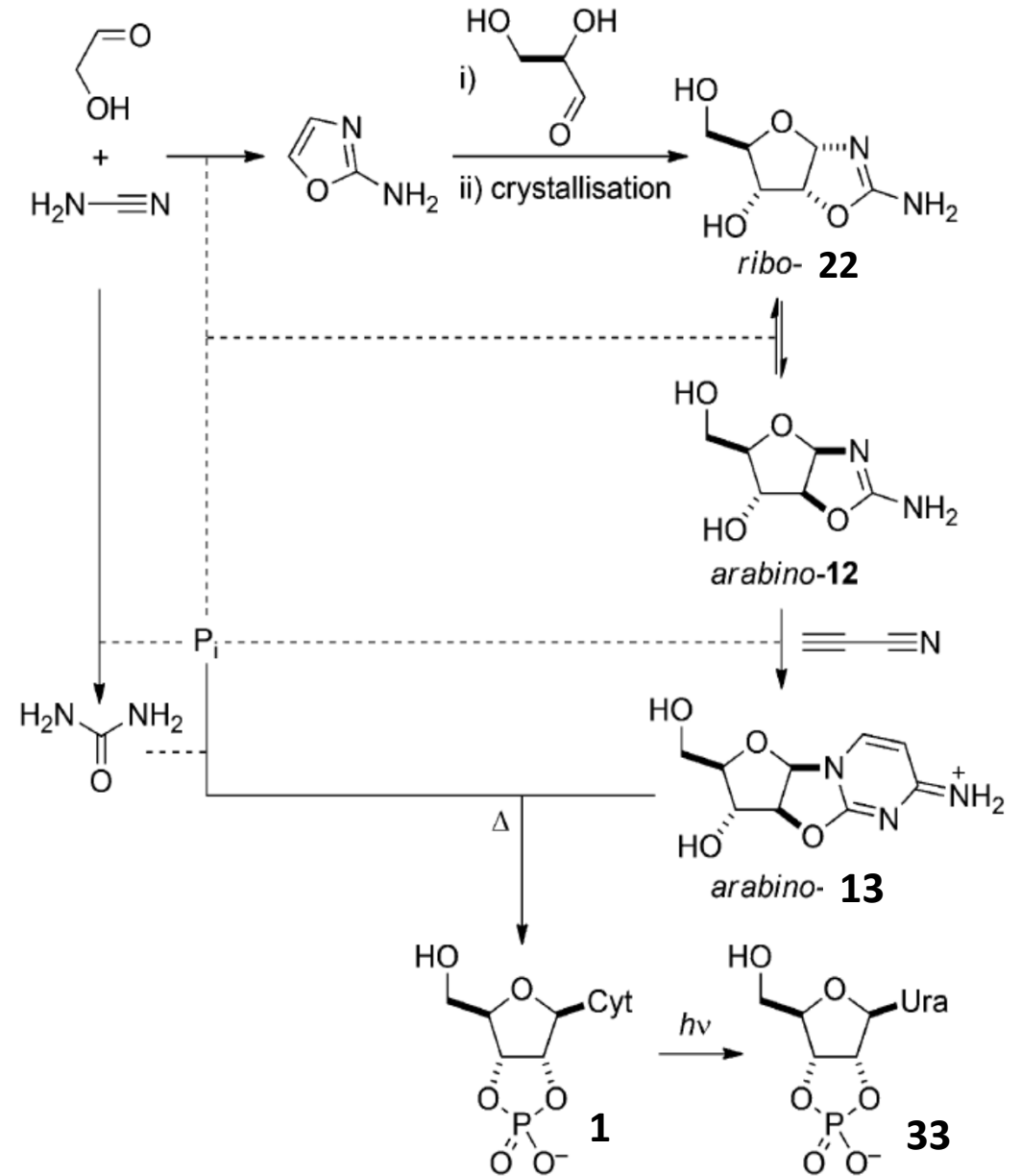
Prof. John Sutherland
Laboratory of Chemical Biology
Cambridge, UK



Dr. Matthew Powner
University College London, UK

Prebiotic synthesis of activated pyrimidine nucleotides

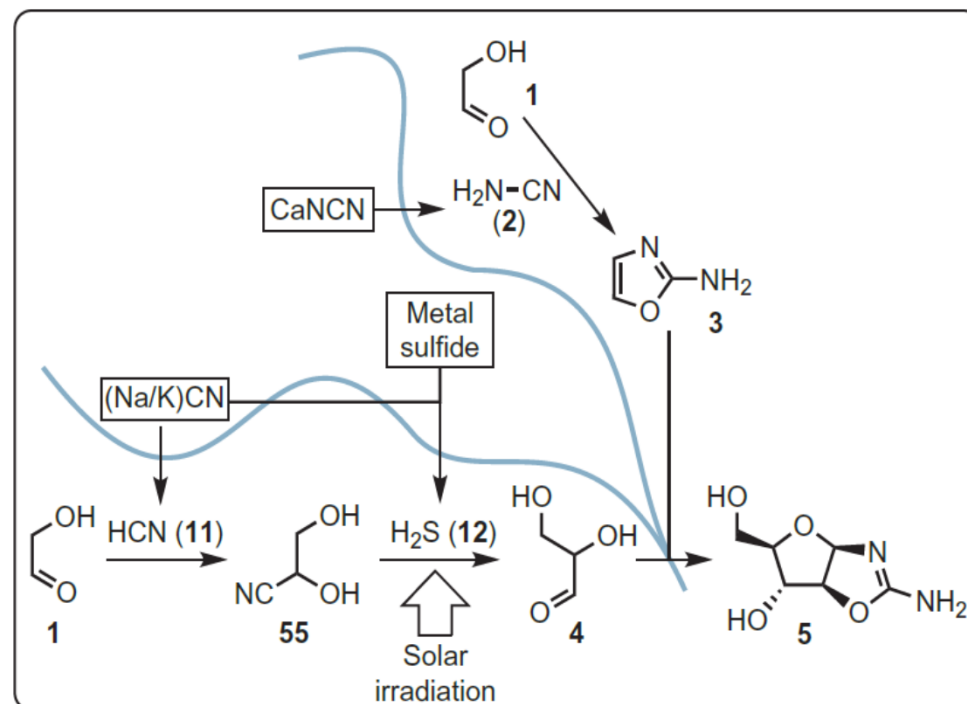
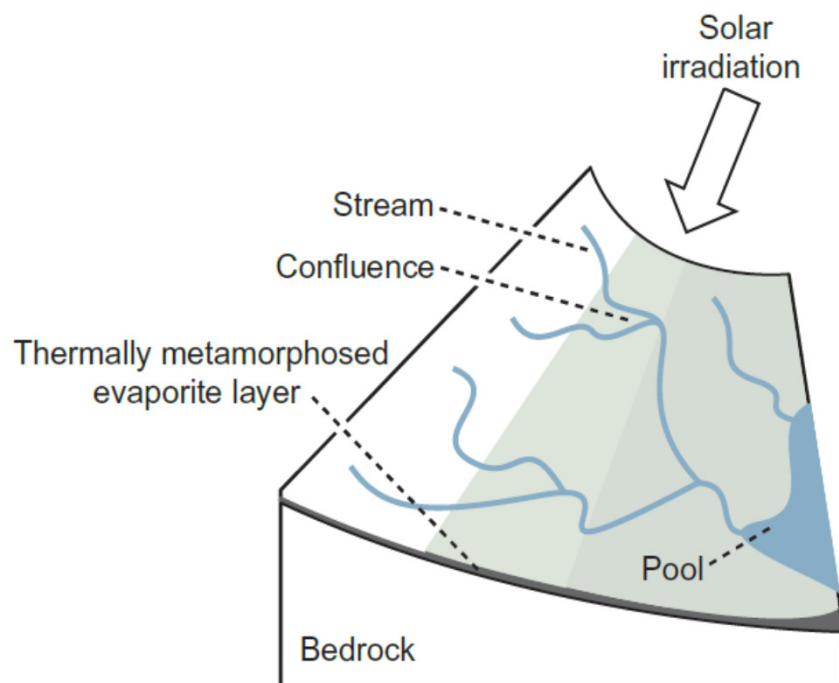
Catalysis, and reaction control through pH and chemical buffering, is indicated by dashed lines.



M. W. Powner, B. Gerland, J. D. Sutherland,
Nature **2009**, *459*, 239–242

Cyanosulfidic chemistry

Rainfall on higher ground (left) leads to rivulets or streams that flow downhill, sequentially leaching feedstocks from the thermally metamorphosed evaporite layer. Solar irradiation drives photoredox chemistry in the streams. Convergent synthesis can result when streams with different reaction histories merge (right), as illustrated here for the potential synthesis of arabinose aminooxazoline (5) at the confluence of two streams that contained glycolaldehyde (1), and leached different feedstocks before merging.



Cyanosulfidic chemistry system

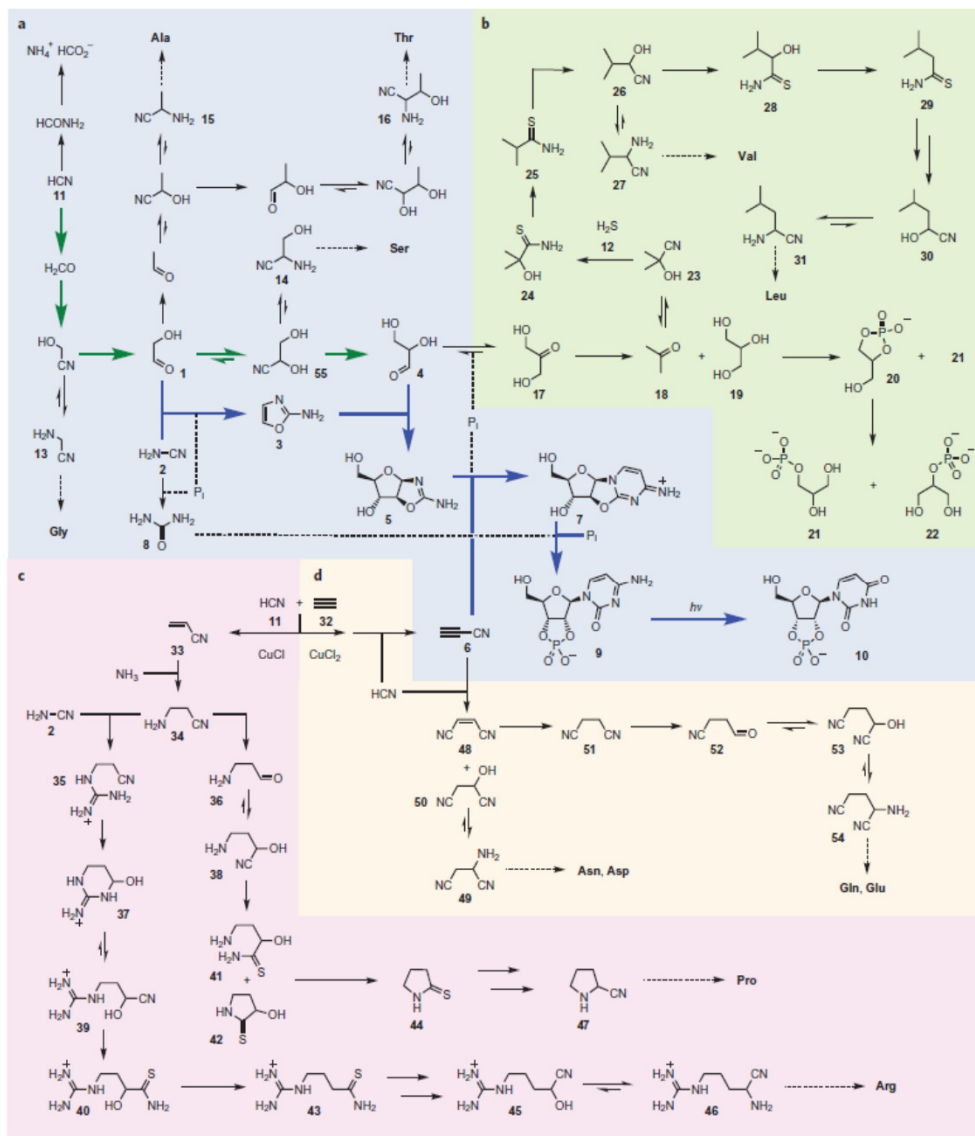


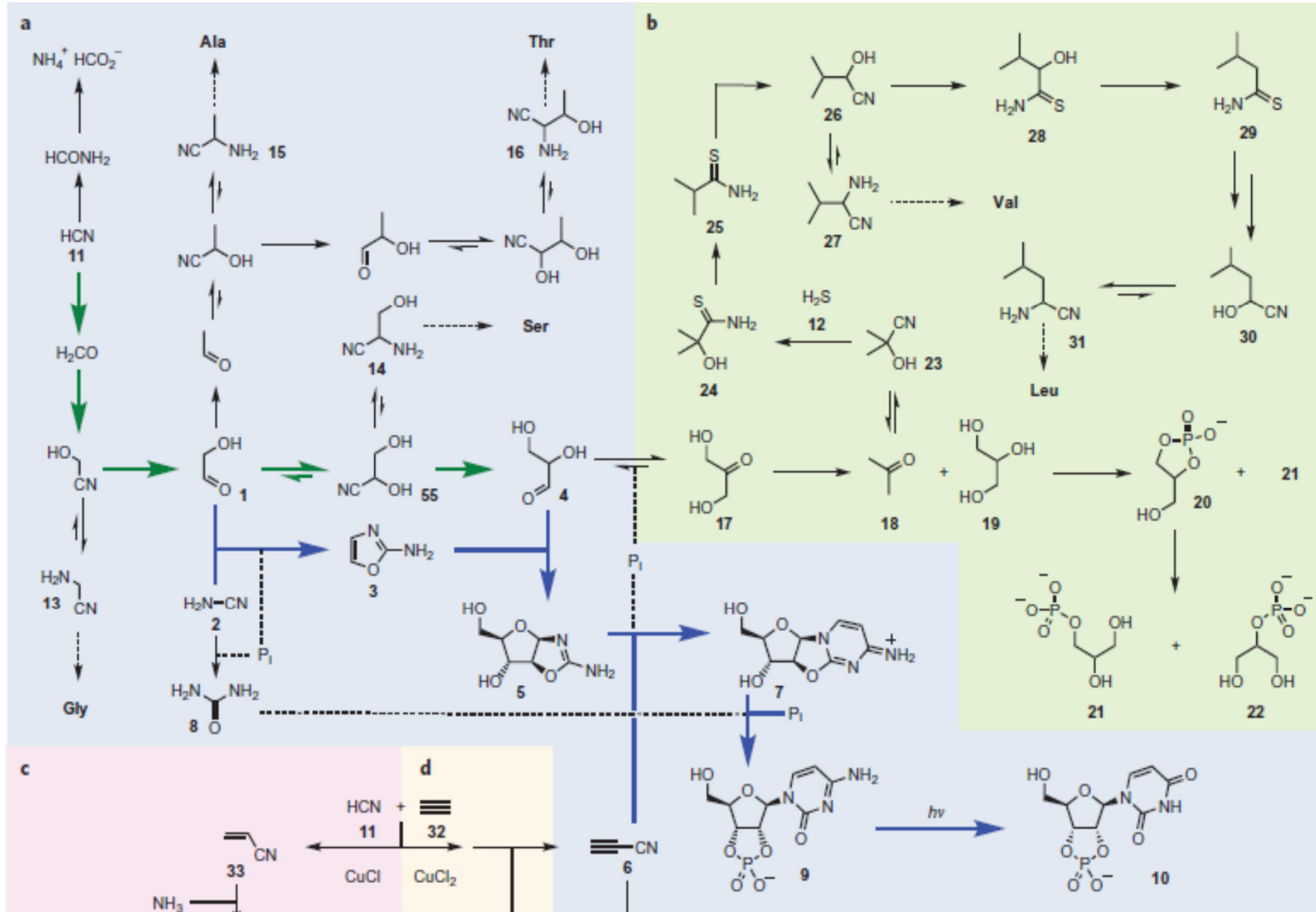
Table 1 | Yields for the part of the reaction network shown in Fig. 1b.

Conversion	Number of steps	Yield (%)	Conversion	Number of steps	Yield (%)
4 → 17	1	59	26 → 28	1	57
17 → 18 + 19	1	29	28 → 29	1	75
18 → 24	2	62	26 → 29	2	43
24 → 25	1	41	29 → 30	2	66
25 → 26	2	78	30 → 31	1	42
26 → 27	1	42	19 → 21 + 22	2	31
					40

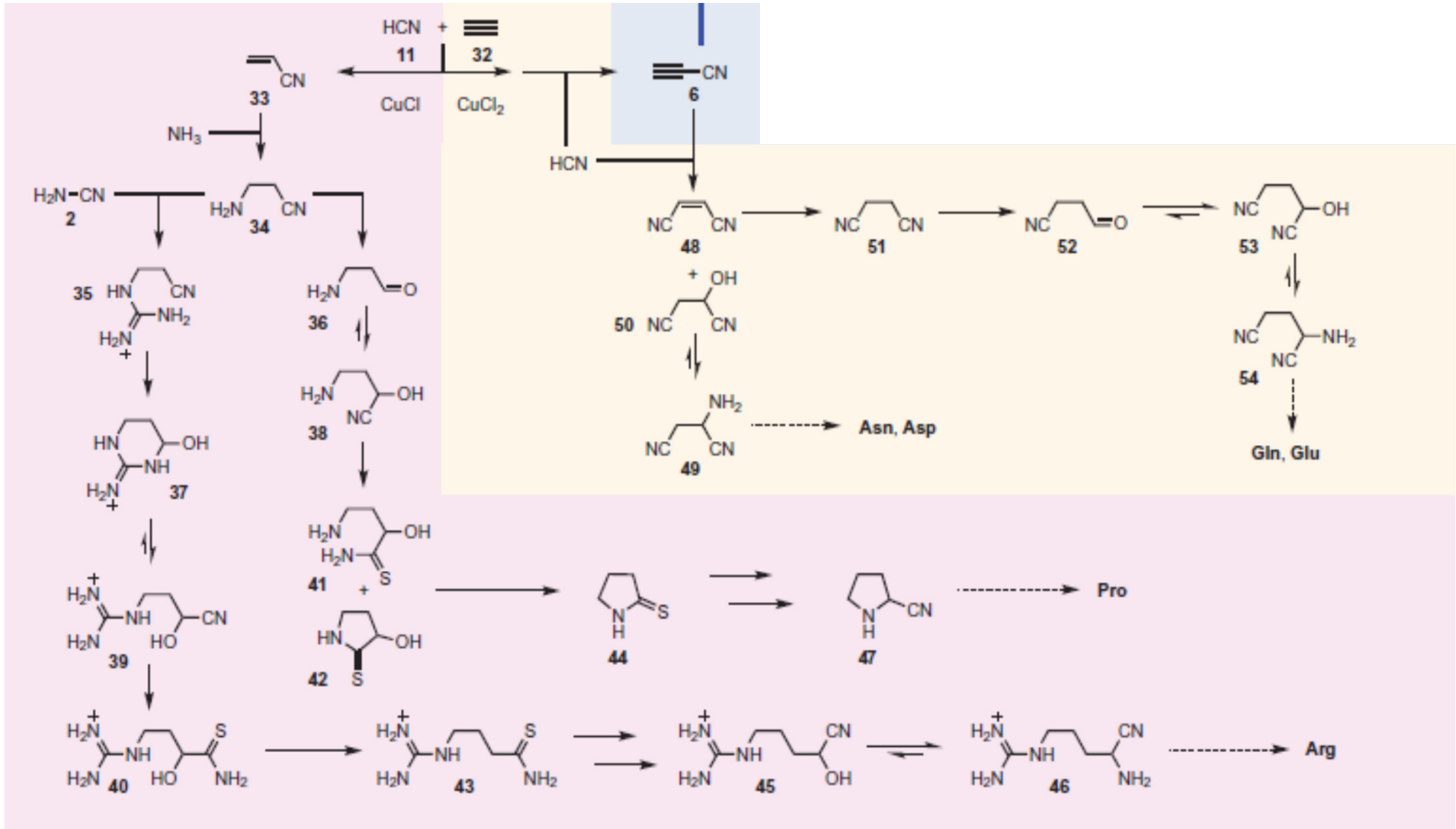
Table 2 | Yields for the parts of the reaction network shown in Fig. 1c,d.

Conversion	Number of steps	Yield (%)	Conversion	Number of steps	Yield (%)
33 → 34	1	83	38 → 41 + 42	1	30
34 → 35	1	55	38 → 44	2	70
34 → 37	2	77	44 → 47	2	32
34 → 36	1	45	45 → 46	1	90
37 → 39	1	77	6 → 48 + 49 + 50	1	50
					25
					16
37 → 40	2	~100	48 → 51	1	90
37 → 43	3	~70	51 → 52	1	89
37 → 45	5	~50	52 → 53	1	~100
36 → 38	1	~100	52 → 54	2	~70

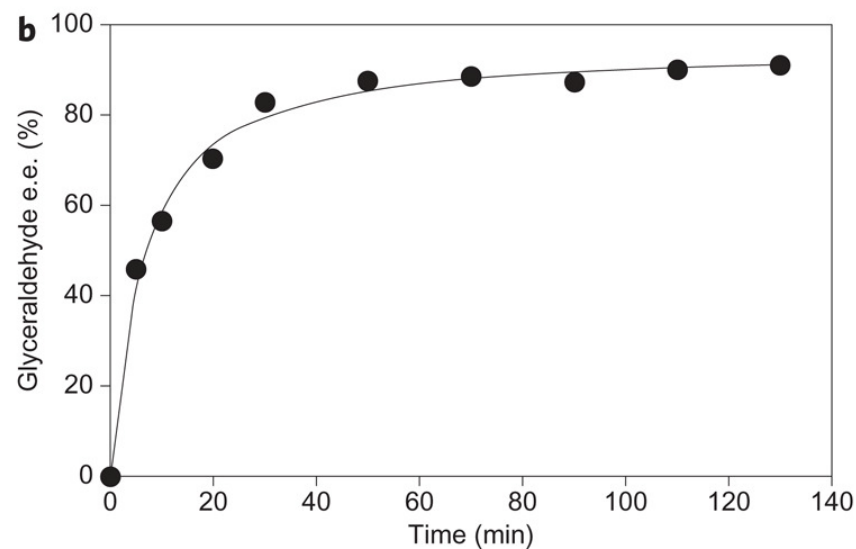
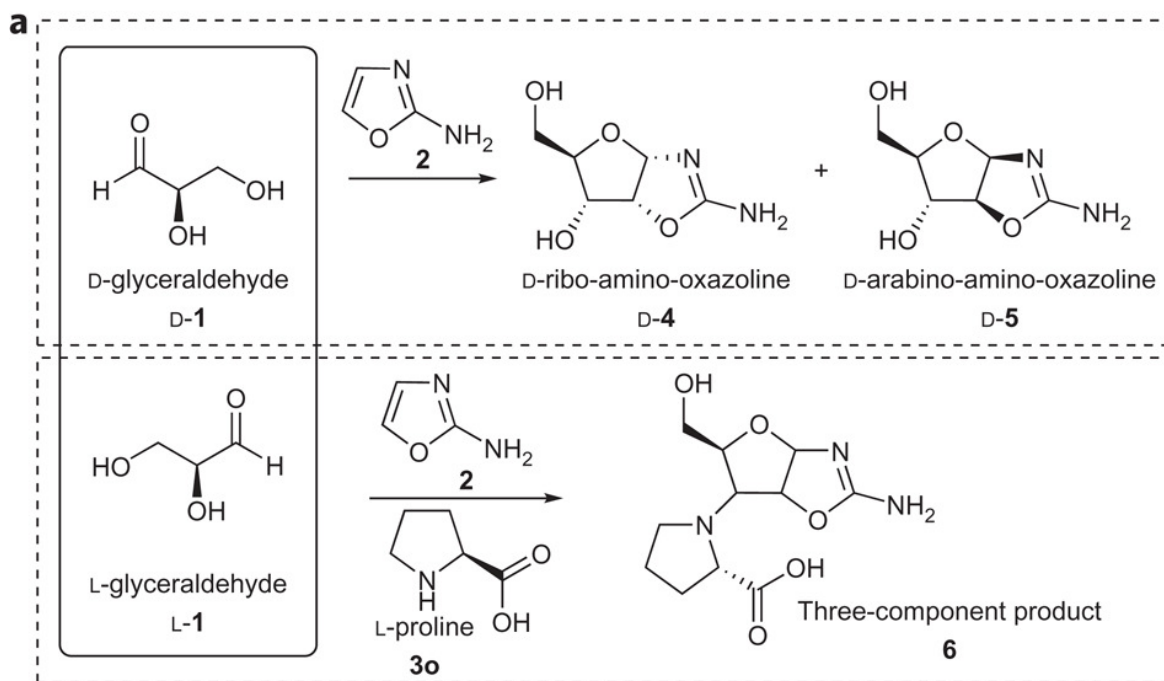
Cyanosulfidic chemistry system



Cyanosulfidic chemistry system



Enantiomeric excess in the cyanosulfidic chemistry



a, In the presence of an enantioenriched L-proline ([3o](#)), the diastereoselective formation of a three-component side product ([6](#)) effectively sequesters the unnatural L-glyceraldehyde ([L-1](#)).

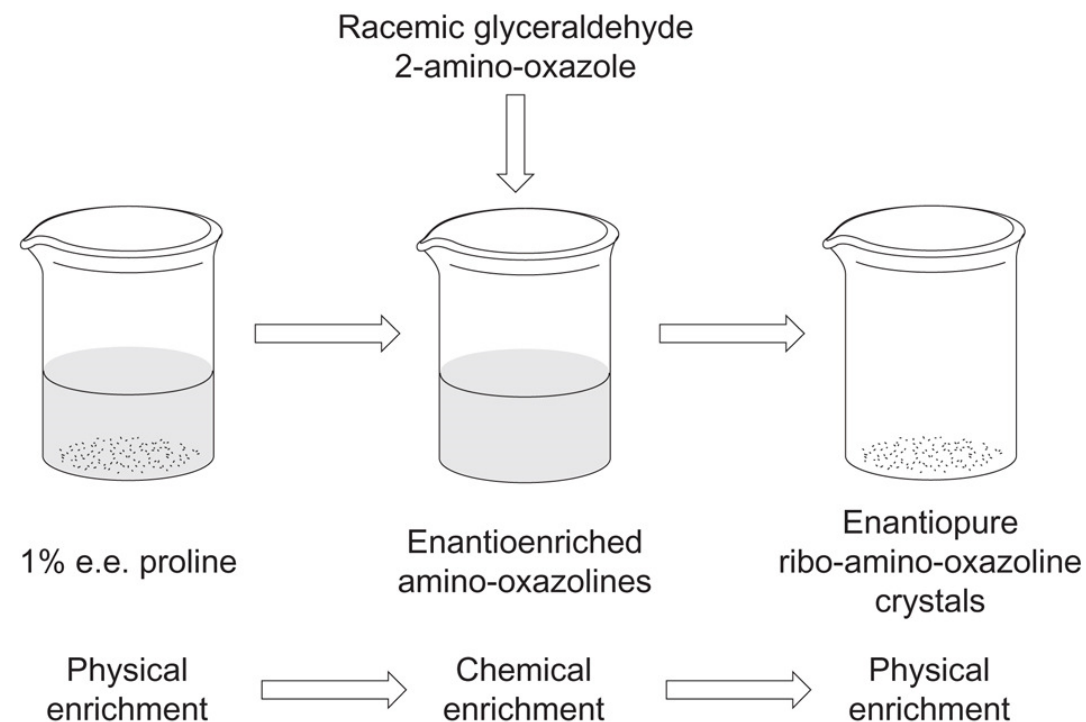
b, The side reaction acts as a kinetic resolution of glyceraldehyde, giving enantiorichment of greater than 90% e.e. [D-1](#), which reacts with [2](#) to form the enantioenriched amino-oxazoline RNA precursors [D-4](#) and [D-5](#). e.e. values are $\pm 2\%$.

Enantiomeric excess in the cyanosulfidic chemistry

Table 1 | Formation of enantioenriched amino-oxazolines in the presence of L-amino acids.

Amino acid	Three-component product* 6	Ribose amino-oxazoline D-4 (% e.e.)	Arabinose amino-oxazoline D-5 (% e.e.)
Ala (3a)	++	8.9	8.1
Arg (3b)	++	4.1	7.3
Asn (3c)	+	1.1	0.5
Asp (3d)	+	2.1	1.4
Cys (3e)	++ +	n.a.	1.4
Gln (3f)	+	1.2	1.1
Glu (3g)	+	0.8	0.1
Gly (3h)	++	-	-
His (3i)	++	7.5 (L)	8.1 (L)
Ile (3j)	+	2.1	0.5 (L)
Leu (3k)	+	1.1	2.1
Lys (3l)	++ +	n.a.	n.a.
Met (3m)	++ +	n.a.	n.a.
Phe (3n)	++ +	2.5	5.4
Pro (3o)	++	55	58
Ser (3p)	++ +	3.0	1.9
Thr (3q)	++	1.1	2.6
Trp (3r)	++	10.2	9.8
Tyr (3s)	+	0.5	2.6
Val (3t)	++	2.0	1.0 (L)

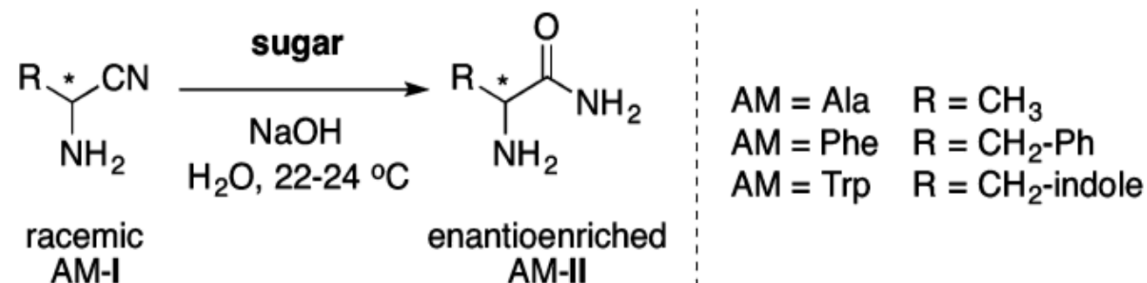
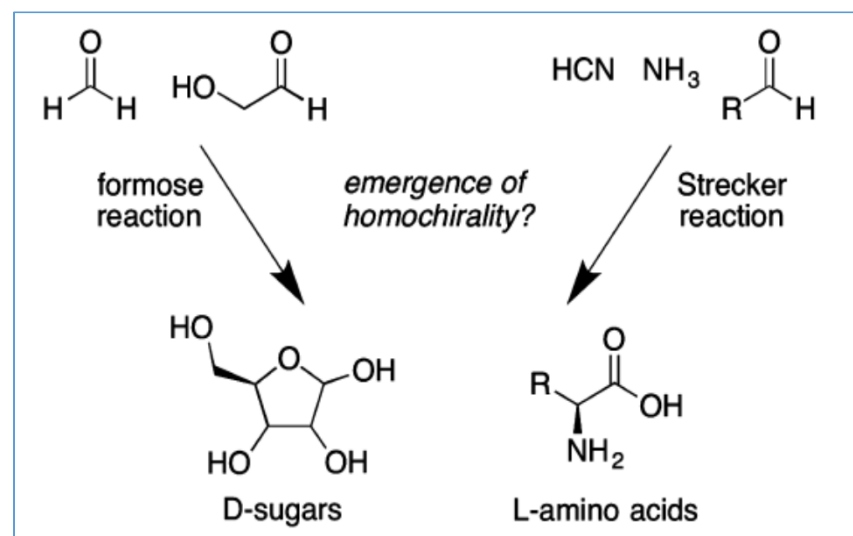
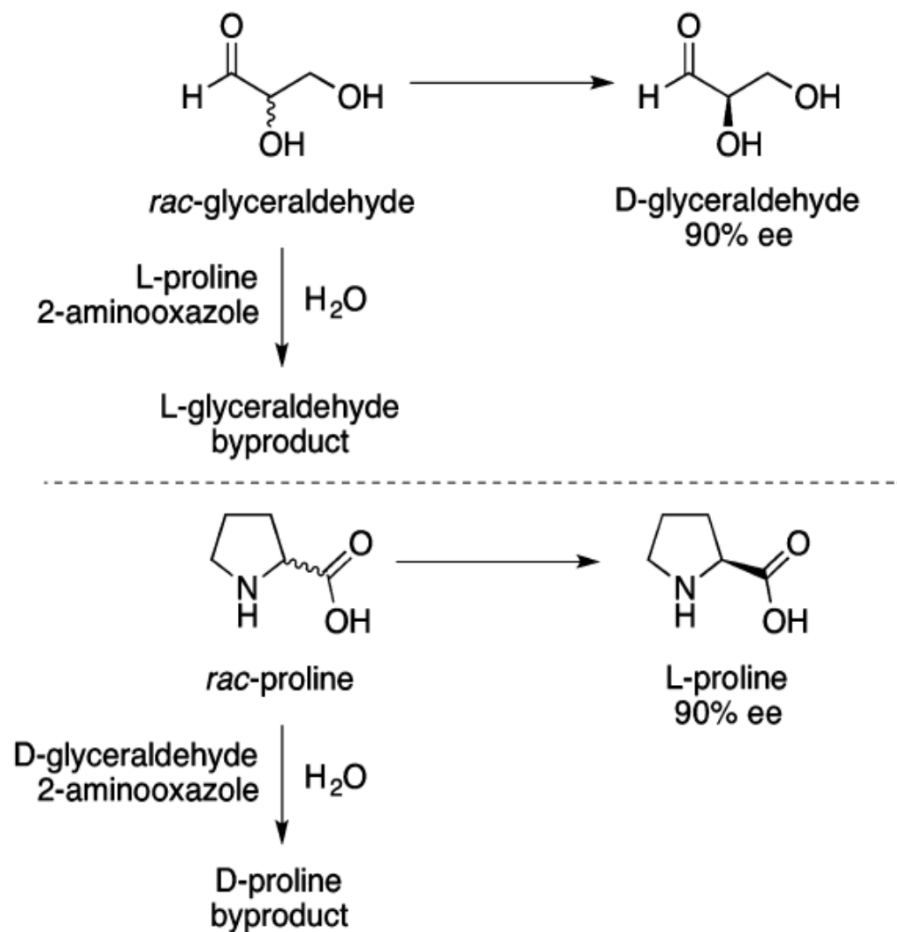
*Yield of side product 6: +, low; ++, medium; +++, high. n.a., no products isolated or observed by chiral LC



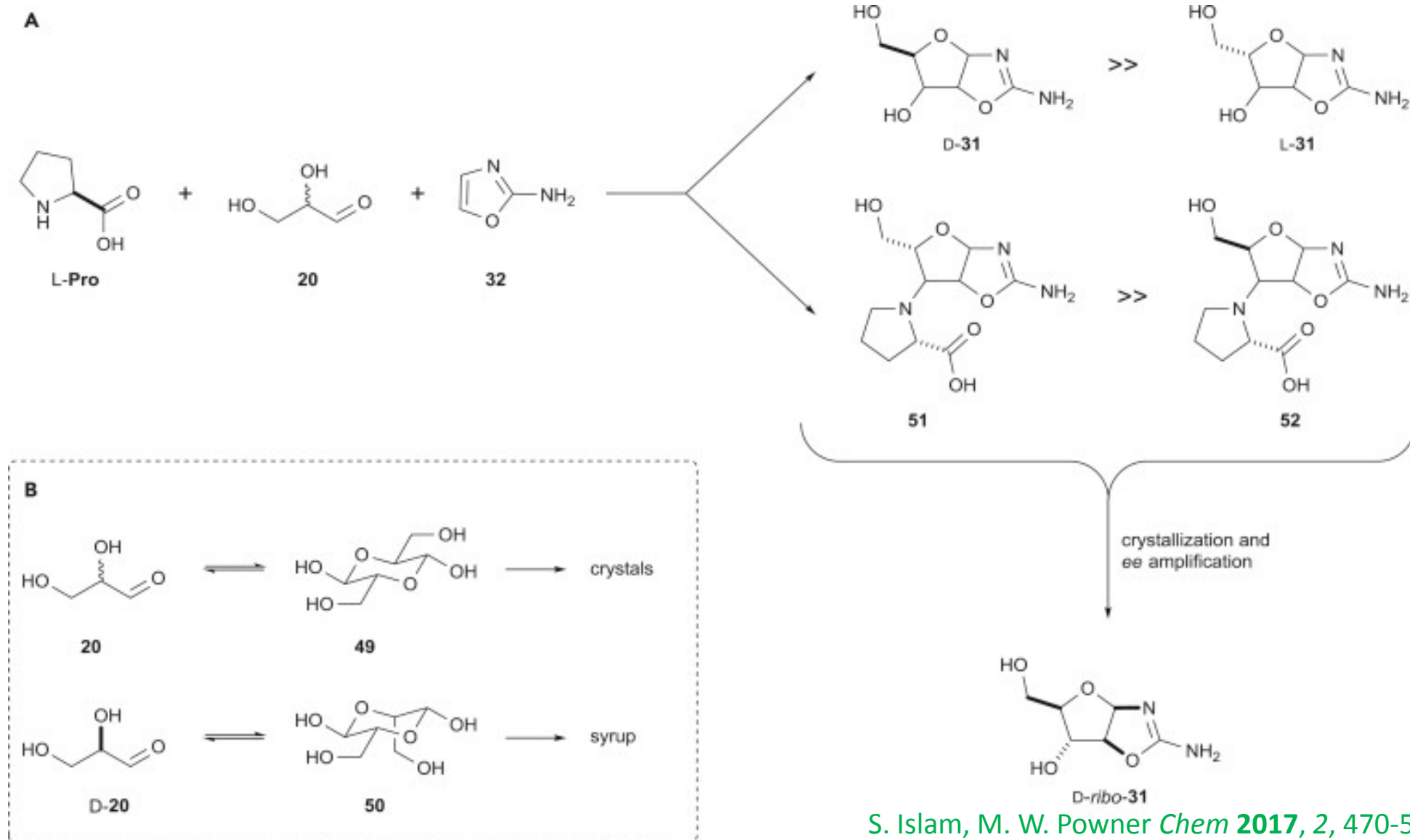
1% e.e. L-proline (**3o**) is suspended in solvent (either CHCl_3 or EtOH). After equilibration, the remaining solid is removed and the solvent is evaporated from the supernatant. Racemic glyceraldehyde DL-**1** and amino-oxazole **2b** are then added and the mixture is dissolved in water. The ensuing reaction produces amino-oxazolines **4** and **5** in 20–80% e.e. Cooling the mixture to 4 °C induces crystallization of enantiopure ribo-amino-oxazoline crystals.

J. E. Hein, E. Tse, D. G. Blackmond, *Nature Chem.*, **2011**, *3*, 704-706

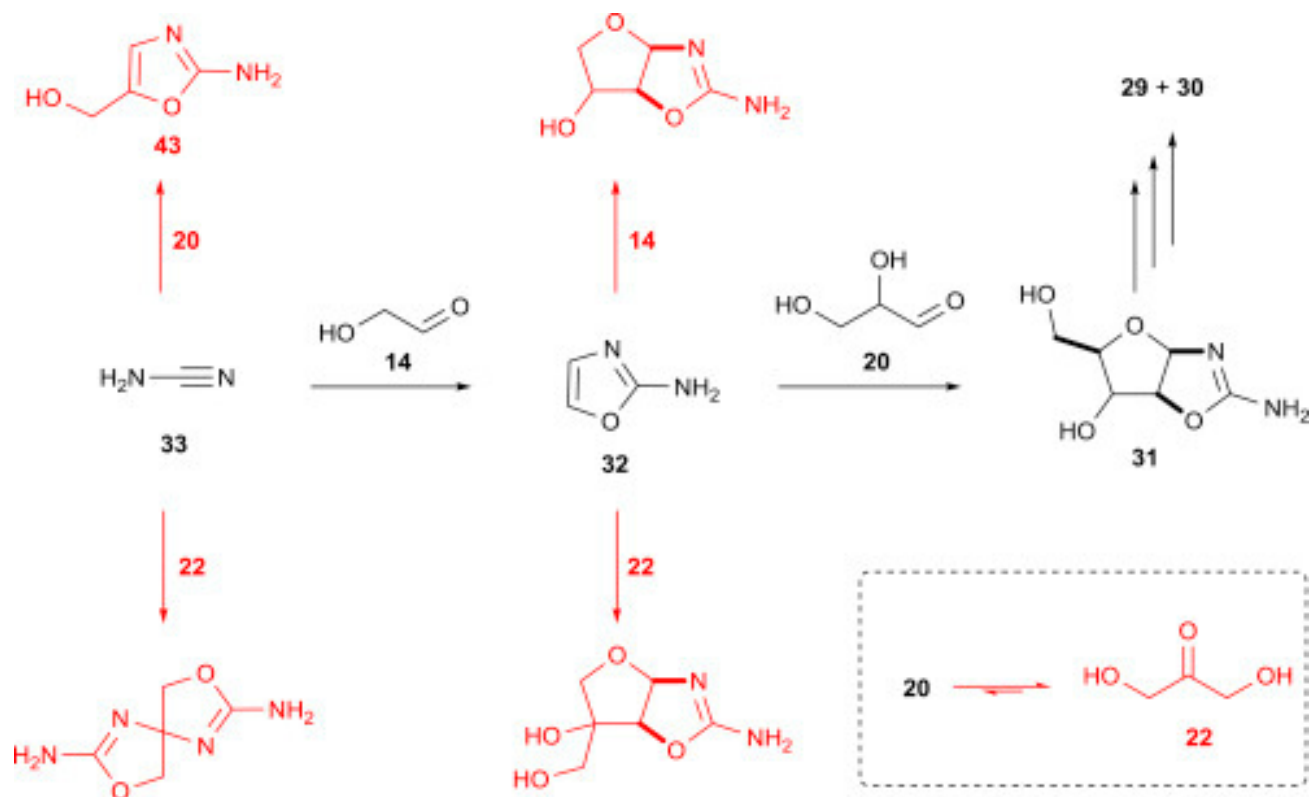
Chiral sugars drive enantioenrichment in prebiotic aminoacid synthesis



Strategies toward Enantio-enriched Glyceraldehyde and Ribonucleotide Precursors



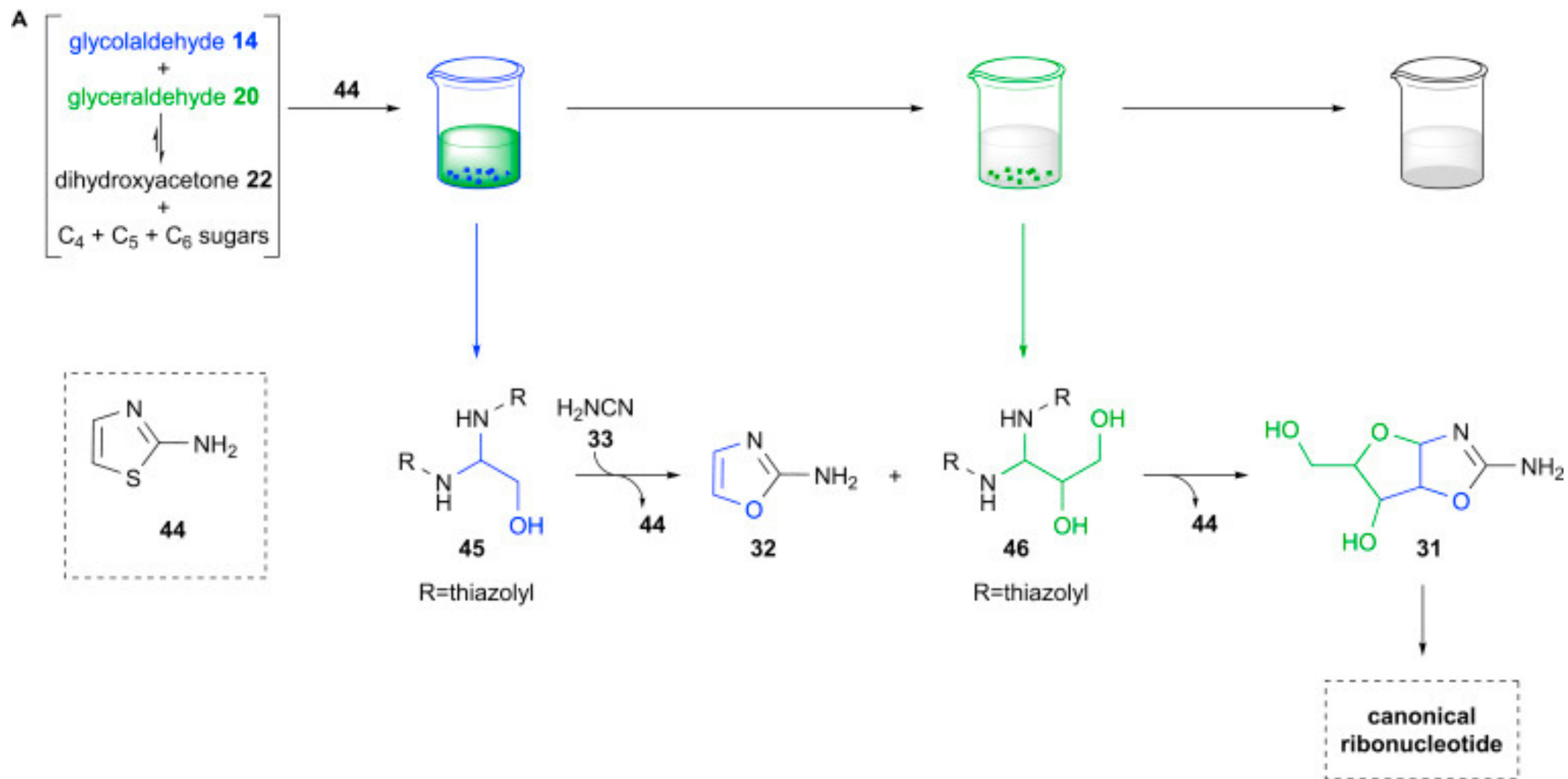
Overcome of the Formation of Prebiotic Clutter.



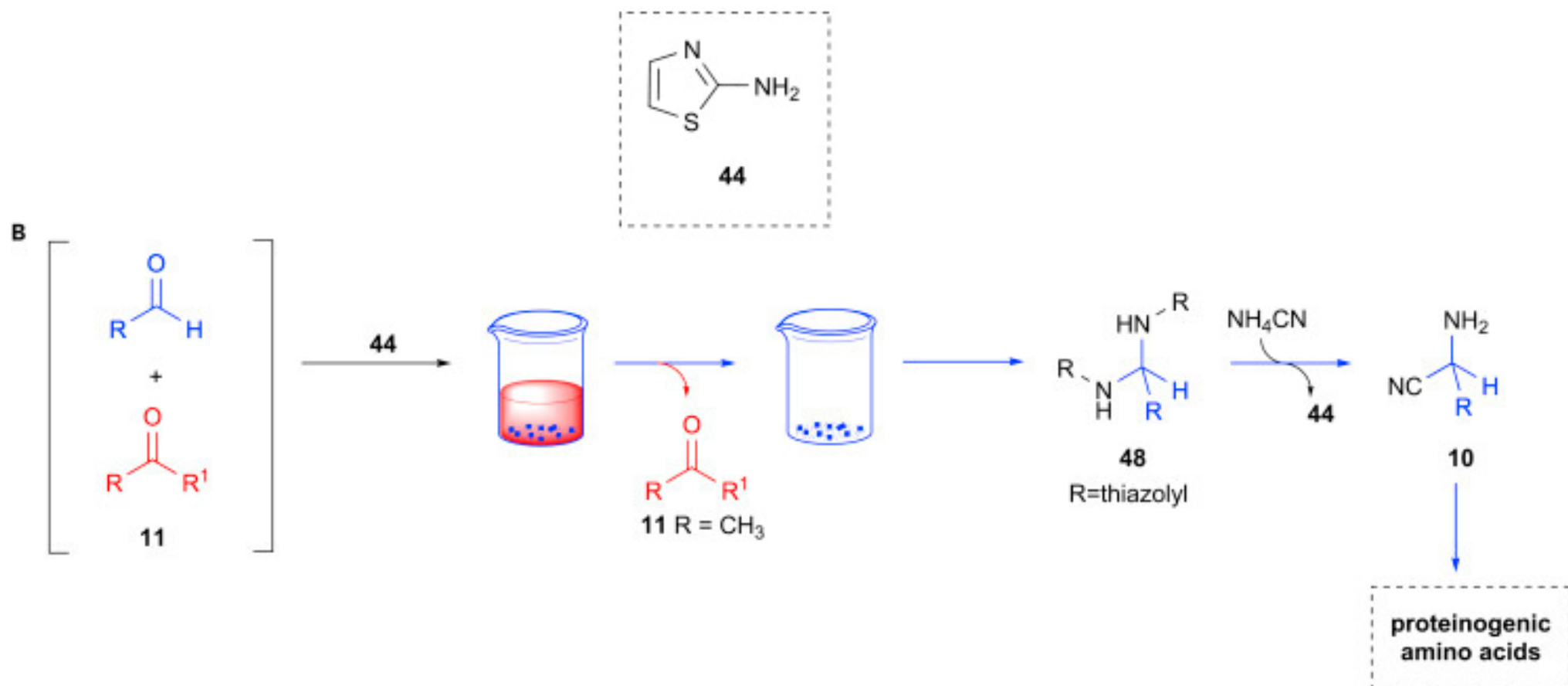
The synthesis of activated pyrimidine ribonucleotides **29** and **30** is dependent on the controlled formation of pentose aminooxazolines **31** (black), but the synthesis of **31** is wholly reliant on the ordered introduction of pure glycolaldehyde **14** (to cyanamide **33**) and glyceraldehyde **20** (to 2-aminooxazole **32**) to prevent the formation of numerous deleterious by-products (red). Ribonucleotide synthesis fails without the adherence to this order of synthetic steps. Glyceraldehyde **20** is highly susceptible to equilibration with dihydroxyacetone **22**, especially in phosphate buffer, which results in diminishing amounts of pentose aminooxazolines **31** being formed (inset).

S. Islam, M. W. Powner *Chem* **2017**, *2*, 470-501

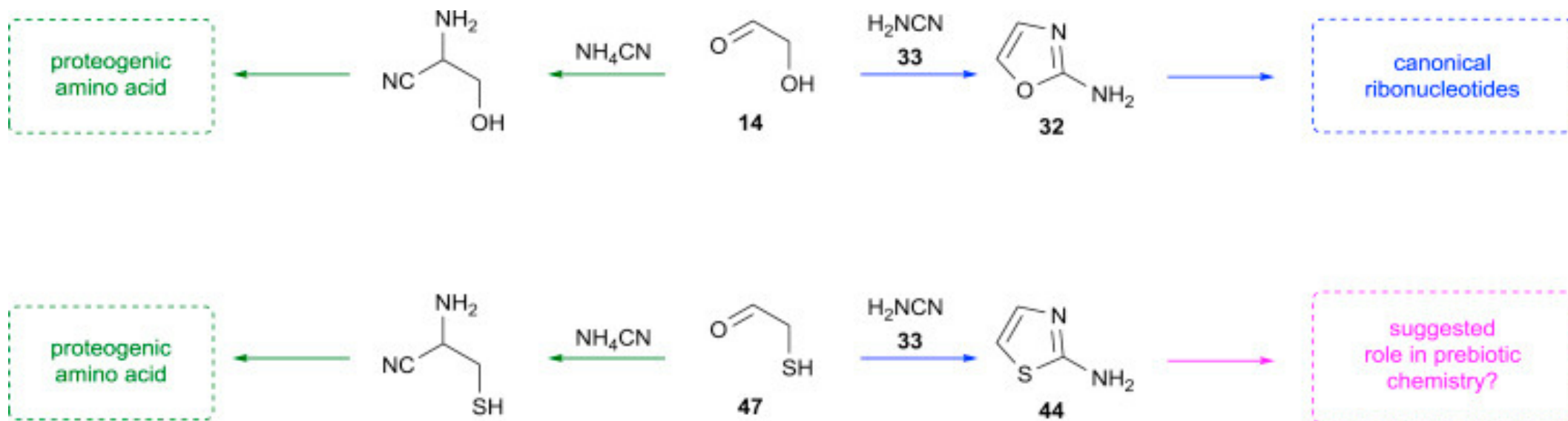
2-Aminothiazole-Controlled Aldehyde Sequestration



2-Aminothiazole-Controlled Aldehyde Sequestration

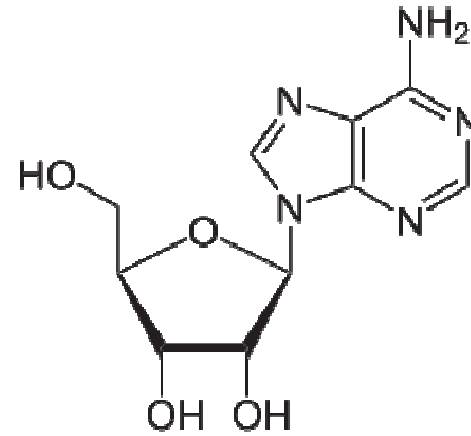
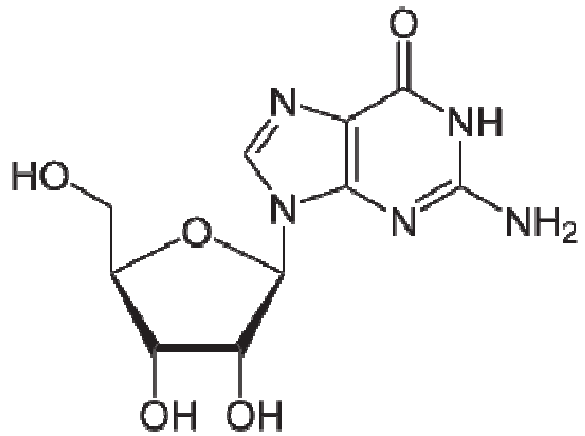
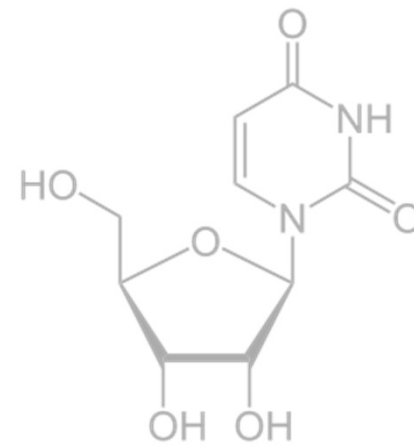
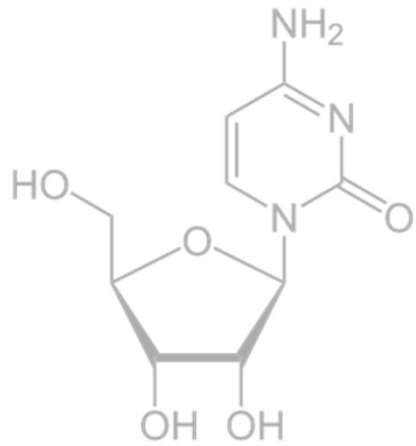


Systems Chemical Analysis of Amino Acid and Nucleotide Syntheses

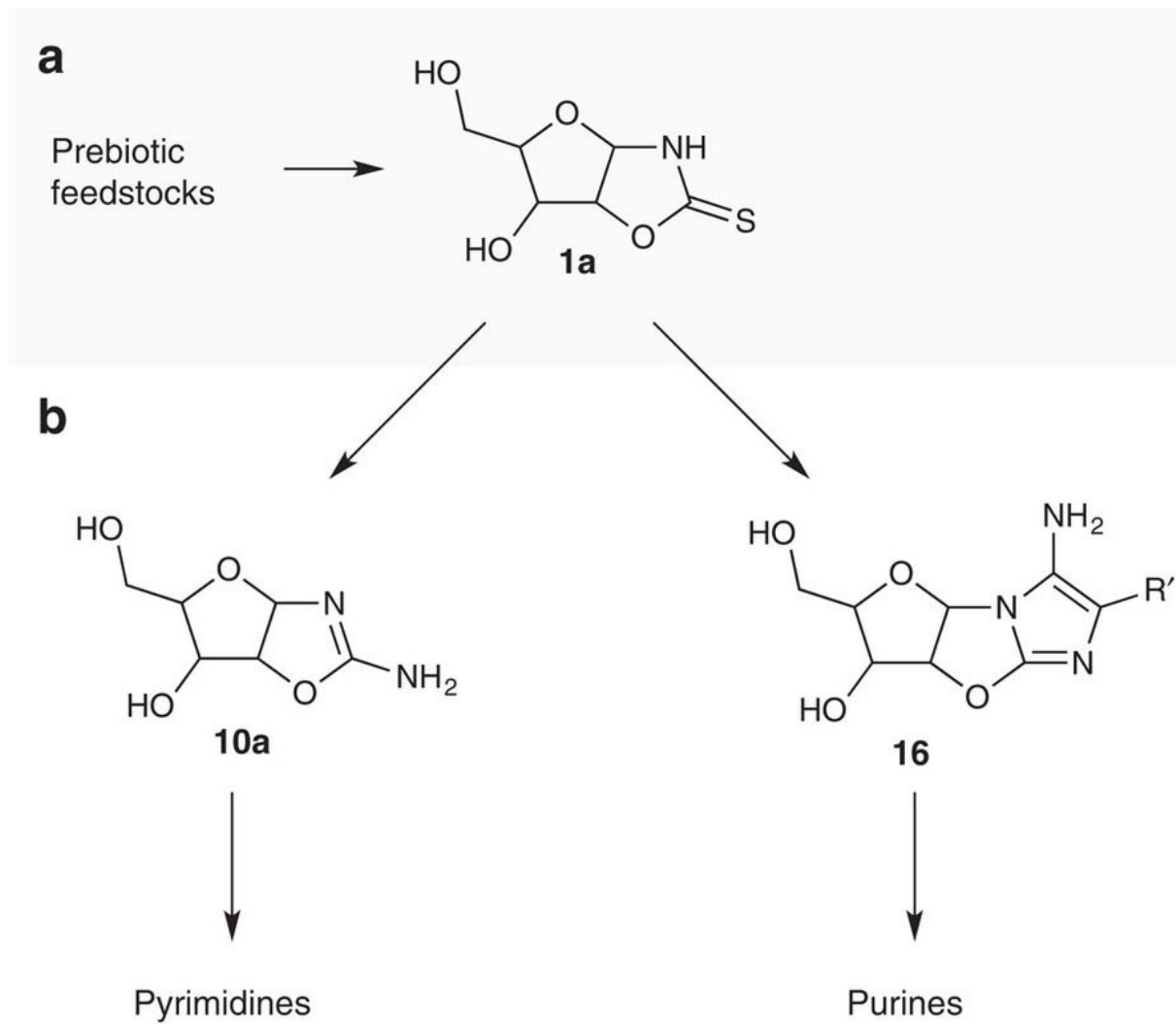


Analysis of the prebiotic amino acid and nucleotide syntheses reveal that glycolaldehyde **14**—a serine and ribonucleotide precursor—lies at a generational node between these two metabolite classes. The same analysis applied to cysteine suggested that b-mercaptoacetaldehyde **47** would be as important as glycolaldehyde **14** and that the reactivity of 2-aminothiazole **44** might have key implications for the concomitant prebiotic synthesis of amino acid and nucleotides

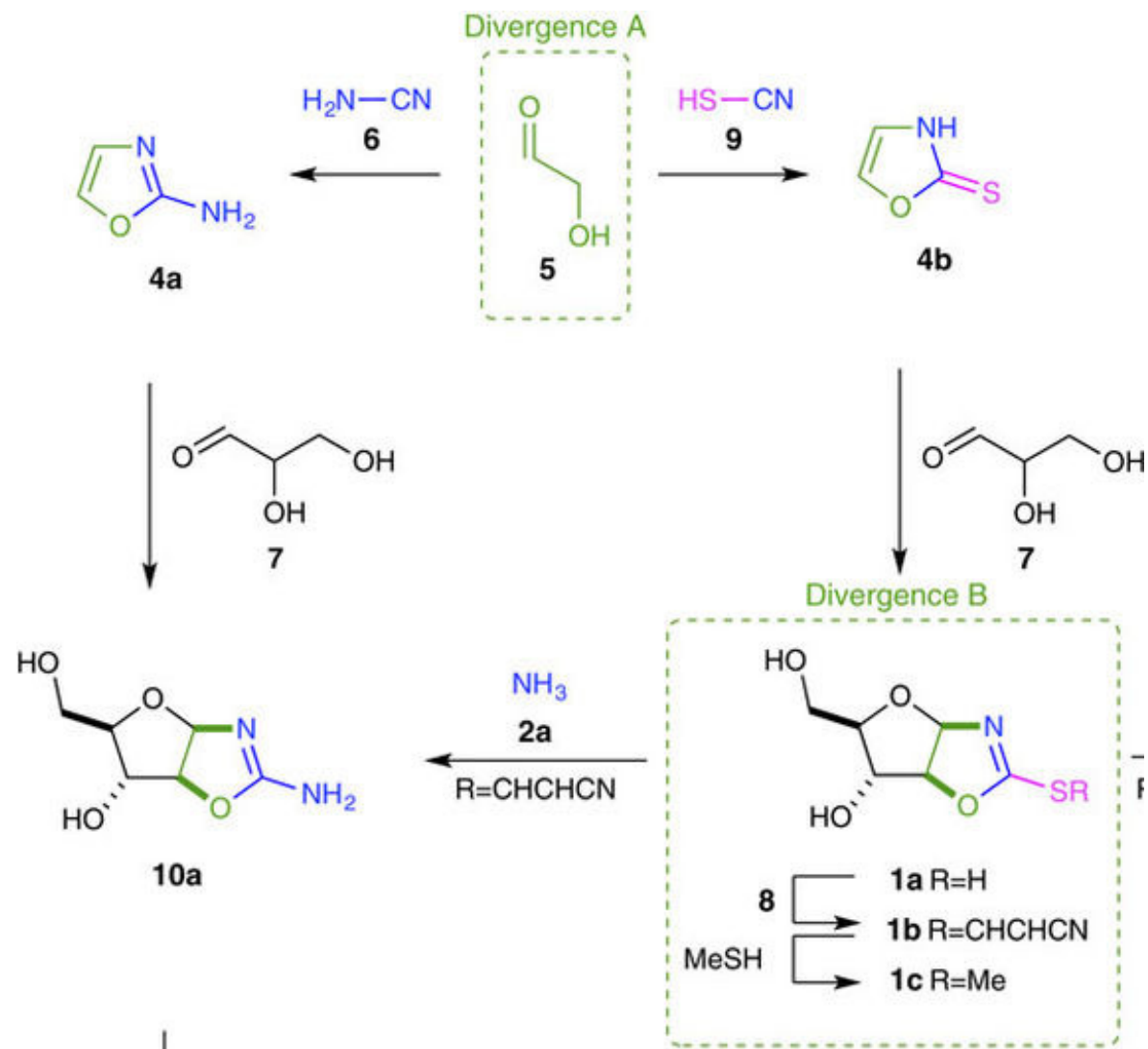
Purine nucleoside synthesis via cyanosulfidic chemistry



8-Oxo-purine nucleoside synthesis via cyanosulfidic chemistry

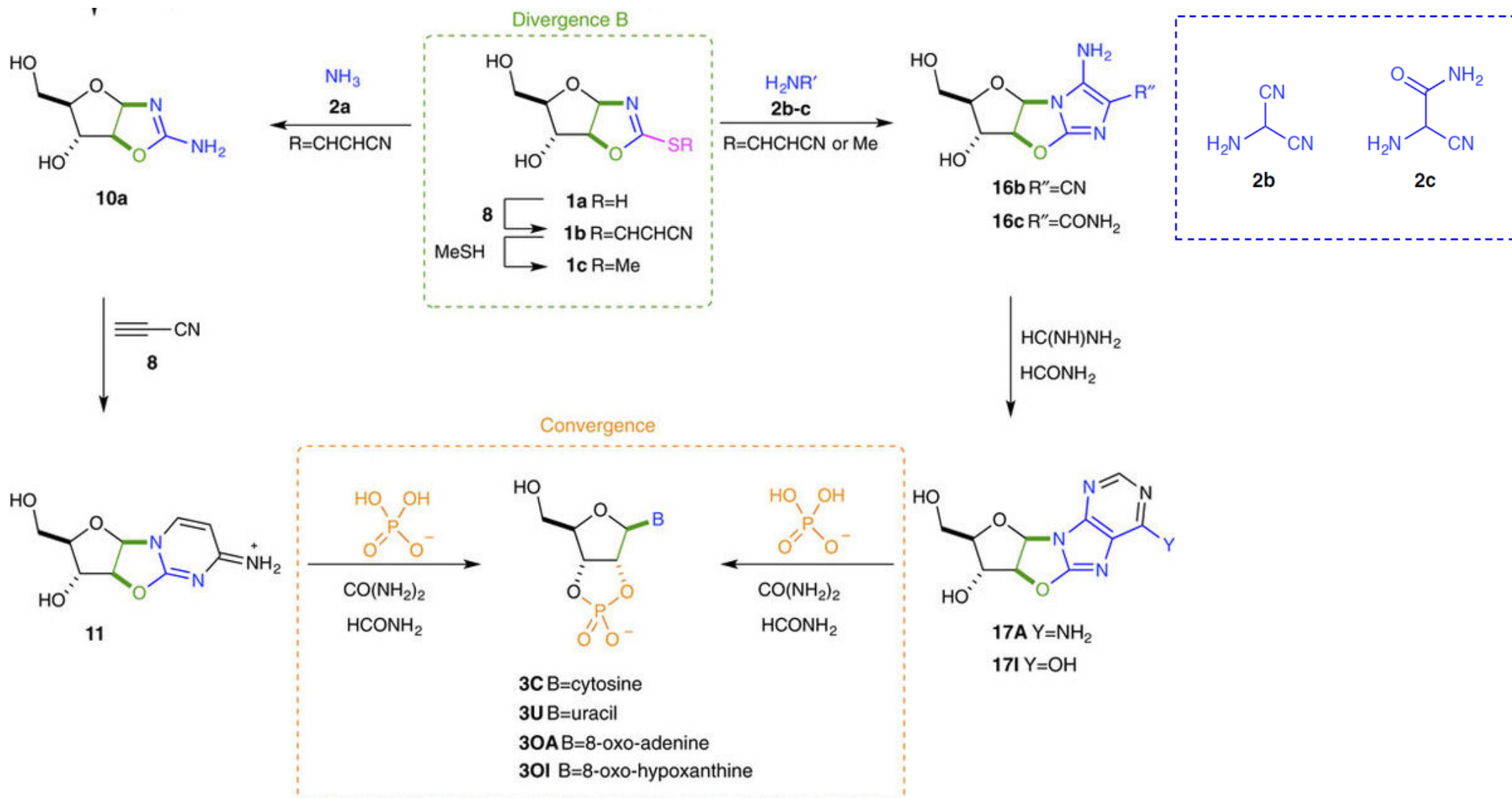


8-Oxo-purine nucleoside synthesis via cyanosulfidic chemistry



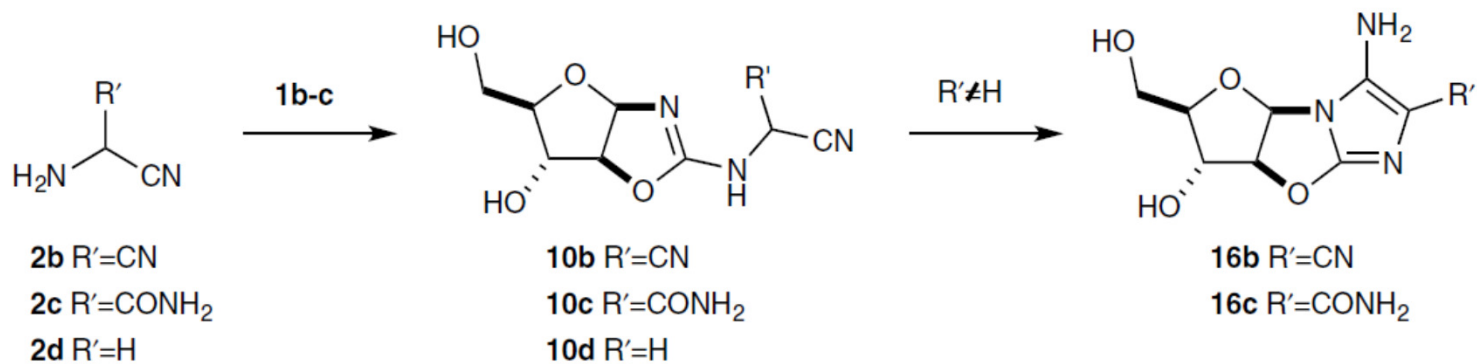
S. Stairs, A. Nikmal, D-K. Bucar, S-L. Zheng, J. W. Szostak, M. W. Powner *Nature Commun.* 8:15270

8-Oxo-purine nucleoside synthesis via cyanosulfidic chemistry

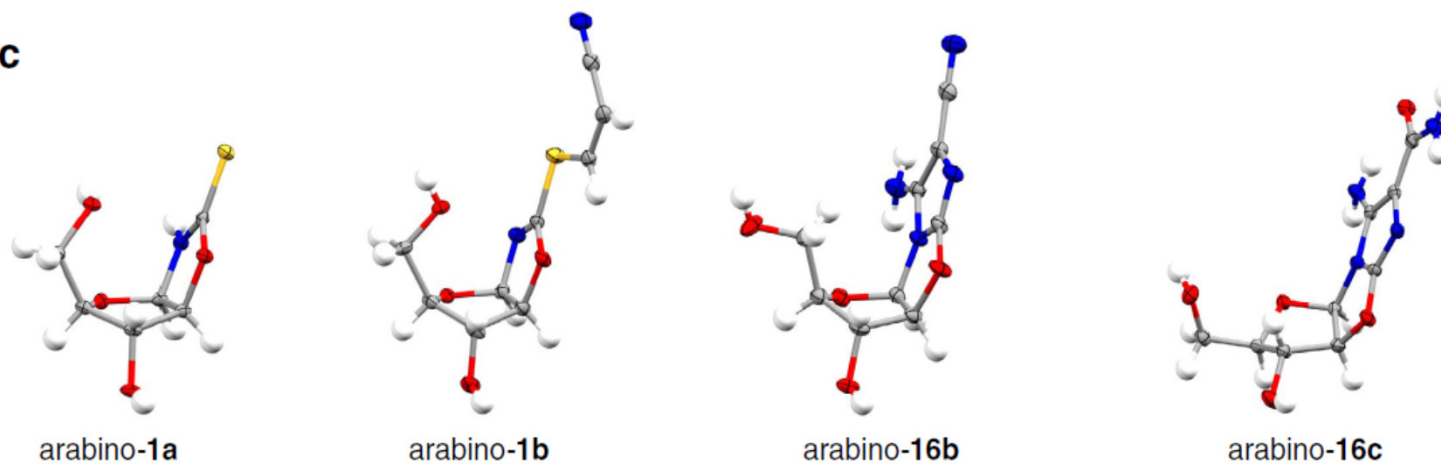


8-Oxo-purine nucleoside synthesis via cyanosulfidic chemistry

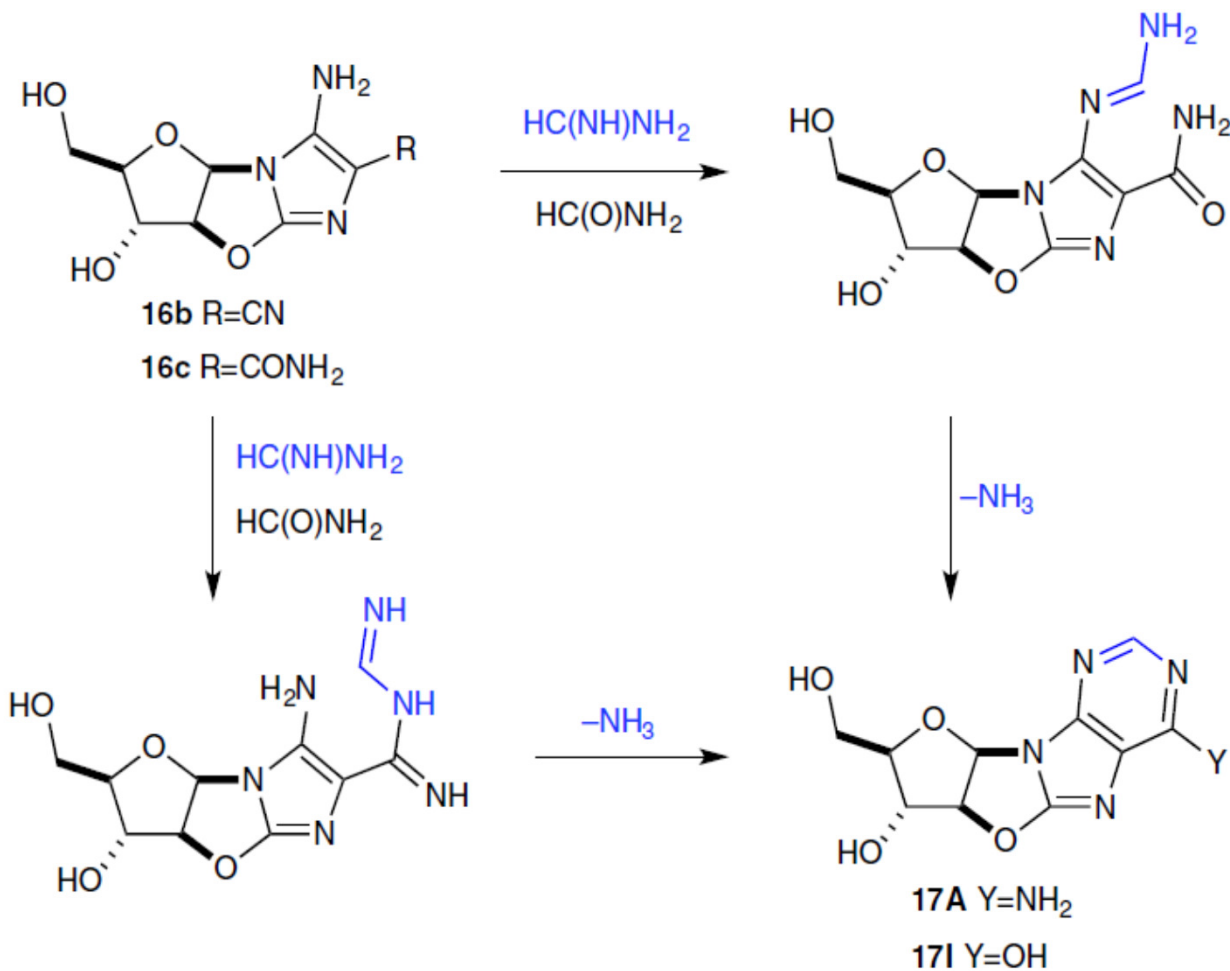
b



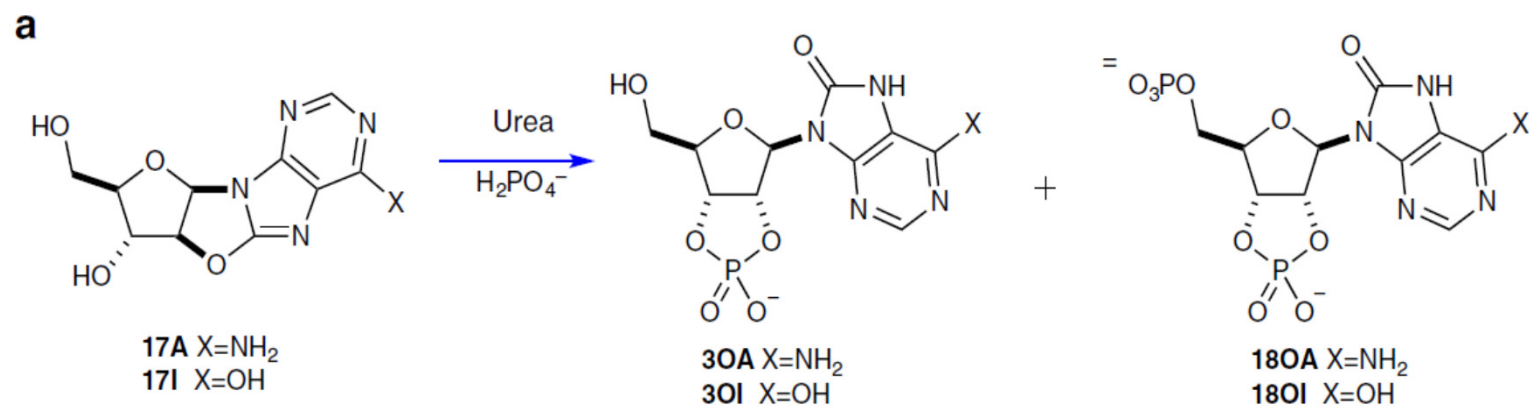
c



8-Oxo-purine nucleoside synthesis via cyanosulfidic chemistry

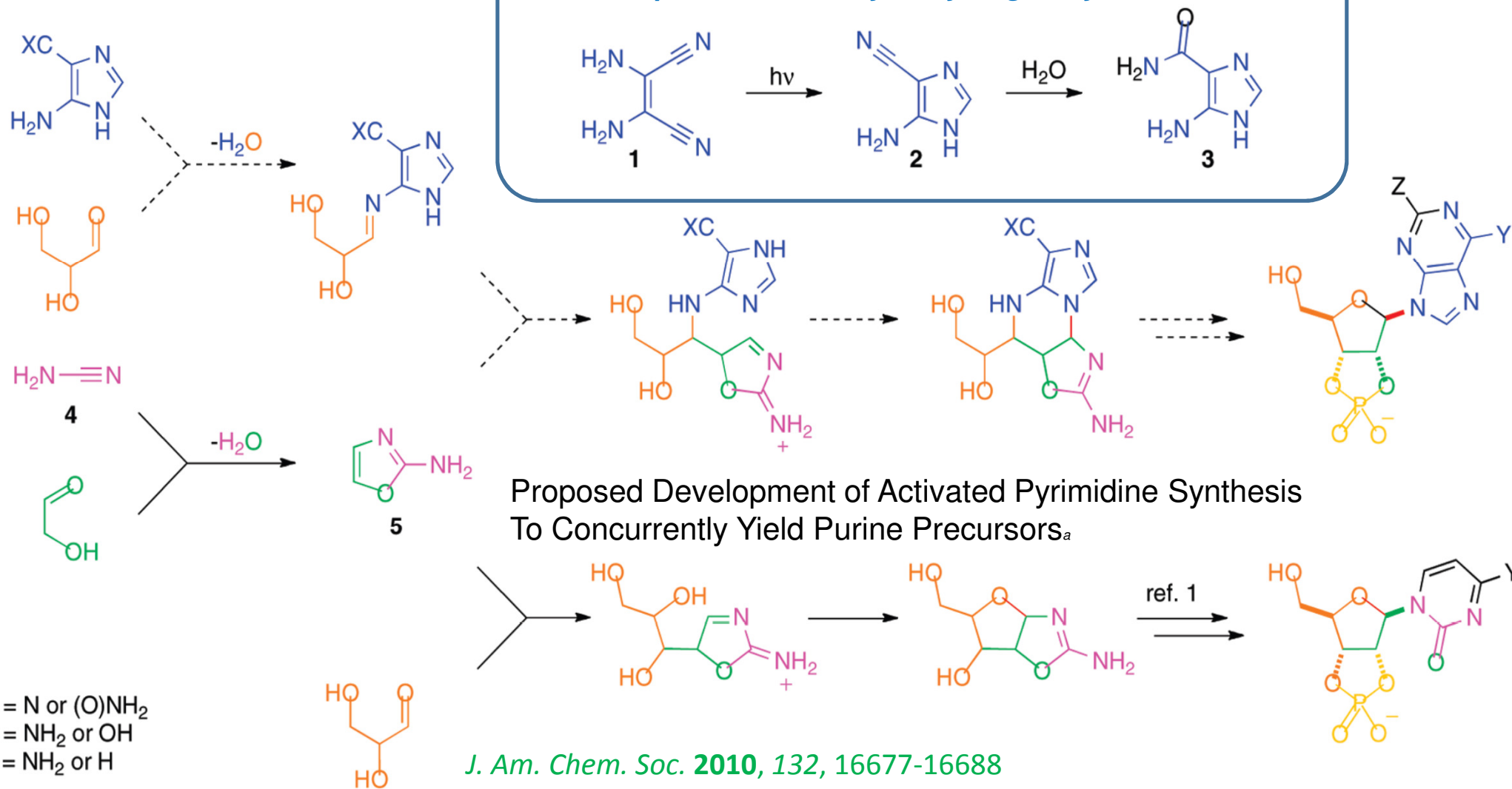


8-Oxo-purine nucleoside synthesis via cyanosulfidic chemistry



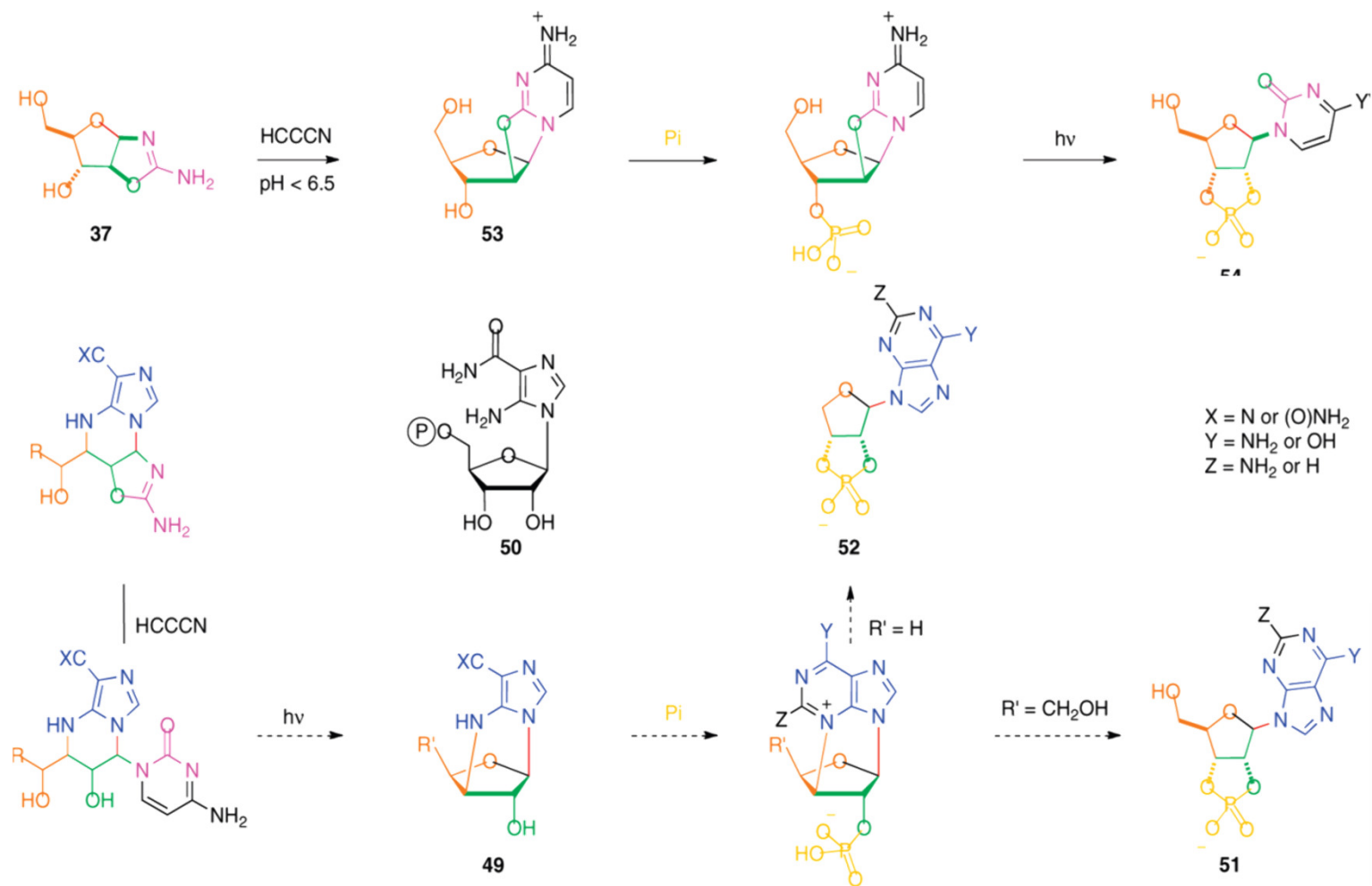
Canonical purine nucleoside synthesis via cyanosulfidic chemistry

Multicomponent Assembly of Hydrogen Cyanide Tetramers



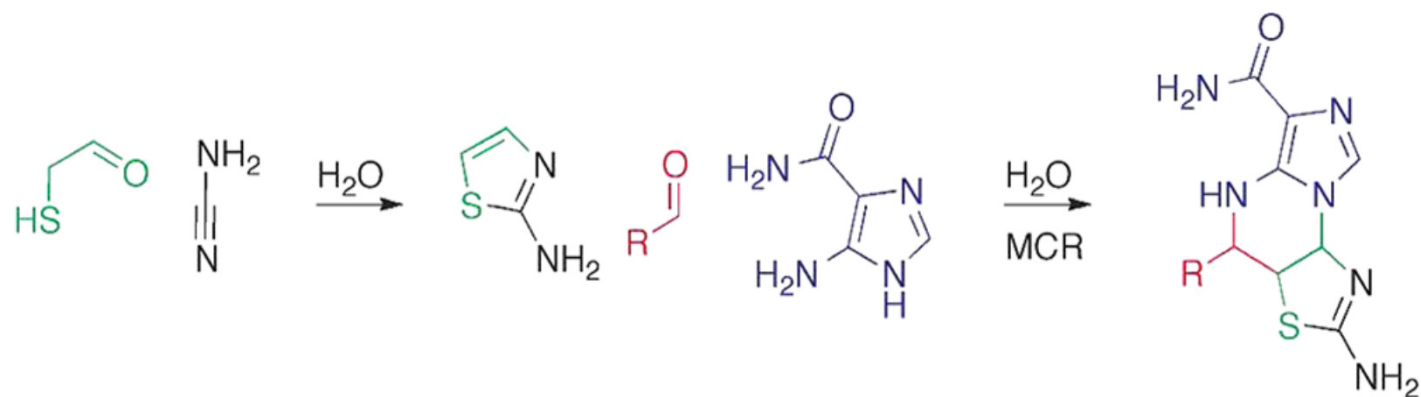
Canonical purine nucleoside synthesis via cyanosulfidic chemistry

beta-Ribofuranosyl-pyrimidine nucleotide assembly and potential stepwise, regioselective beta-ribofuranosyl-purine assembly
Pathway via the intermediacy of tetrahydroimidazo[1',3']-2''-aminooxazolo[1',2']-pyrimidines

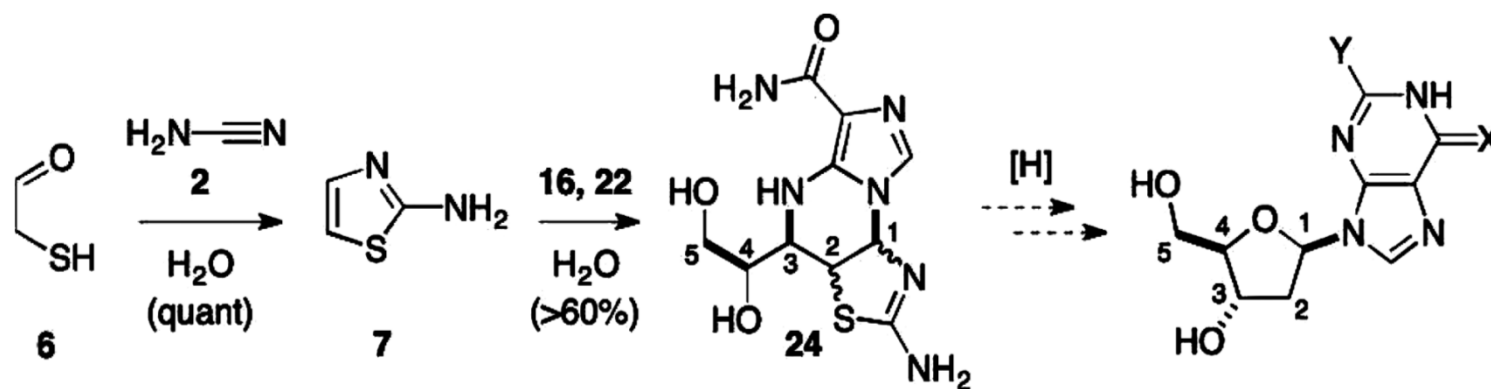


M. W. Powner, J. D. Sutherland, J. W. Szostak *J. Am. Chem. Soc.* **2010**, *132*, 16677-16688

Prebiotic synthesis of deoxyribonucleosides

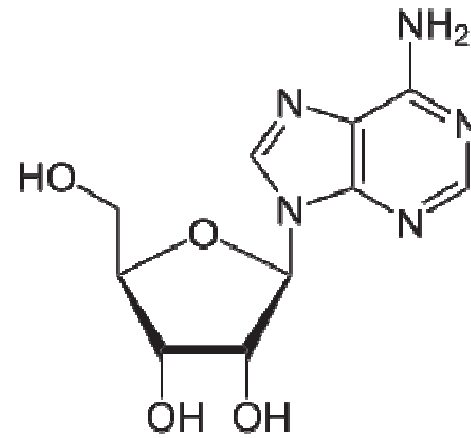
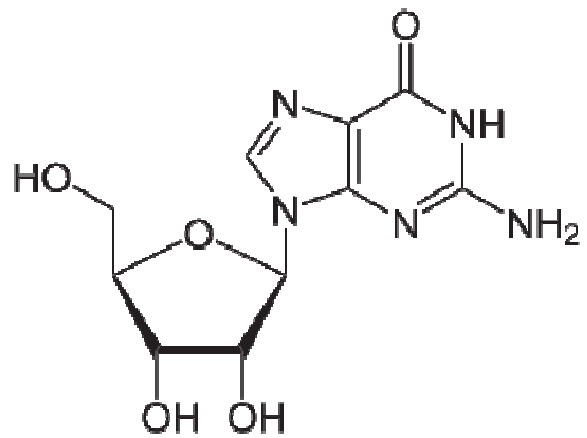
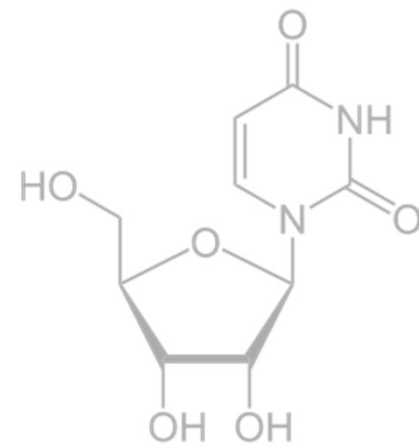
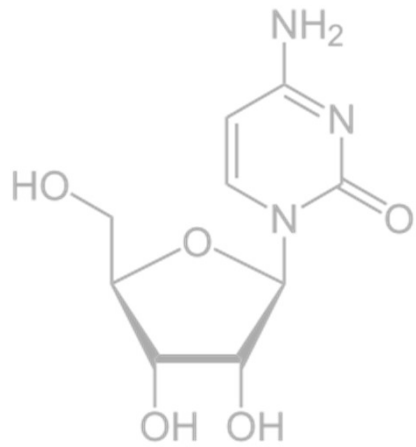


proposed multicomponent deoxyribonucleotide syntheses

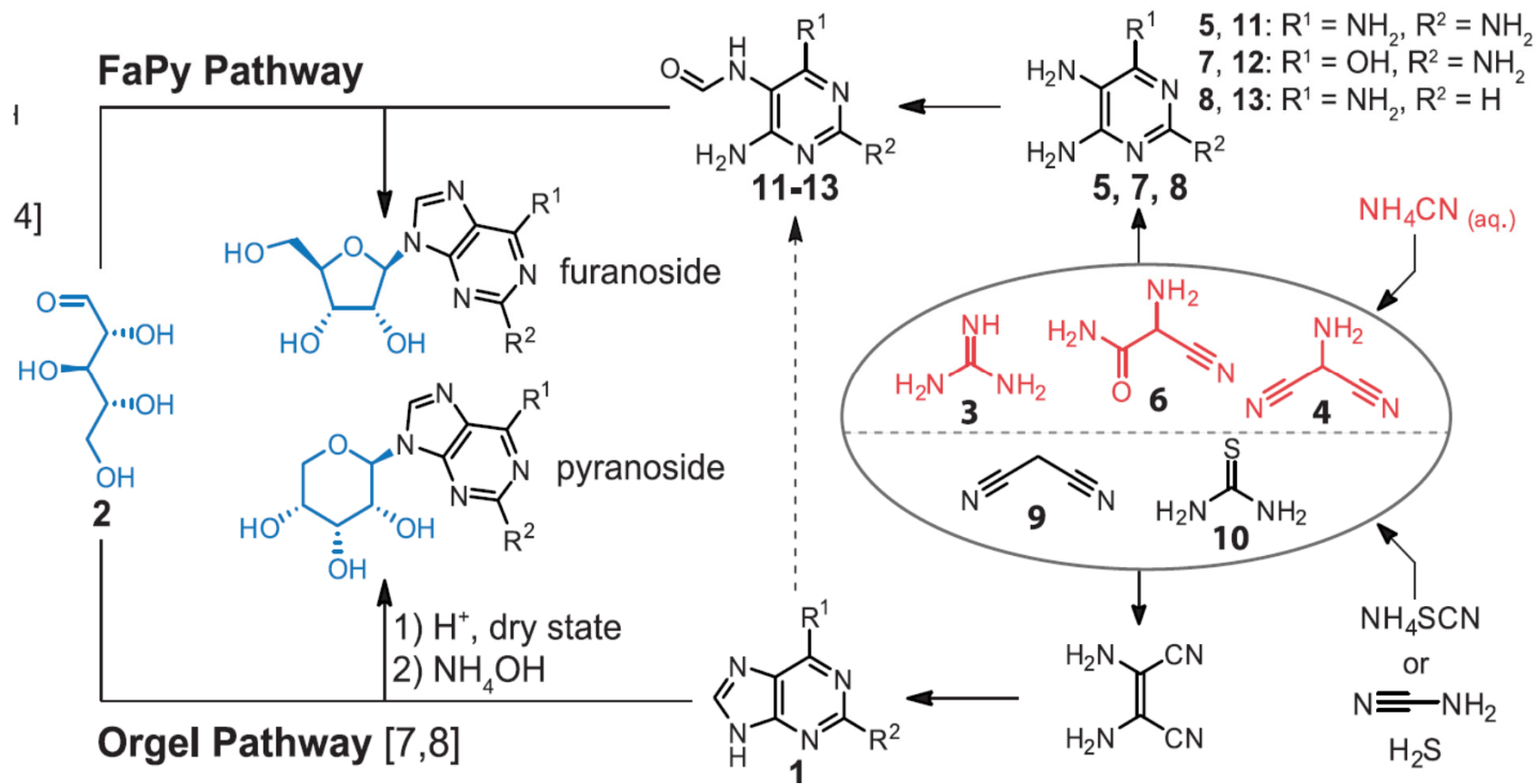


M. W. Powner, S.-L. Zheng, J. W. Szostak *J. Am. Chem. Soc.* **2012**, *134*, 13889-13895

Purine nucleoside synthesis - alternatives

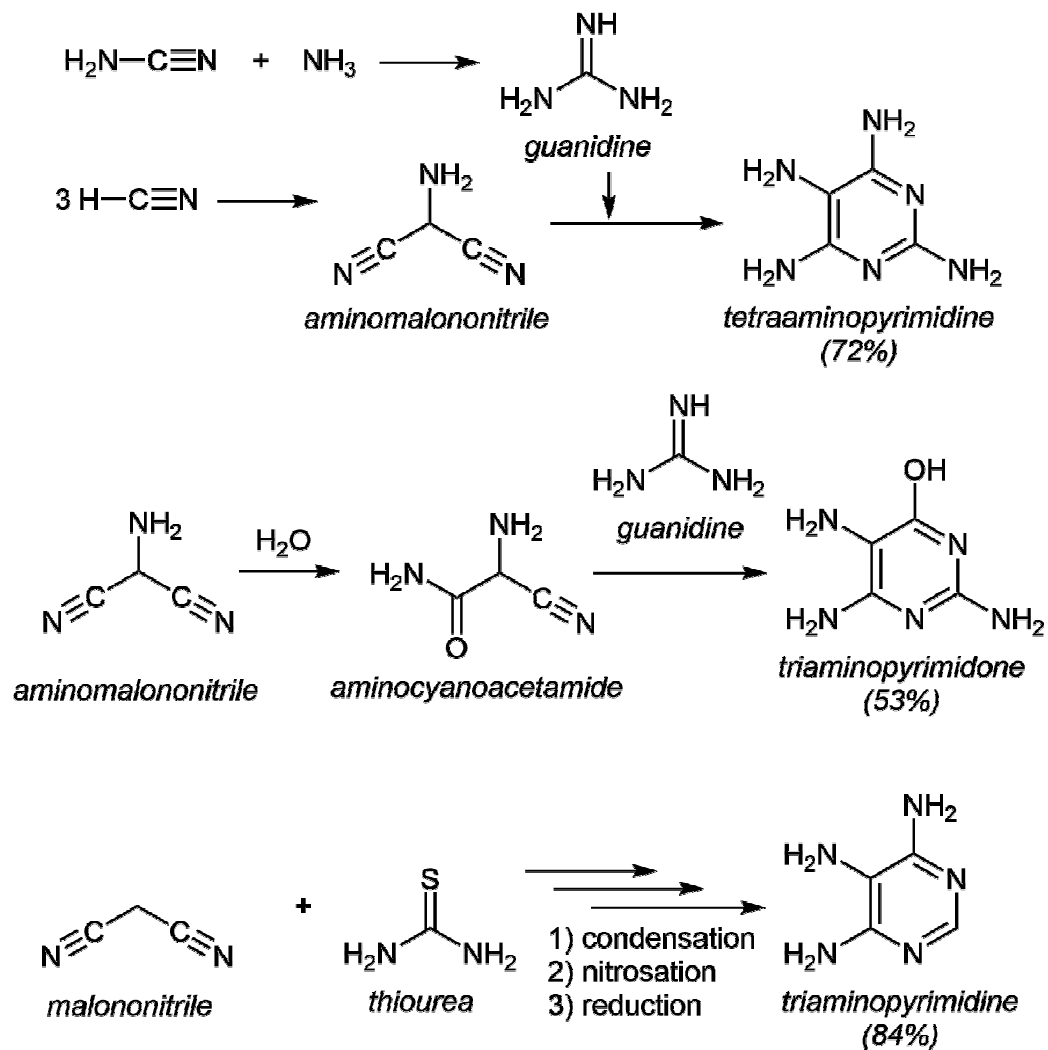


Prebiotic synthesis of purine nucleosides –FaPY pathway



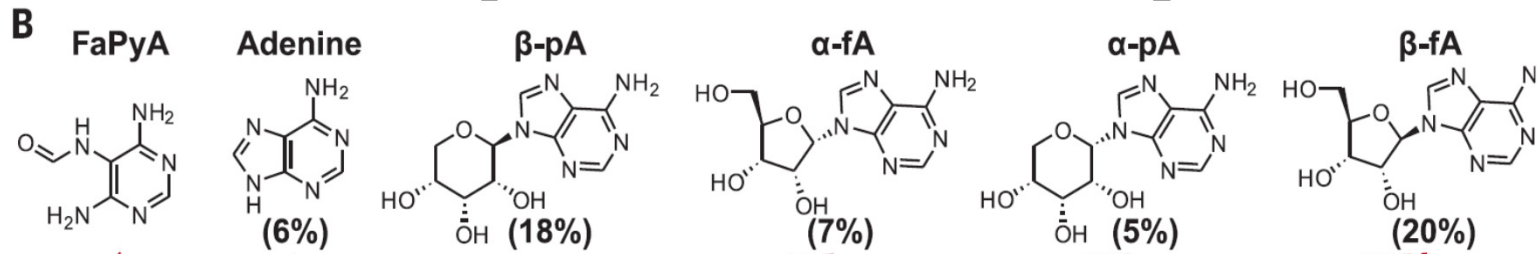
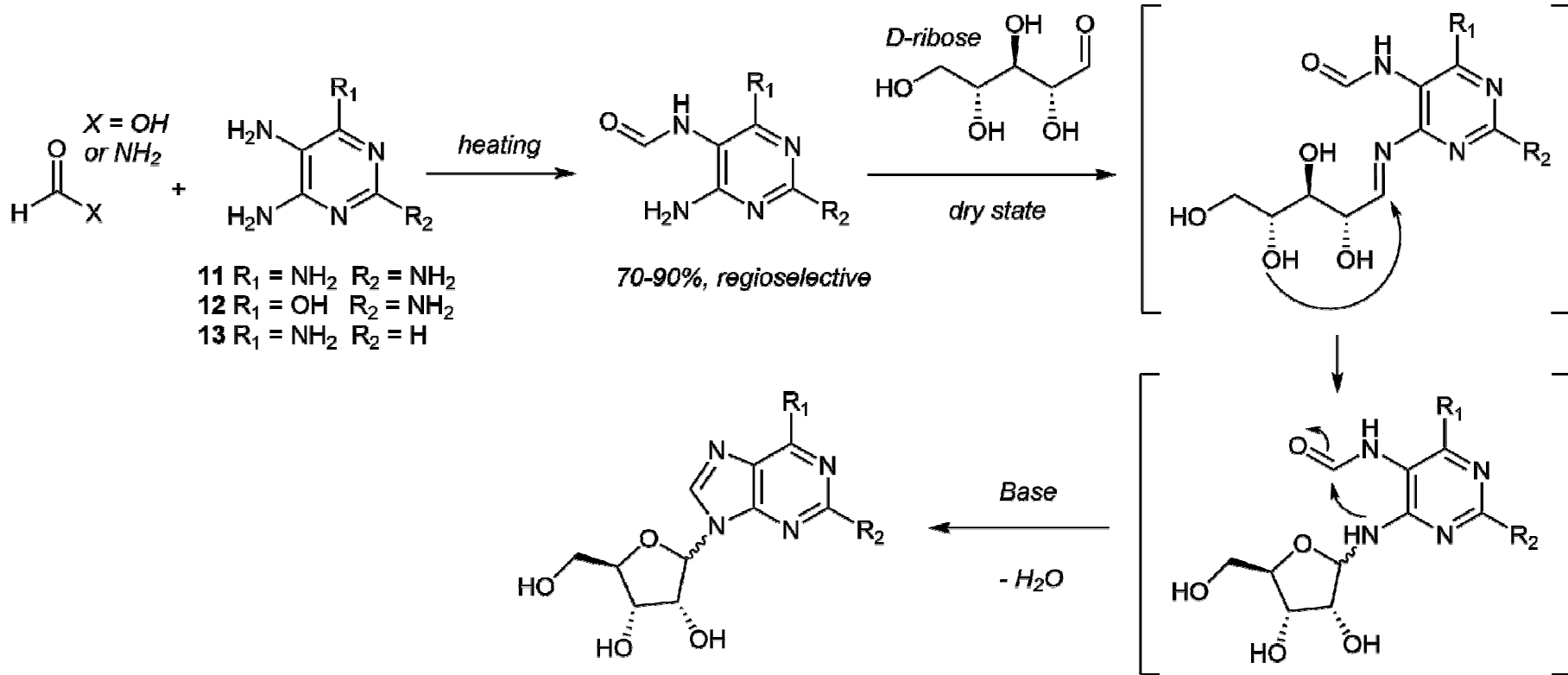
T. Carell, *Nature* **2016**, 352(6287), 833-836

Prebiotic syntheses of aminopyrimidines



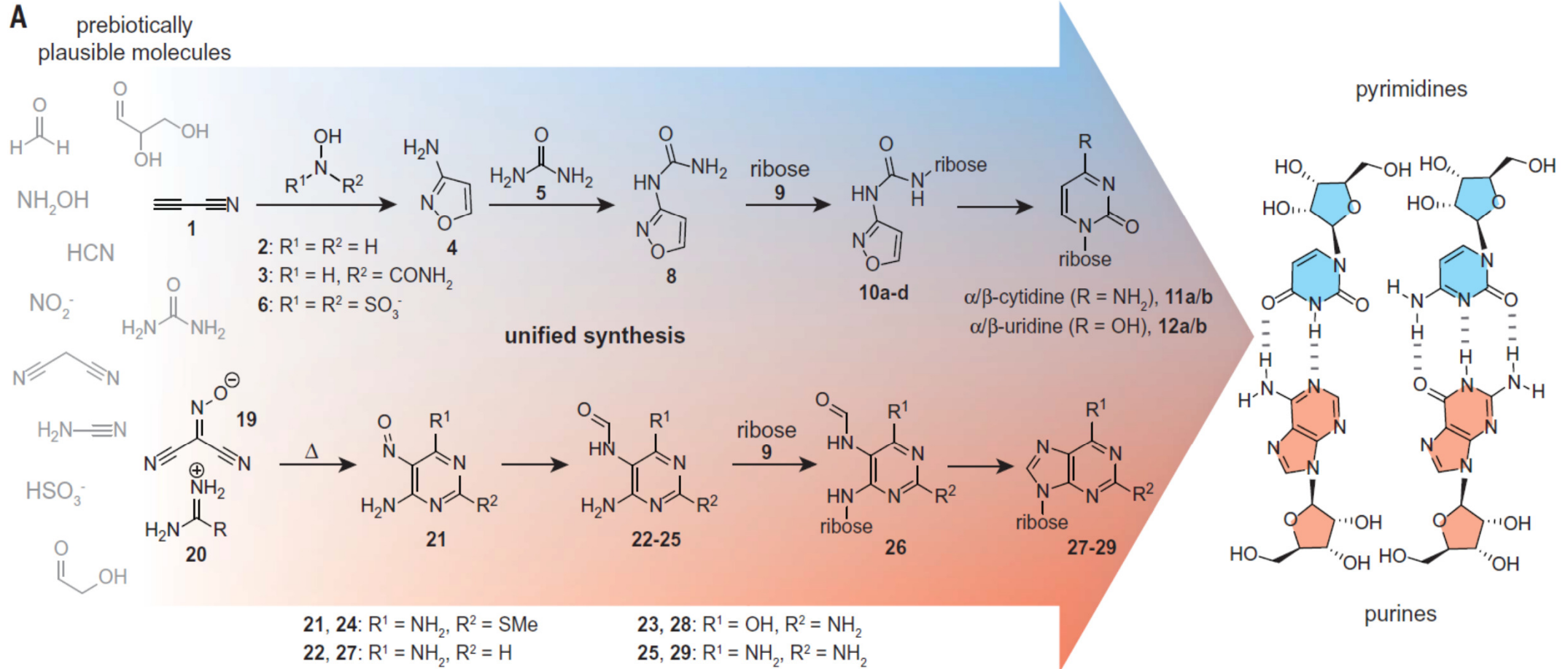
T. Carell, *Nature* **2016**, 352(6287), 833-836

Prebiotic synthesis of purine nucleosides –FaPY pathway



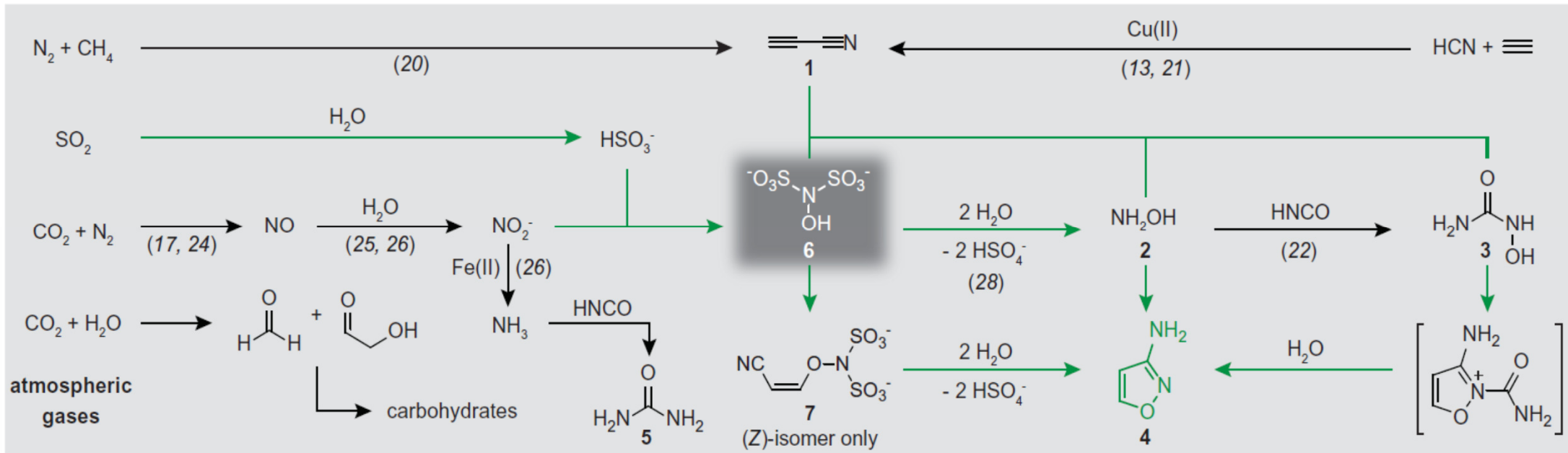
T. Carell, *Nature* **2016**, 352(6287), 833-836

Unified prebiotic synthesis of pyrimidine and purine ribonucleotides



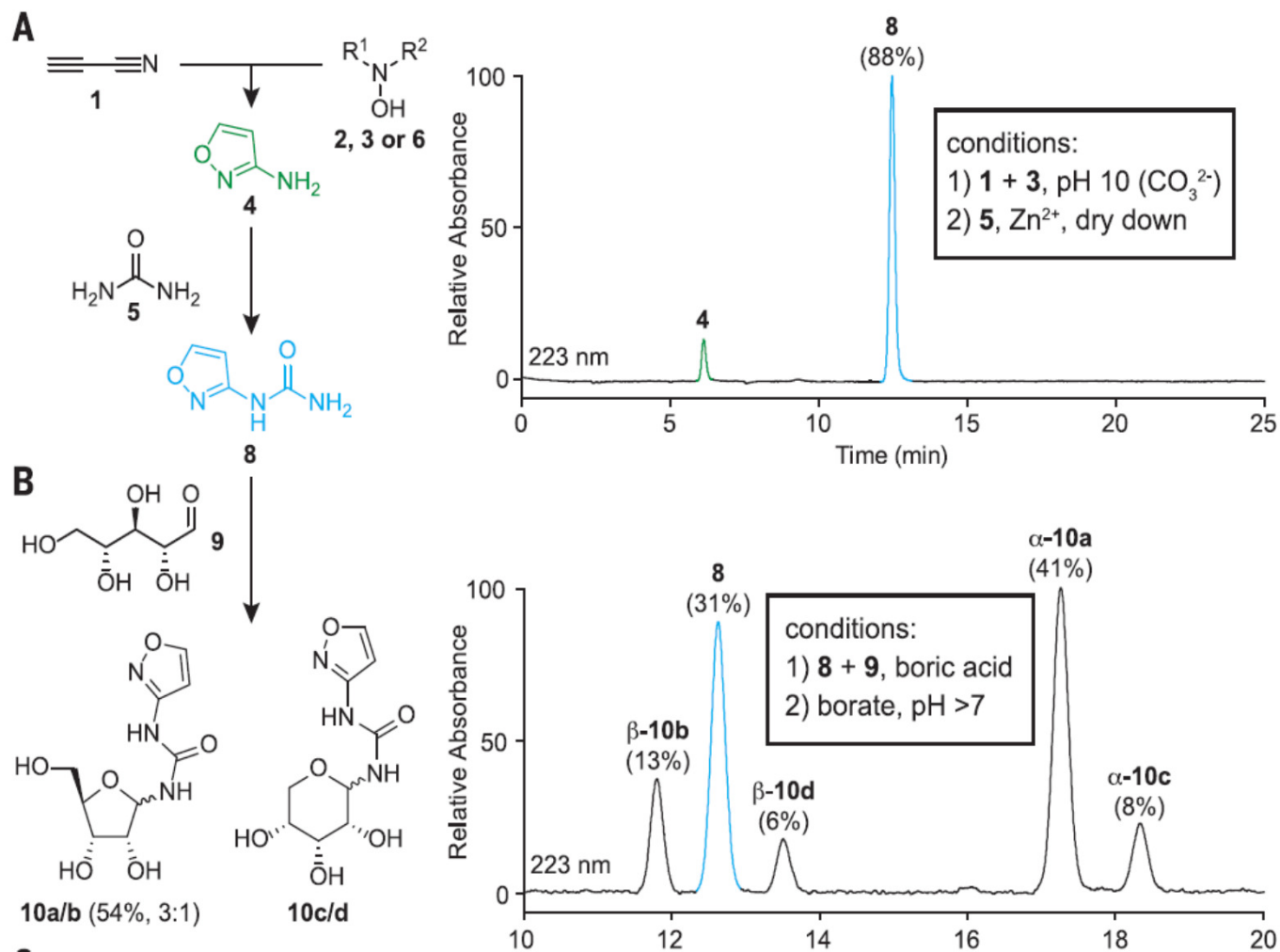
S. Becker, J. Feldmann, S. Wiedemann, ..., T. Carell, *Science* **2019**, *366*, 76-82

Unified prebiotic synthesis of pyrimidine and purine ribonucleotides



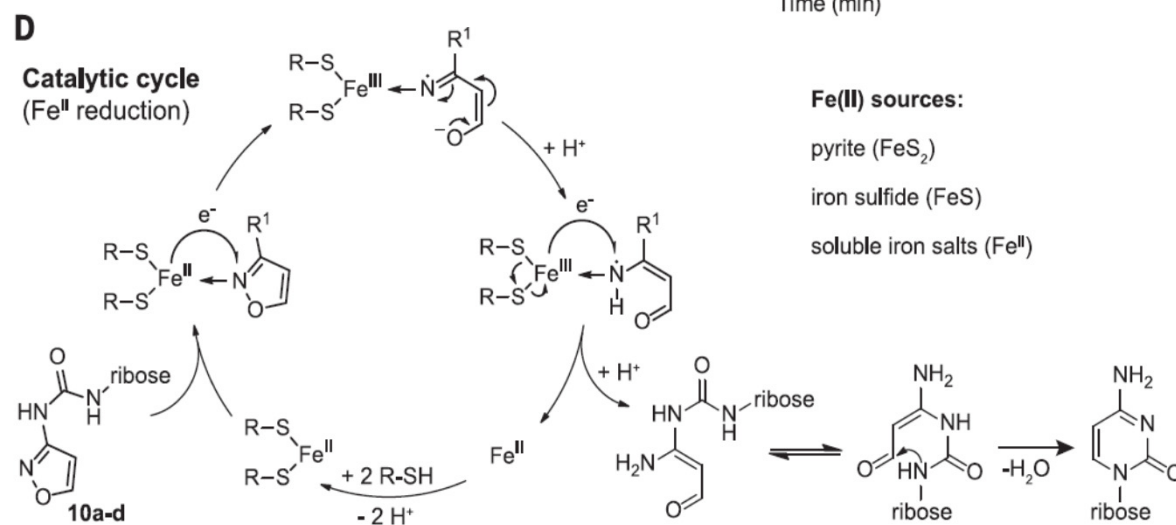
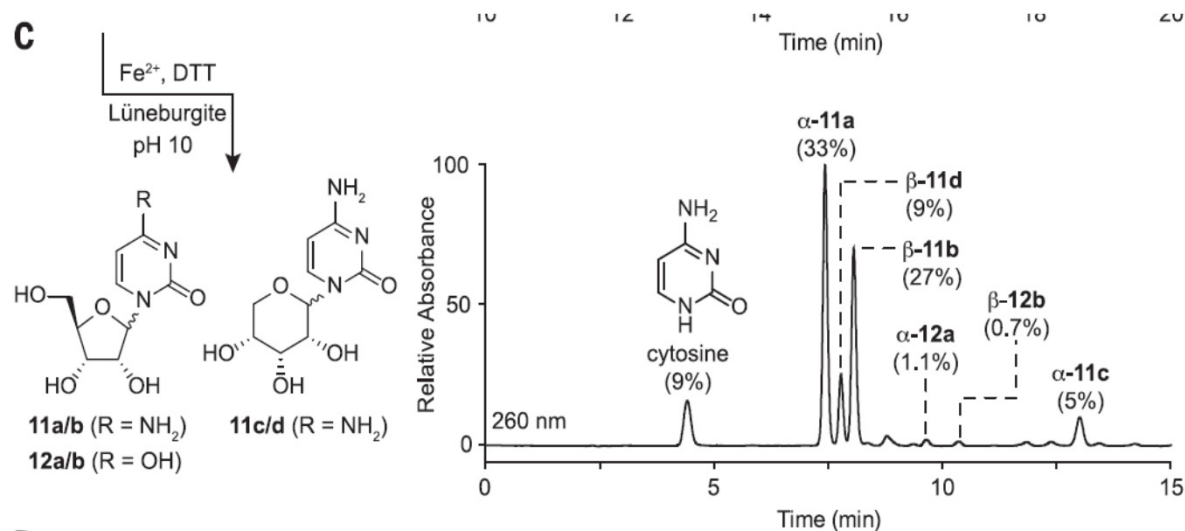
S. Becker, J. Feldmann, S. Wiedemann, ..., T. Carell, *Science* **2019**, 366, 76-82

Unified prebiotic synthesis of pyrimidine and purine ribonucleotides



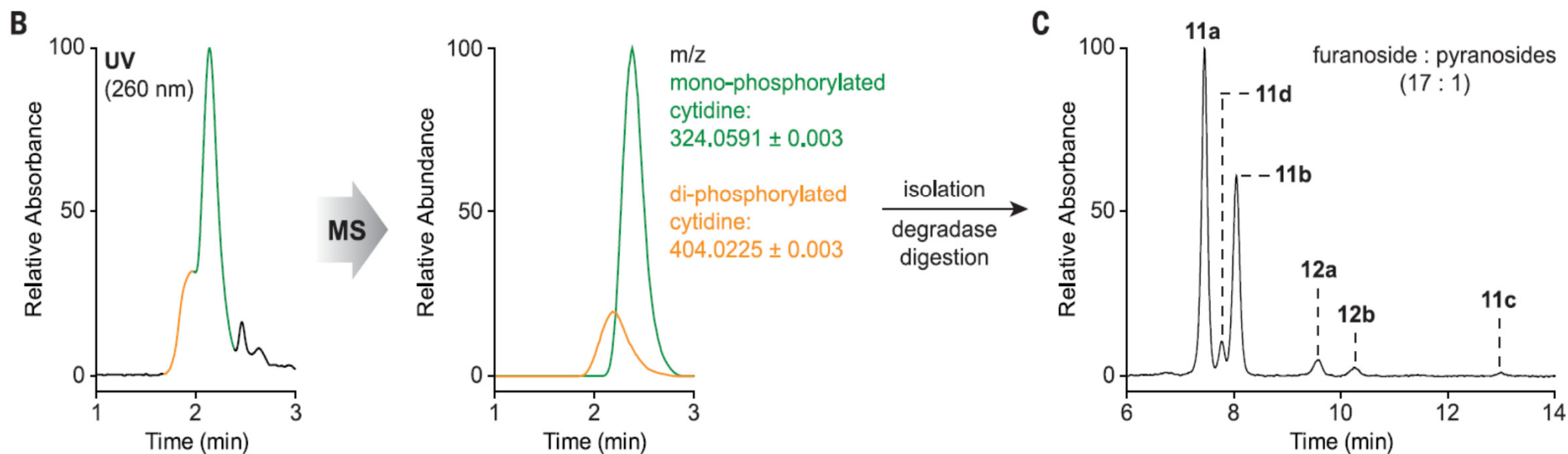
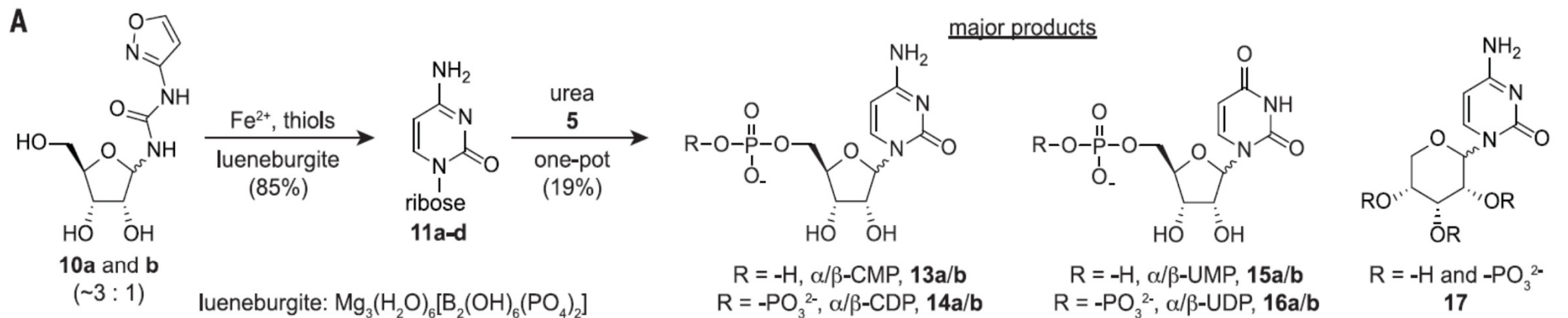
S. Becker, J. Feldmann, S. Wiedemann, ..., T. Carell, *Science* **2019**, *366*, 76-82

Unified prebiotic synthesis of pyrimidine and purine ribonucleotides



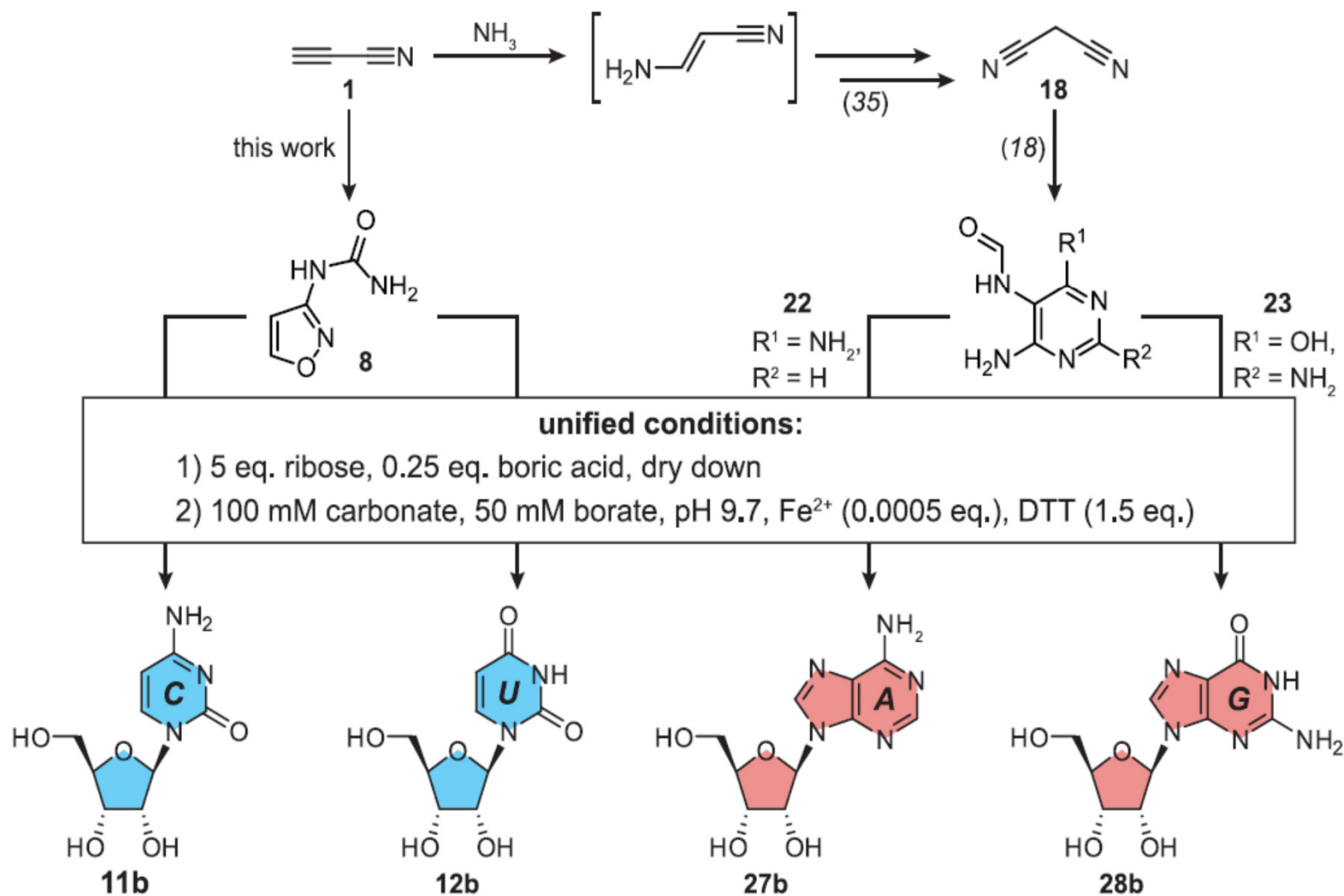
S. Becker, J. Feldmann, S. Wiedemann, ..., T. Carell, *Science* **2019**, *366*, 76-82

Unified prebiotic synthesis of pyrimidine and purine ribonucleotides



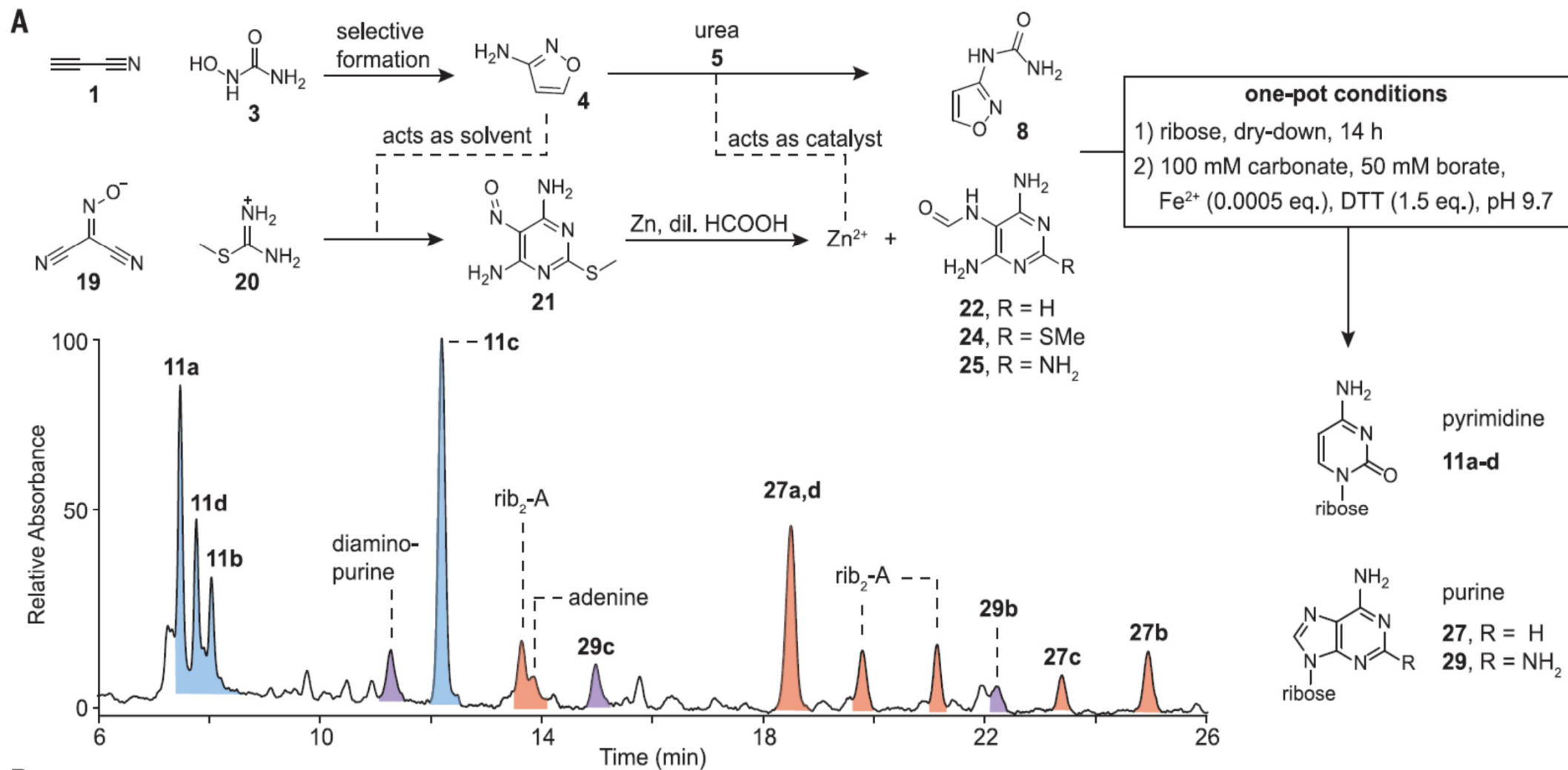
S. Becker, J. Feldmann, S. Wiedemann, ..., T. Carell, *Science* **2019**, *366*, 76-82

Unified prebiotic synthesis of pyrimidine and purine ribonucleotides

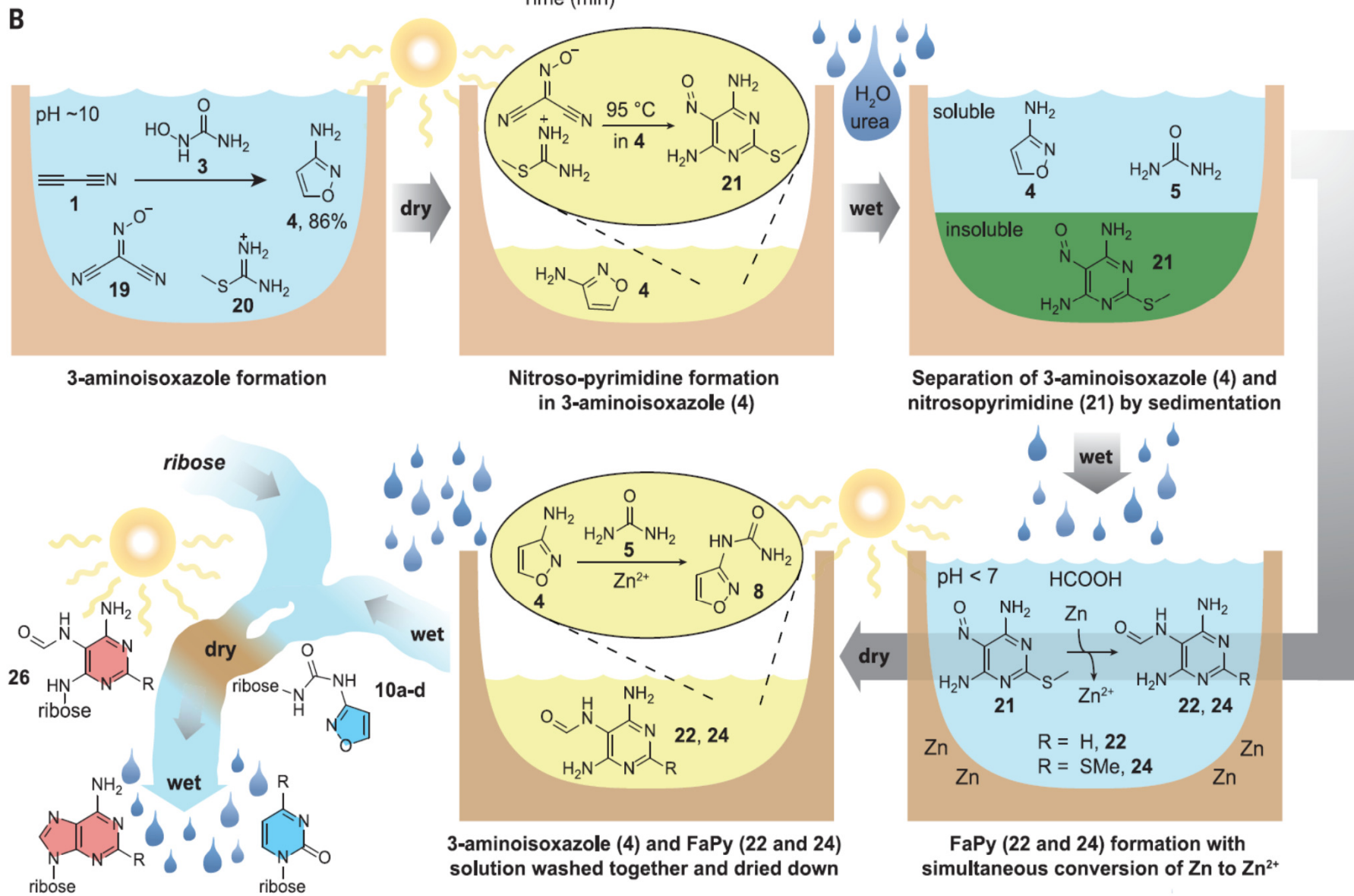


S. Becker, J. Feldmann, S. Wiedemann, ..., T. Carell, *Science* **2019**, *366*, 76-82

Unified prebiotic synthesis of pyrimidine and purine ribonucleotides



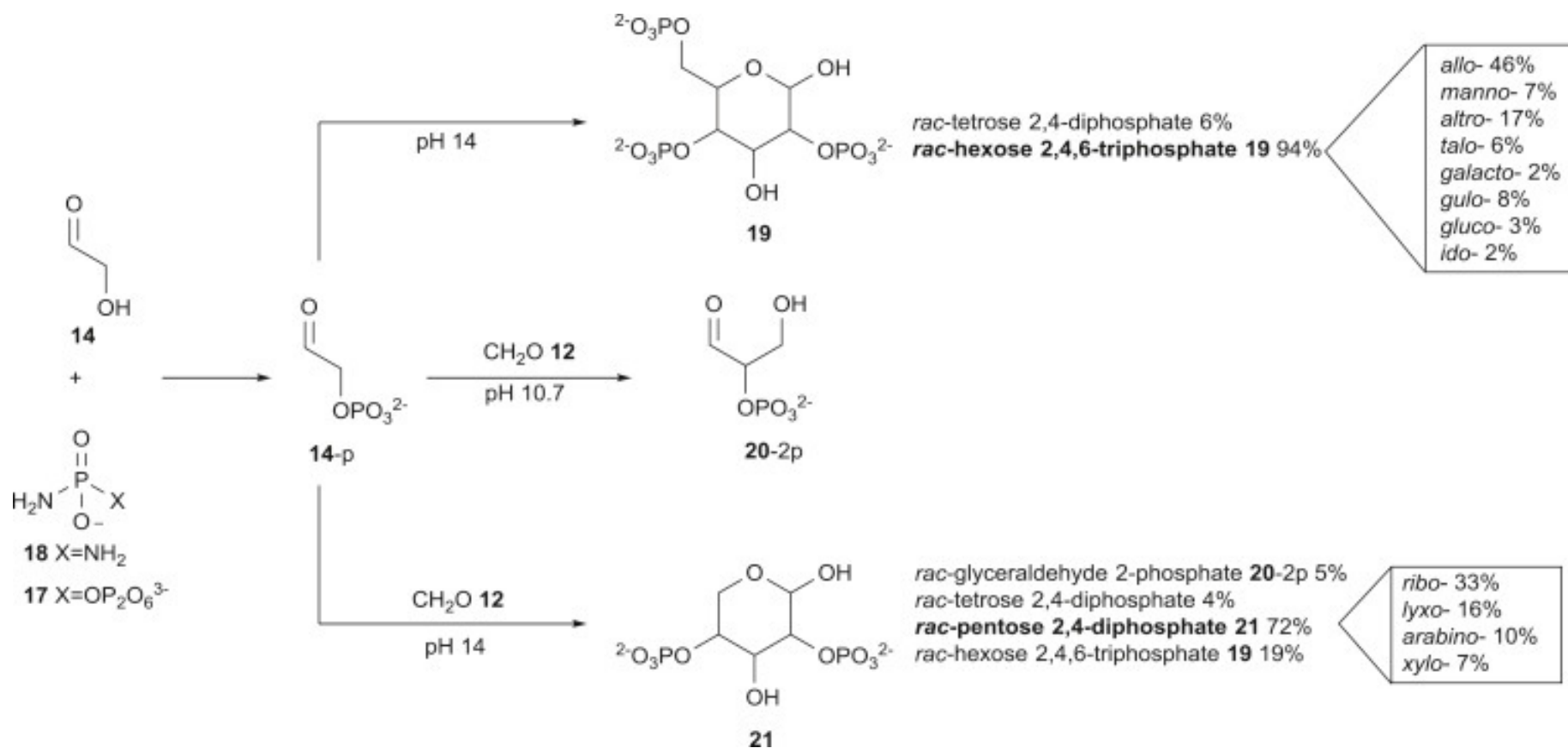
S. Becker, J. Feldmann, S. Wiedemann, ..., T. Carell, *Science* **2019**, *366*, 76-82



S. Becker, J. Feldmann, S. Wiedemann, ..., T. Carell, *Science* **2019**, *366*, 76-82

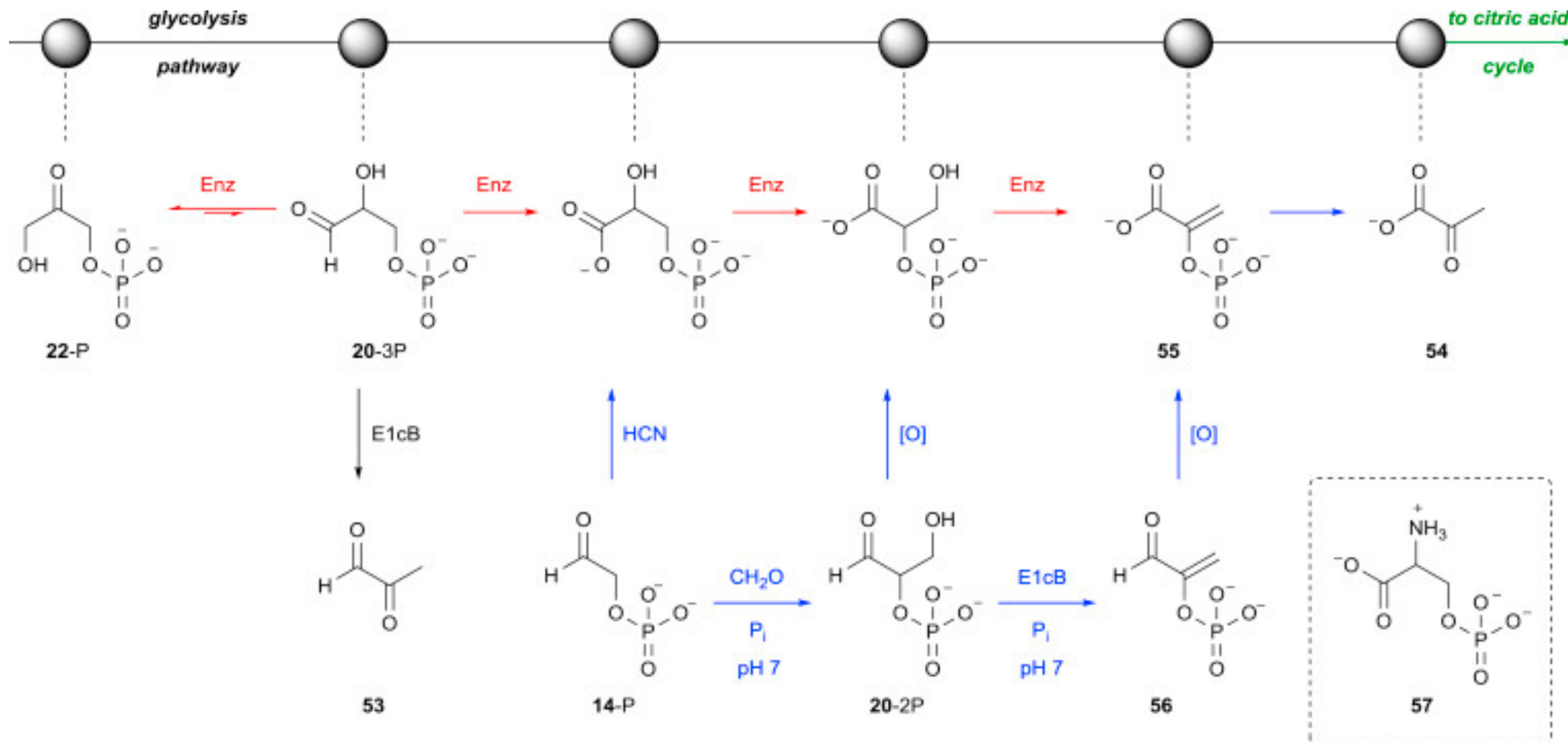
Prebiotic phosphorylations and the origins of protometabolism

Selective Phosphorylation of Glycolaldehyde and Aldol Reactions of Glycolaldehyde Phosphate

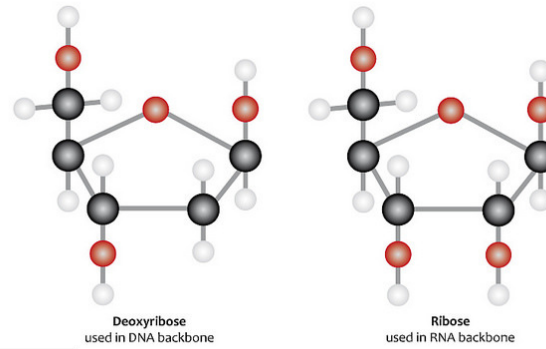
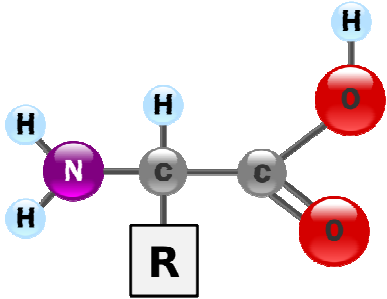


S. Islam, M. W. Powner *Chem* **2017**, *2*, 470-501

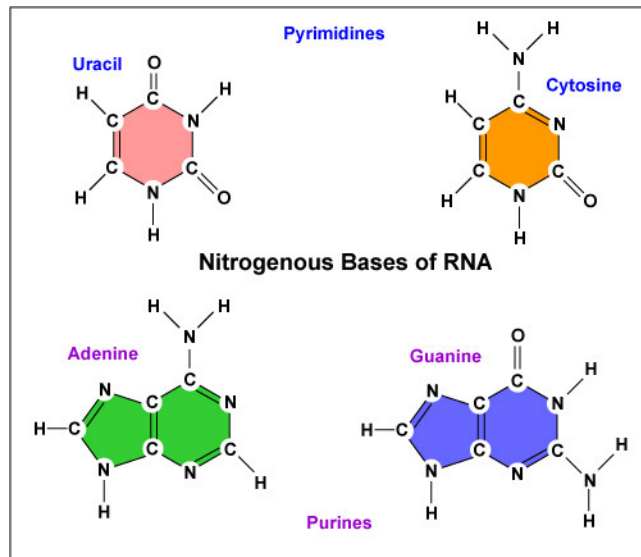
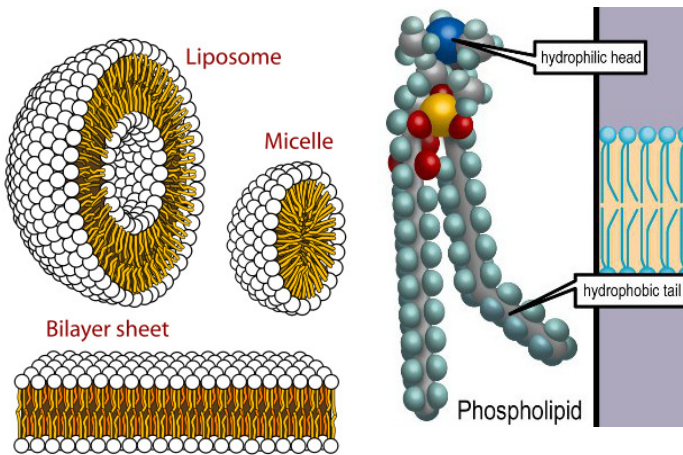
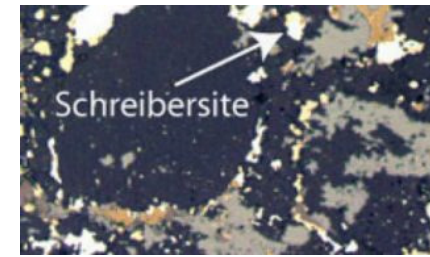
Prebiotic Reconstruction of the Triose Glycolysis Pathway by Selective α -Phosphorylation of Sugars



Prebiotic soup - summary

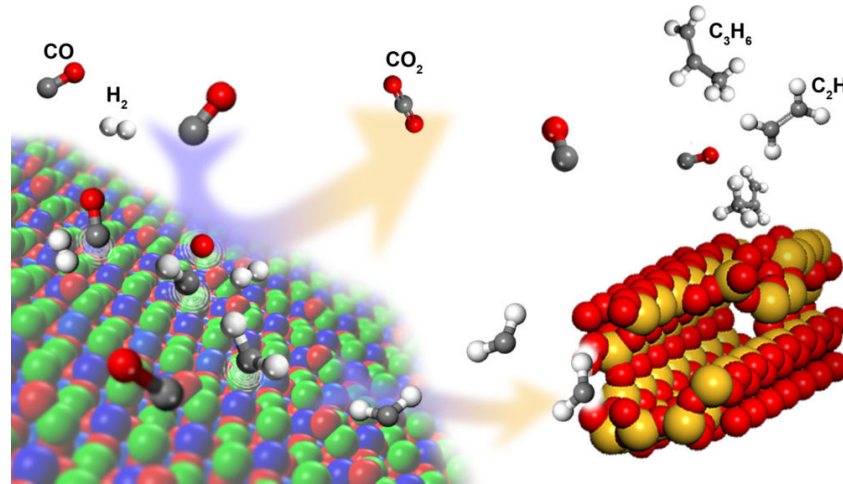


Key
 ○ Hydrogen
 ● Oxygen
 ● Carbon

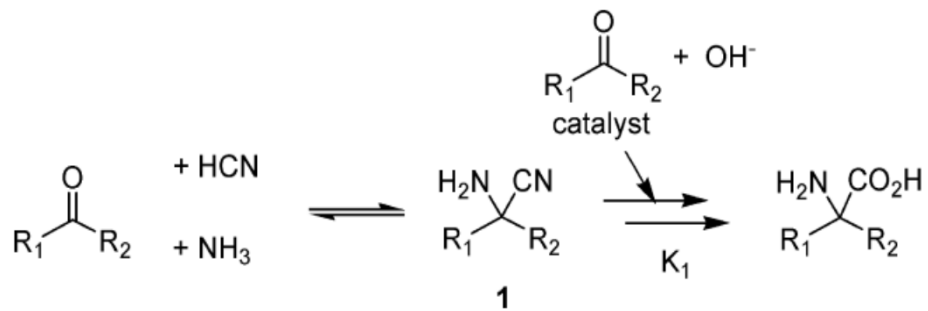


Prebiotic soup - summary

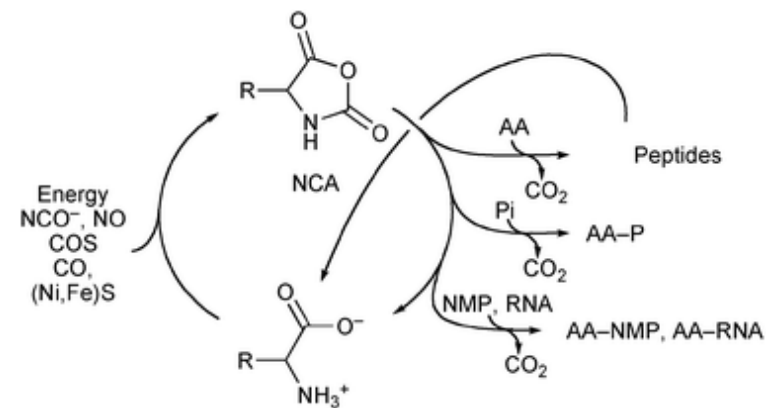
Fischer-Tropsch chemistry - lipids



Strecker chemistry - aminoacids

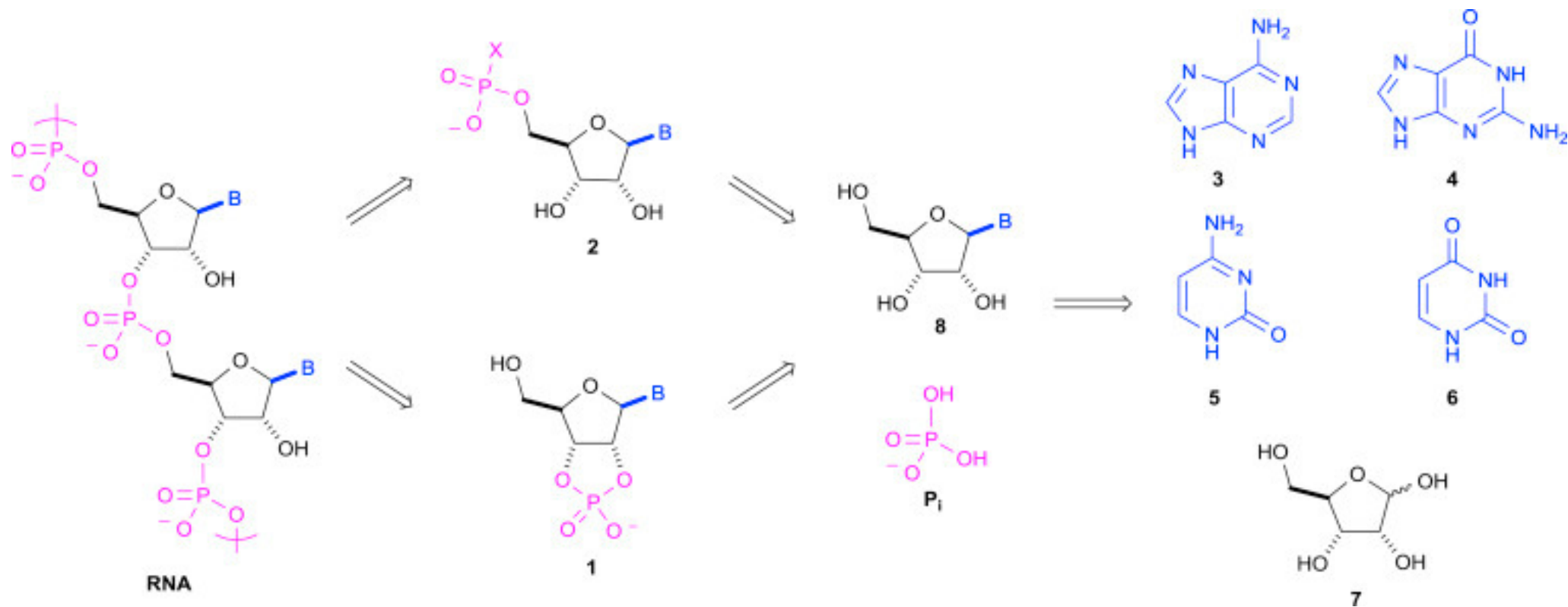


Dehydrating agents (COS, NO) – condensation of AAs to peptides



Prebiotic soup - summary

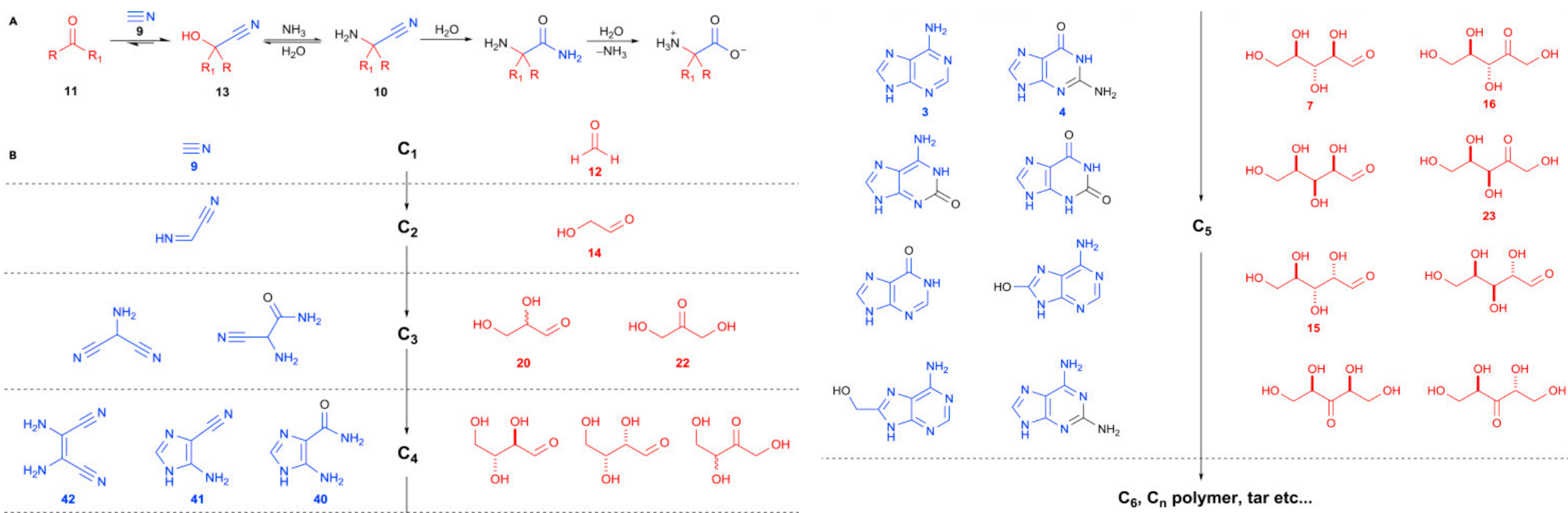
The Traditional Modular Retrosynthetic Analyses Disconnect RNA to Ribofuranosyl Sugar, Inorganic Phosphate, and Canonical RNA Nucleobases.



Prebiotic soup - summary

The Three Pillars of Prebiotic Chemistry

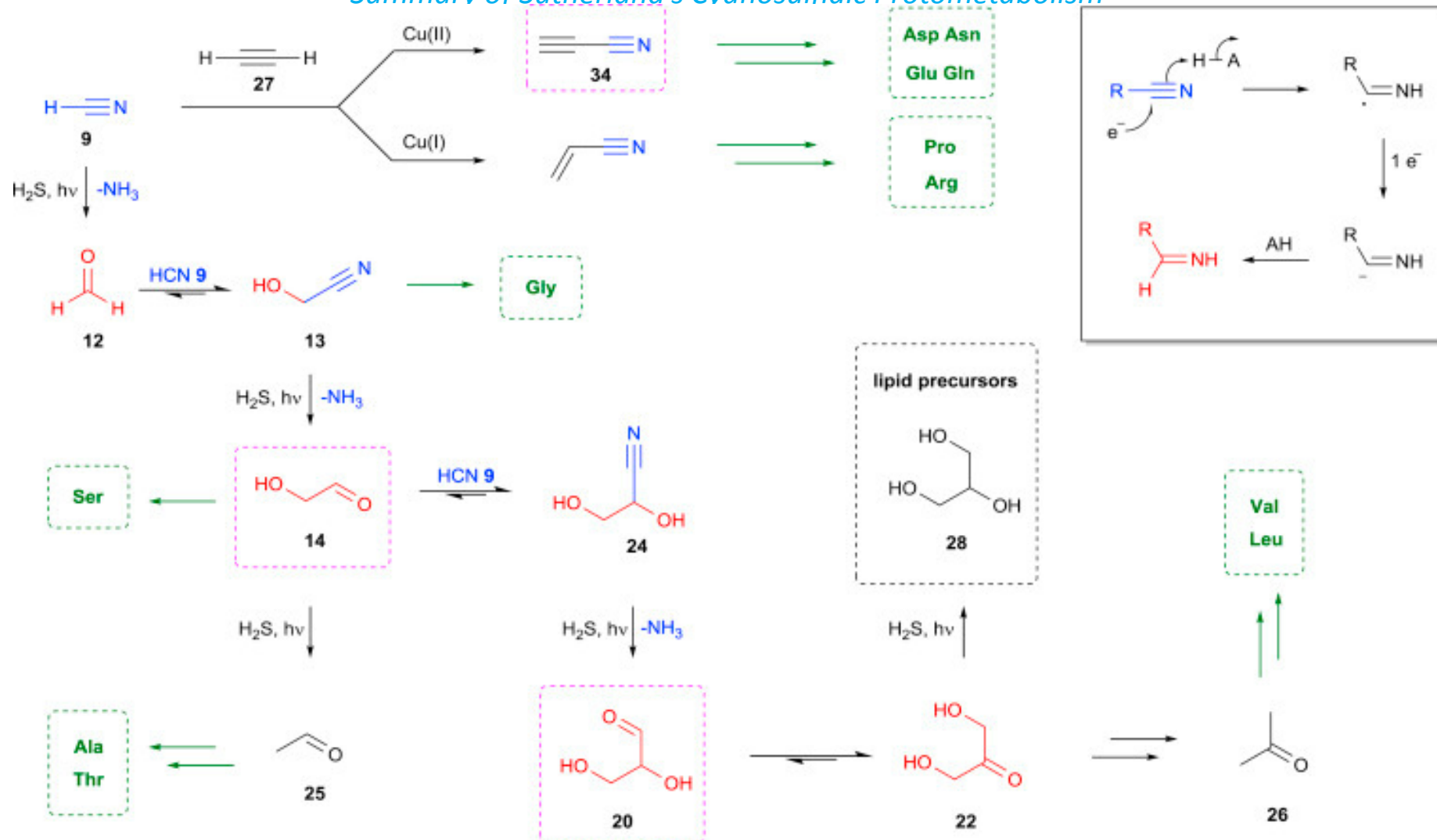
(A) The spark discharge aminonitrile synthesis (The Miller-Urey experiment.),
(B) Nucleobase synthesis by HCN oligomerization, and
(C) Sugar synthesis by the formose reaction.



S. Islam, M. W. Powner *Chem* **2017**, *2*, 470-501

Prebiotic soup - summary

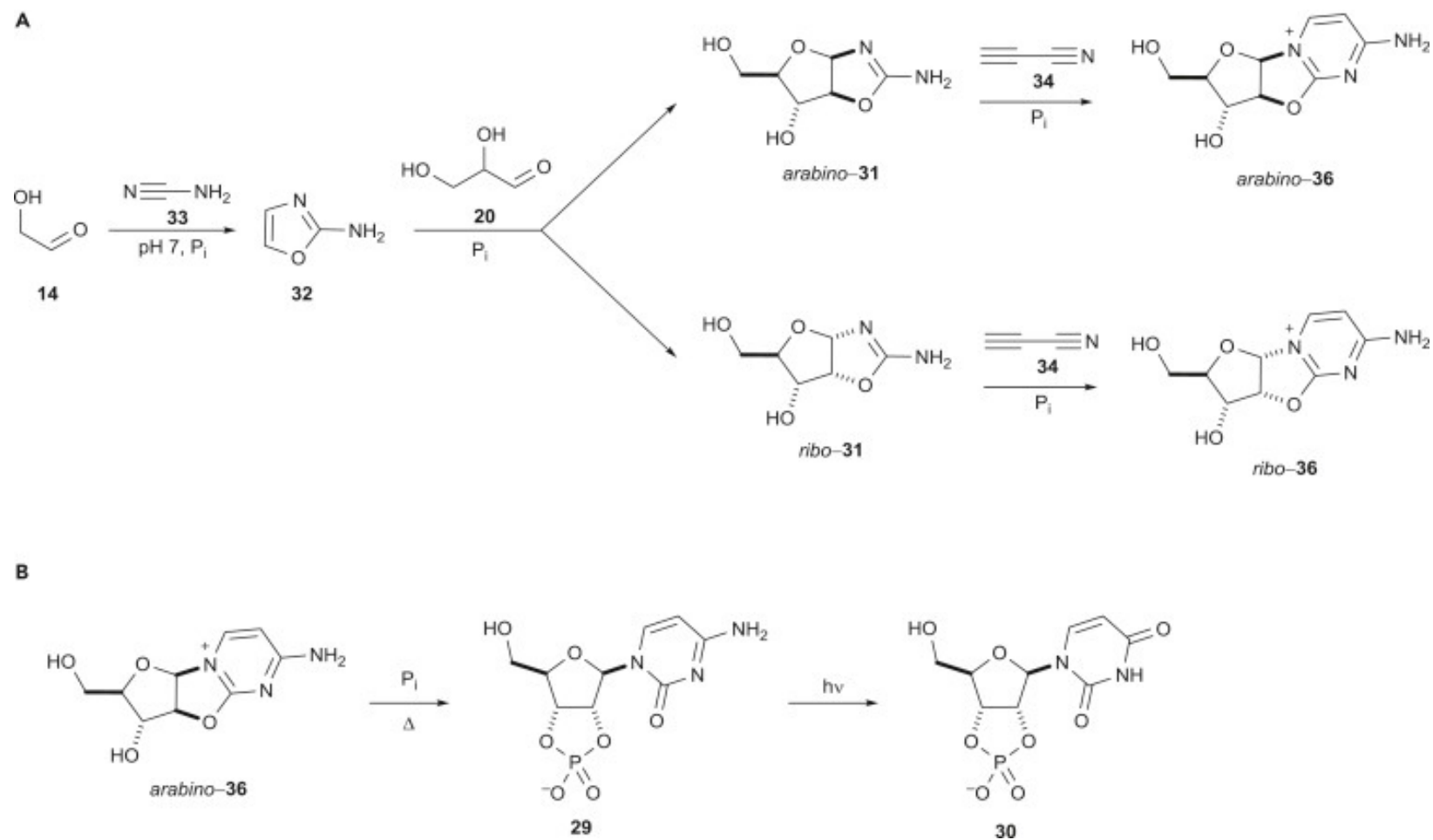
Summary of Sutherland's Cyanosulfidic Protometabolism



S. Islam, M. W. Powner *Chem* **2017**, *2*, 470-501

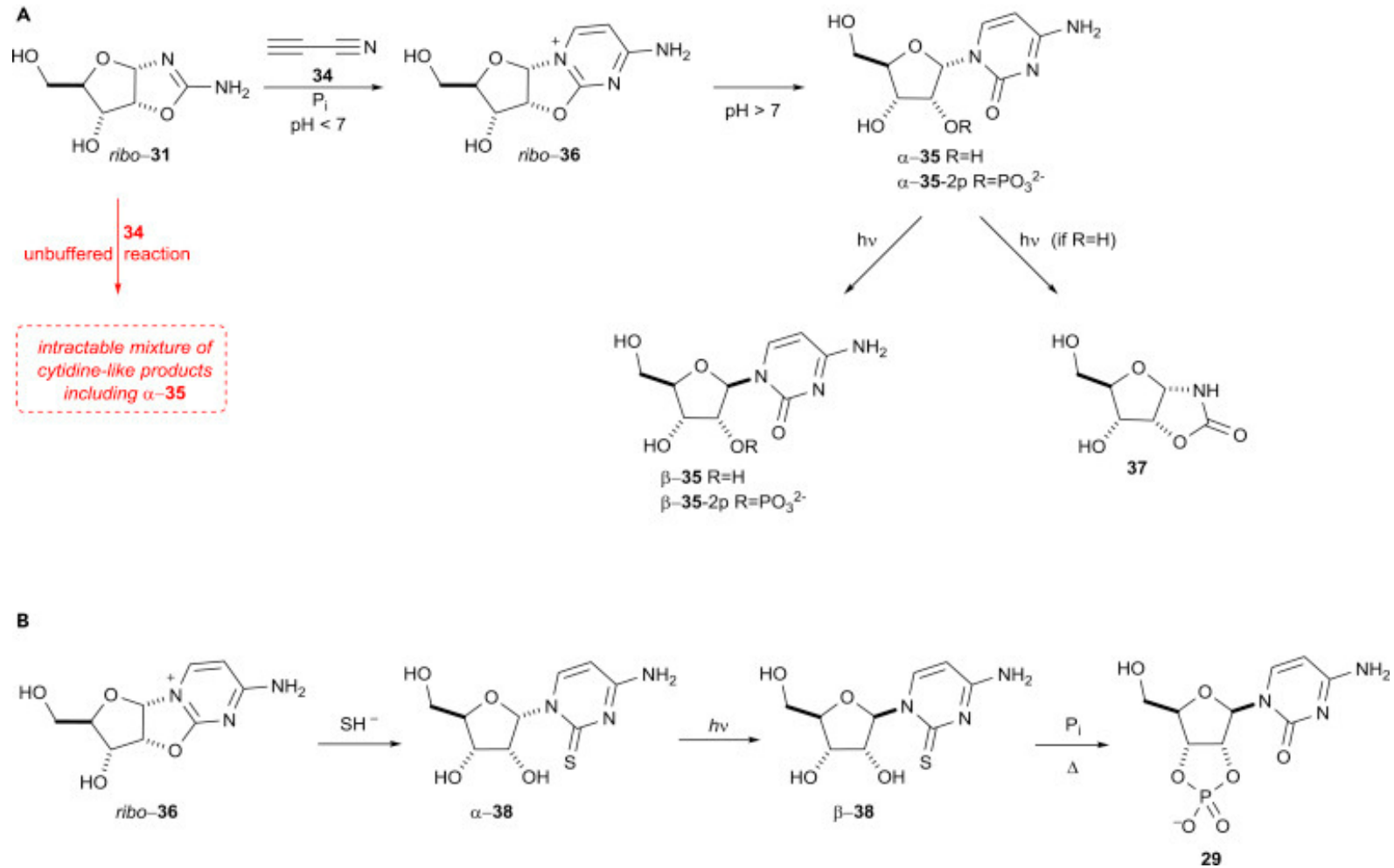
Prebiotic soup - summary

Summary of the Prebiotic Syntheses of the Activated Pyrimidine Ribonucleotides



Prebiotic soup - summary

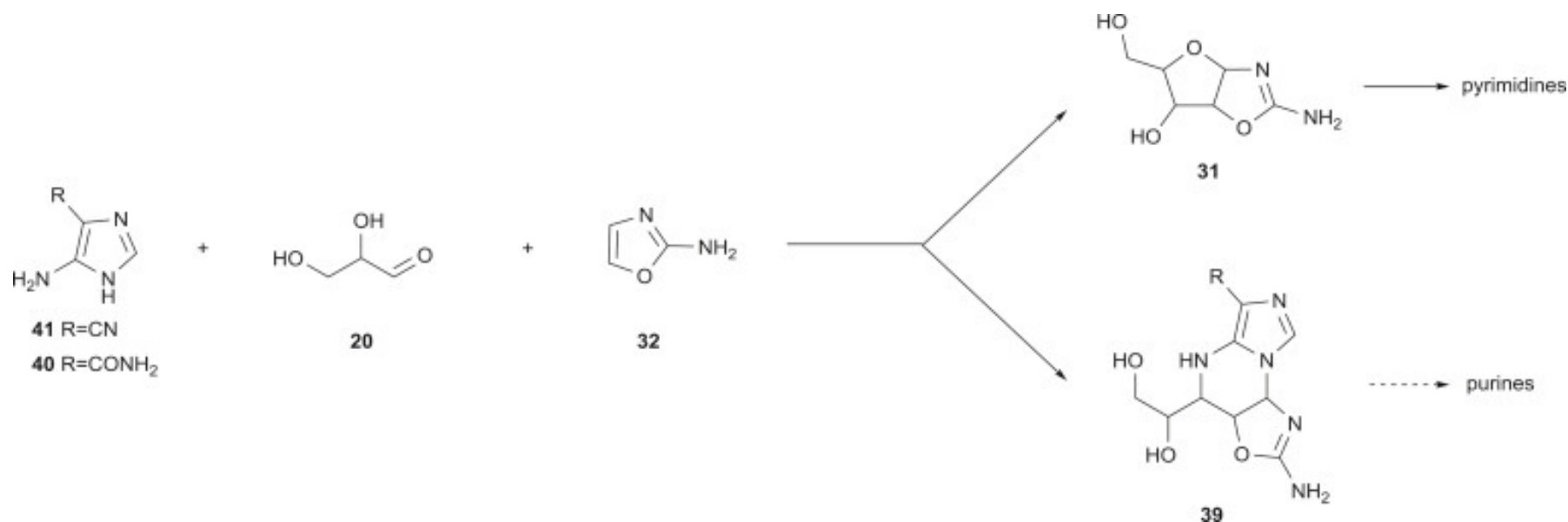
Conversion of Ribose Aminooxazoline to Activated Pyrimidine Ribonucleotides



S. Islam, M. W. Powner *Chem* **2017**, *2*, 470-501

Prebiotic soup - summary

Simultaneous pH-Controlled Multicomponent Assembly of Purine and Pyrimidine Nucleotide Precursors



HCN tetramers AICA **40** and AICN **41** participate in a high-yielding pH-dependent three-component reaction with glyceraldehyde **20** and 2-aminooxazole **32**. This produces potential purine ribonucleotide precursors **39**. The Mannich-type reactivity results in N9-purination with absolute regioselectivity. At pH 6–6.5, both purine **39** and pyrimidine **31** ribonucleotide precursors are observed, suggesting that a divergent synthesis of purine and pyrimidine ribonucleotides from within one pool of reagents is an enticing prospect.

S. Islam, M. W. Powner *Chem* **2017**, *2*, 470-501

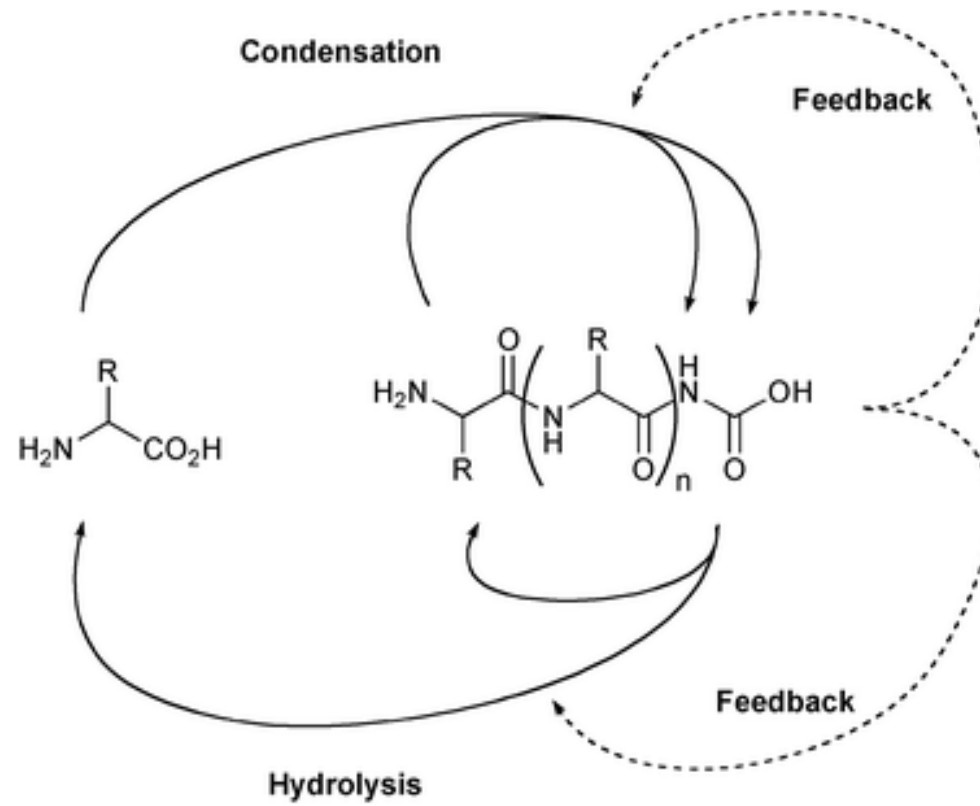
Origin of the Universe – stars, planets, elements

Origin of biorelevant monomers – primordial soup

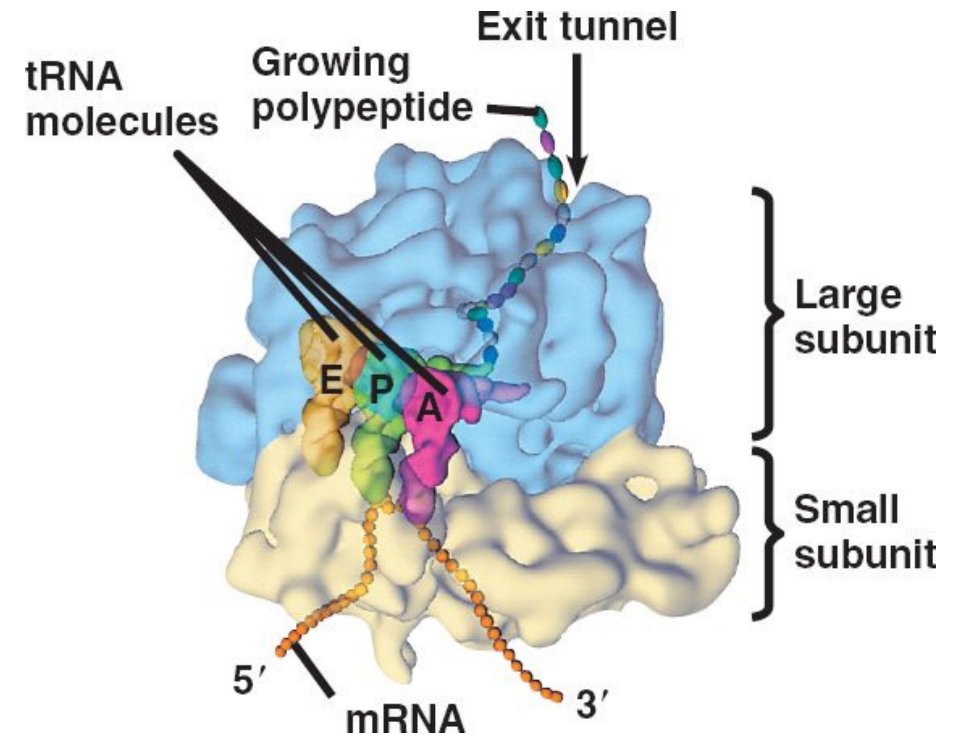
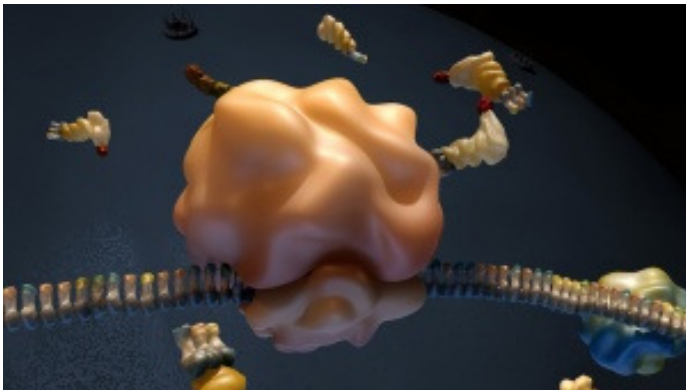
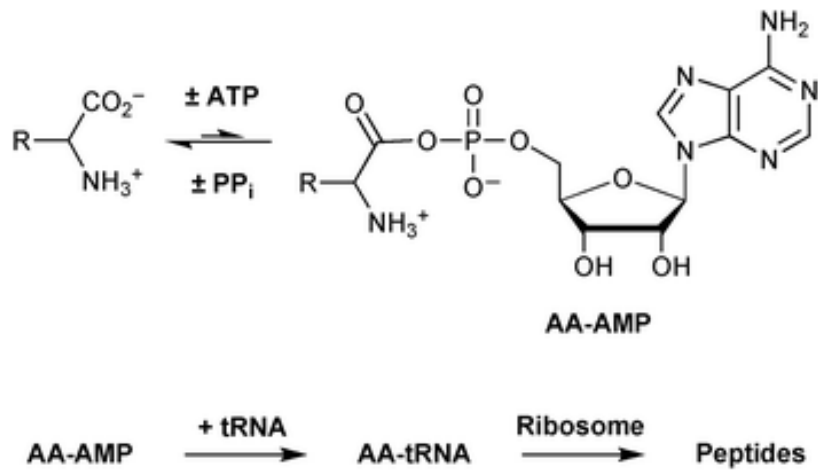
Complex chemical processes on the way to living systems

Protocells and LUCA

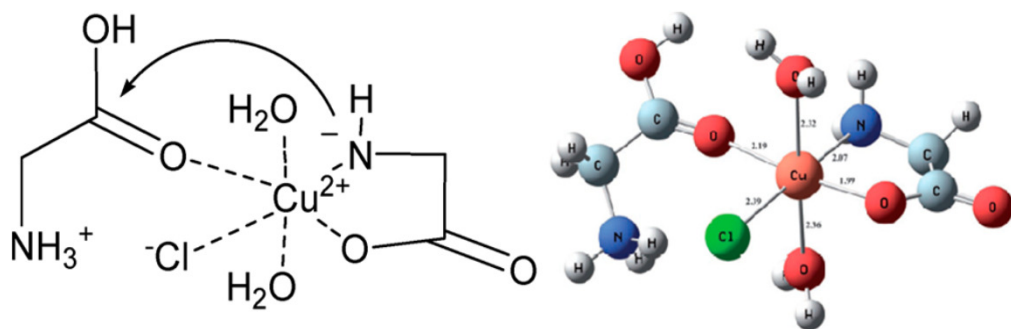
Condensation of aminoacids into peptides



Biochemical condensation of amino acids into peptides



Spontaneous vs. assisted dehydration

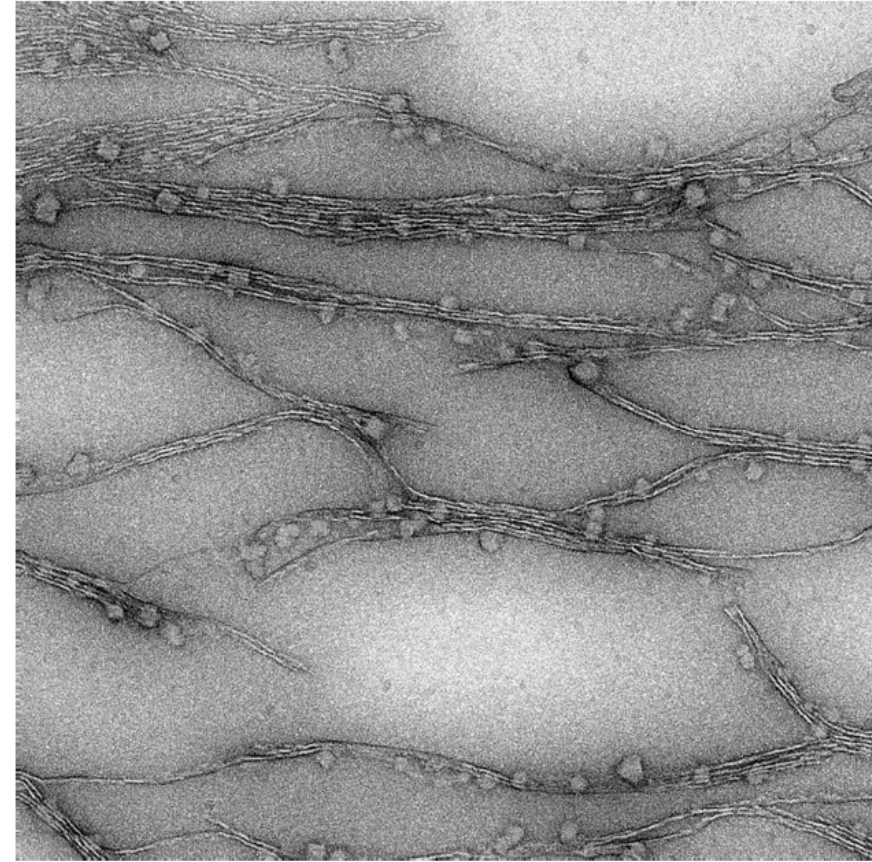
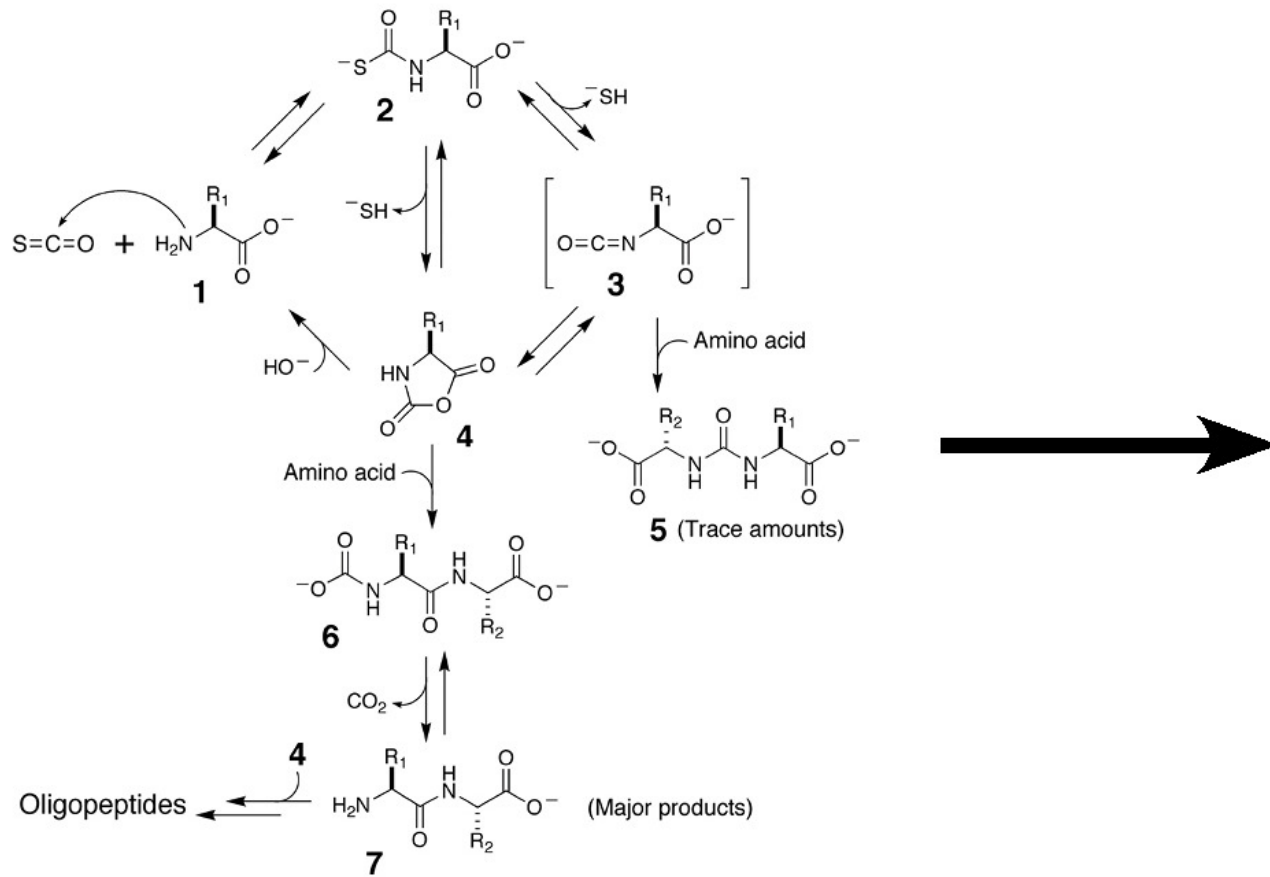


Rode, B. M.; Fitz, D.; Jakschitz, T. *Chem. Biodiversity* **2007**, *4*, 2674.

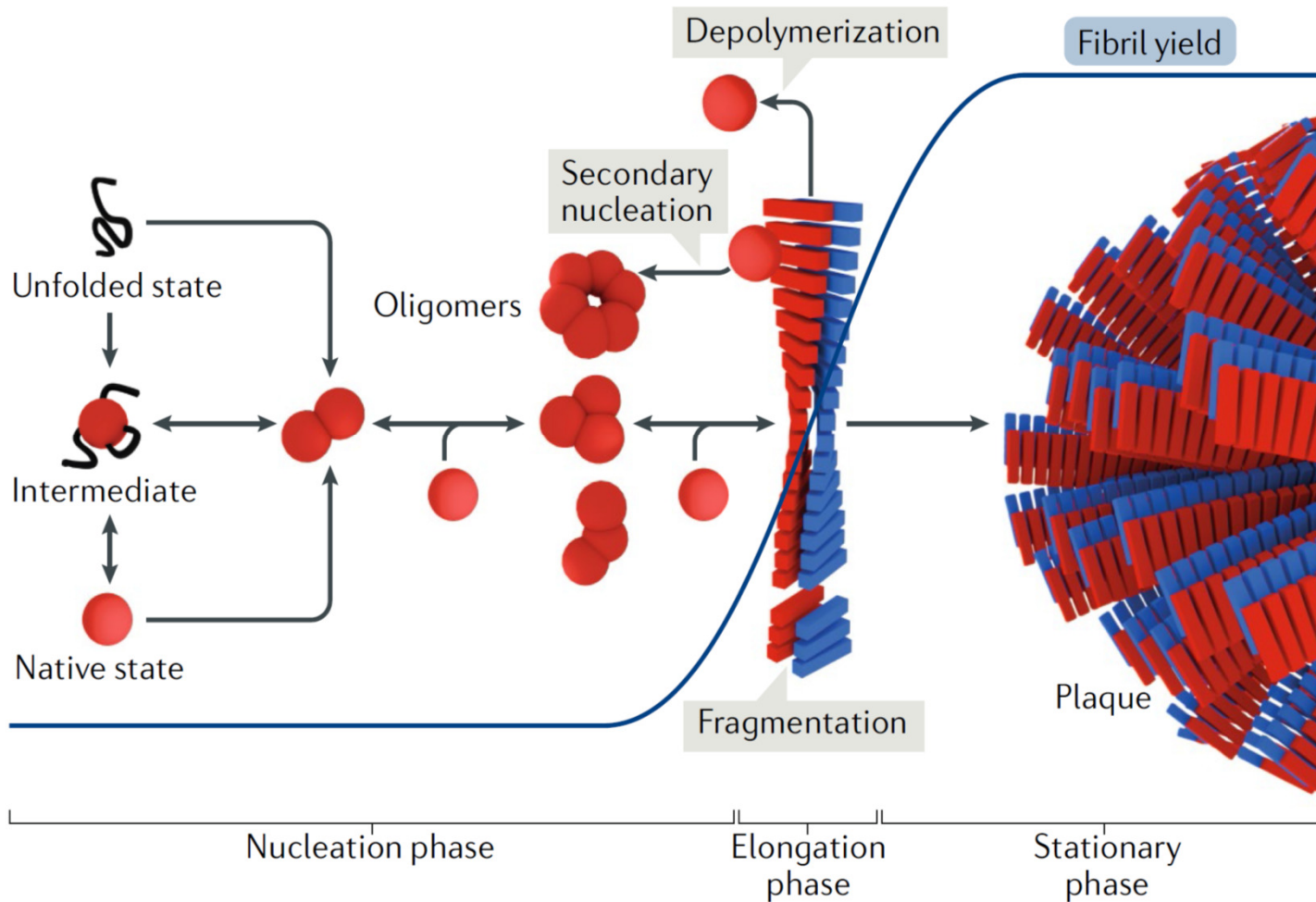
Activating agent	Hydrolysis/ hydration product	ΔG° / kJ mol ⁻¹
NH ₂ CONH ₂	CO ₂ + NH ₃	-16 ^a
COS (g)	CO ₂ + H ₂ S	-17 ^a
Pyrophosphate	Phosphate	-19 ^b
CO (g)	HCO ₂ H	-16 ^a
HNCO	CO ₂ + NH ₃	-54 ^a
HCN	HCO ₂ H + NH ₃	-75 ^a
RCN	RCO ₂ H + NH ₃	-80 ^c
NH ₂ CN	Isourea	-83 ^d
HNCNH	Isourea	-97 ^d
HCCH (g)	CH ₃ CHO	-112 ^a

Danger, G.; Plasson, R.; Pascal, R.
Chem. Soc. Rev. **2012**, *41*, 5416.

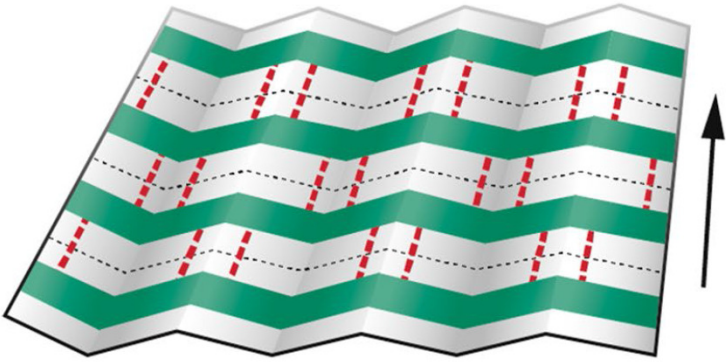
Condensation of amino acids into peptides



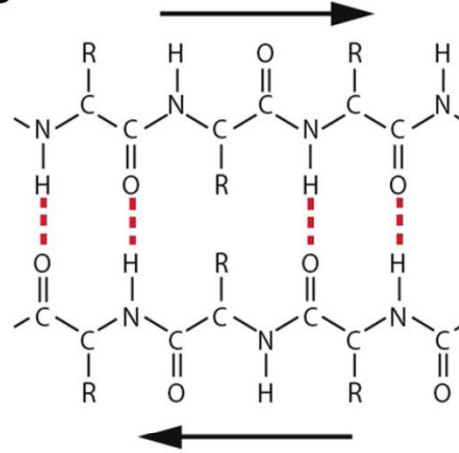
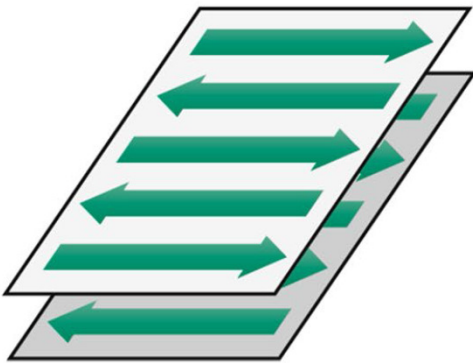
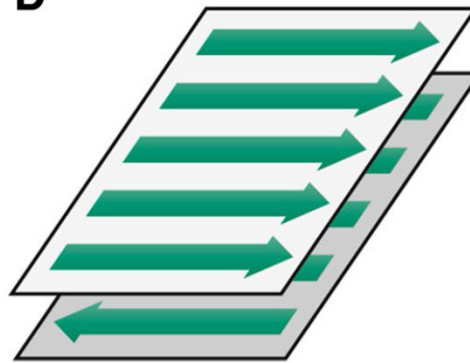
Amyloid world



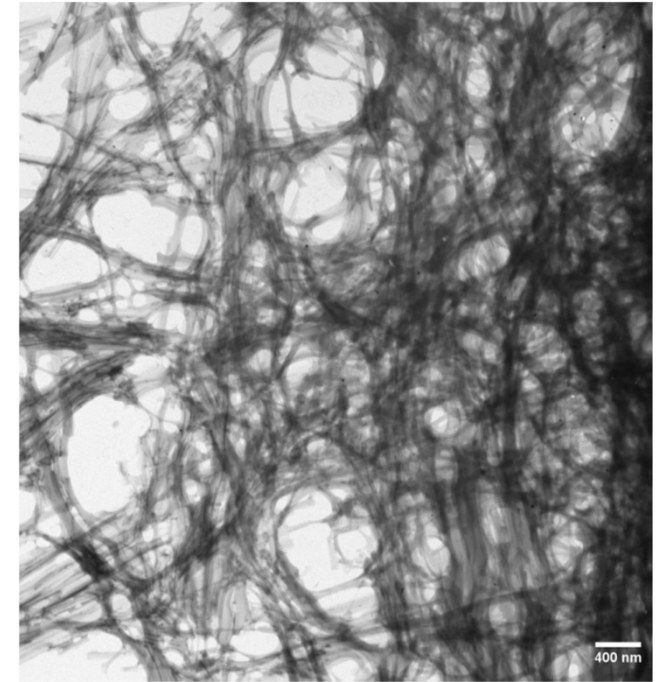
Schematic of amyloid formation. Native proteins are in dynamic equilibrium with their less-structured, partially folded and/or unfolded states. One of these states initiates amyloid fibril formation by assembling into oligomeric species. Oligomeric species can then assemble further to form higher-order oligomers, one or more of which can form a fibril nucleus, which, by rapidly recruiting other monomers, can nucleate assembly into amyloid fibrils.

A

Amyloid world

B**C****D**

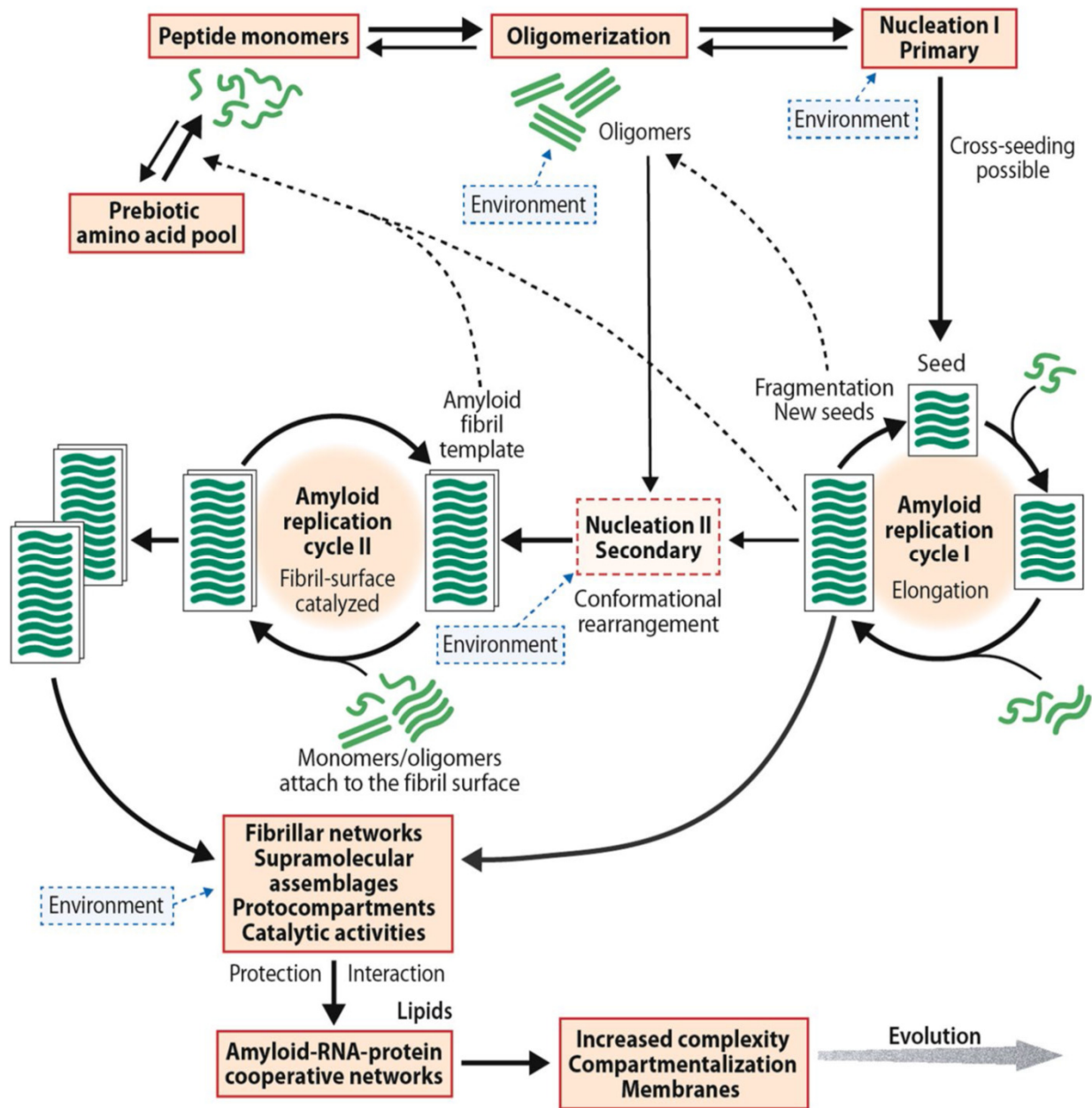
Typically, the repeating unit of the amyloid fibrils consists of two tightly packed layers of β -sheets with side chains within the bilayers forming a dry interdigitating zipper interface.



Electron micrograph of a polymorphic fibrillar amyloid network self-assembled from a prebiotically relevant 9-mer peptide (EGGSVVAAD) in aqueous environment.

Maury CPJ, Liljeström M, Zhao F,
J Biol Res **2012**, *18*, 332–335

C. P. J. Maury *Cellular and Molecular Life Sciences* **2018** *75*, 1499–1507



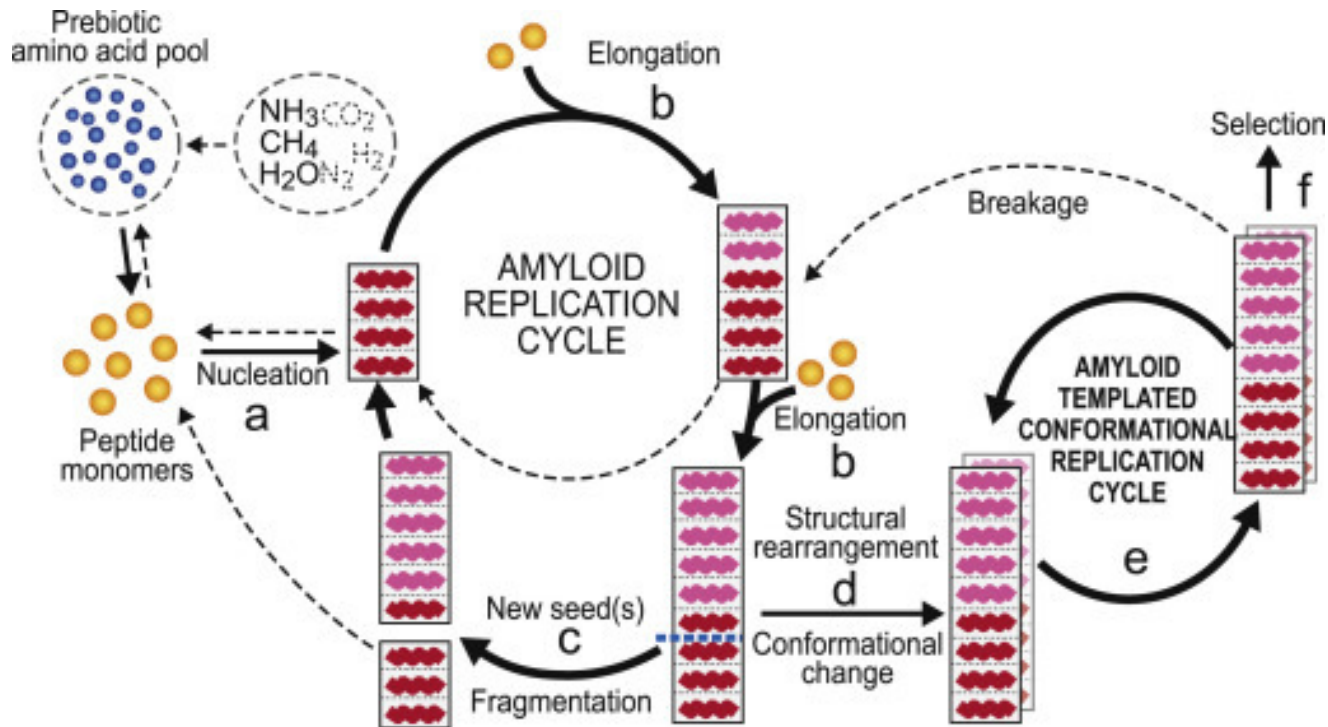
Amyloid world

An initial **slow nucleation** process is followed by a **fast polymerization** phase where peptide monomers are added to the growing end of the protofilament. **Fragmentation** generates new seeds that can initiate **repeated replication cycles**. The same peptide monomer can give rise to different amyloid structures and molecular rearrangements are possible. Specific conformational changes can be replicated in the fibril/protofibril-catalyzed cycle II. Amyloid is also able to **direct the synthesis of its own constituent peptides**. The β -sheet conformers and ribonucleotides interact dynamically and cooperatively, and the amyloid-based supramolecular fibrillar assemblies can function as a primitive metabolic apparatus catalyzing the formation metabolite precursors.

C. P. J. Maury *Cellular and Molecular Life Sciences* 2018 75, 1499–1507

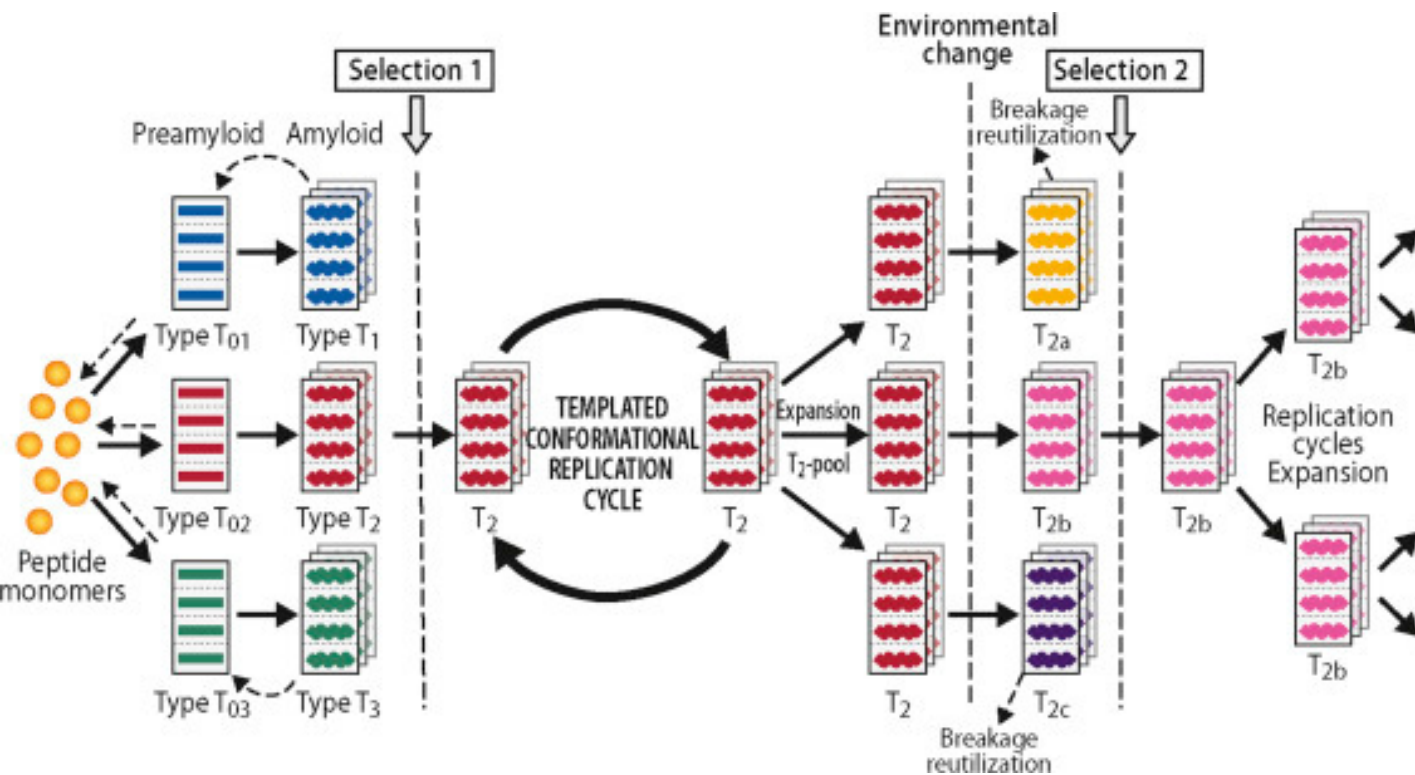
Amyloid world

Schematic representation of the self-replicating cycles of amyloid.



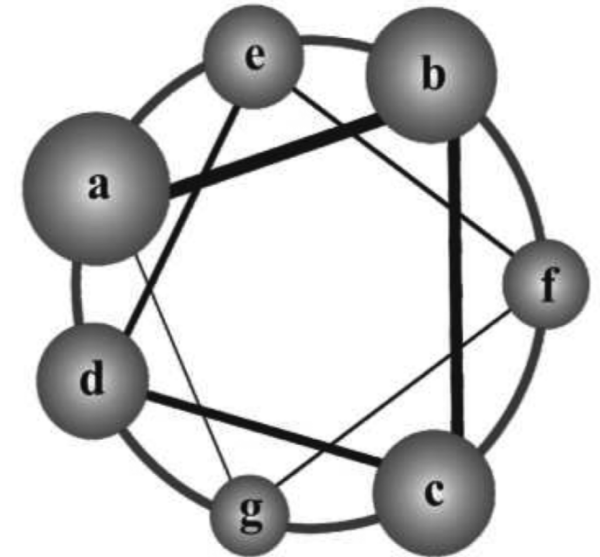
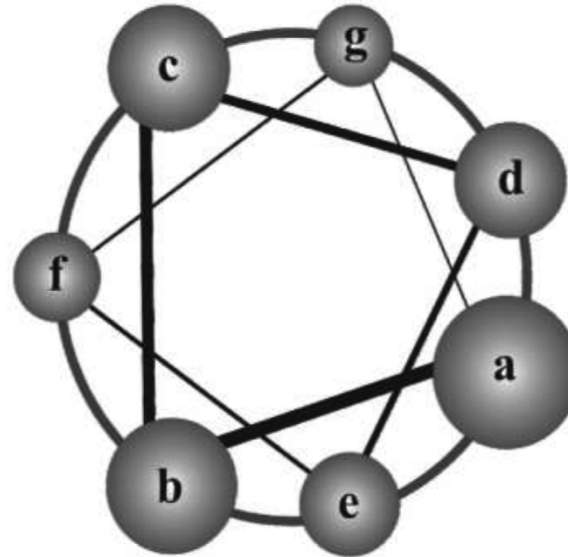
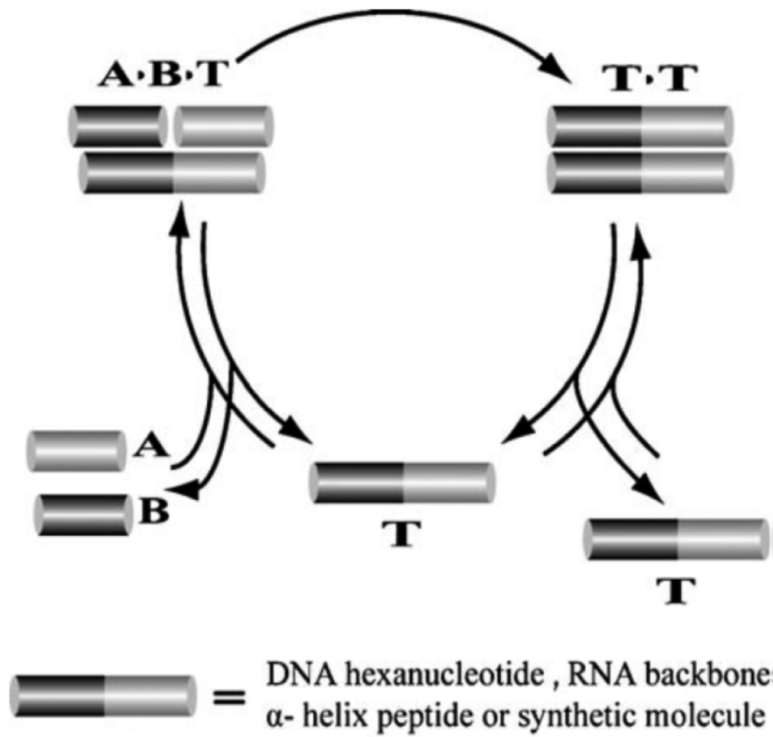
An initial **slow nucleation phase (a)** is followed by a kinetically **fast elongation phase (b)** where monomers (or oligomers) are added sequentially to the growing end of the protofibril. **Breakage** of the fiber results in **new seeds (c)** and repeated replication cycles. Importantly, molecular **rearrangements** and conformational changes in amyloid may occur (**d**) that, by a **templated conformational replication mechanism (e)**, can faithfully be transmitted to other amyloid conformers. The pool of the environmentally fittest variant(s) then **expands (f)**.

The amyloid world model

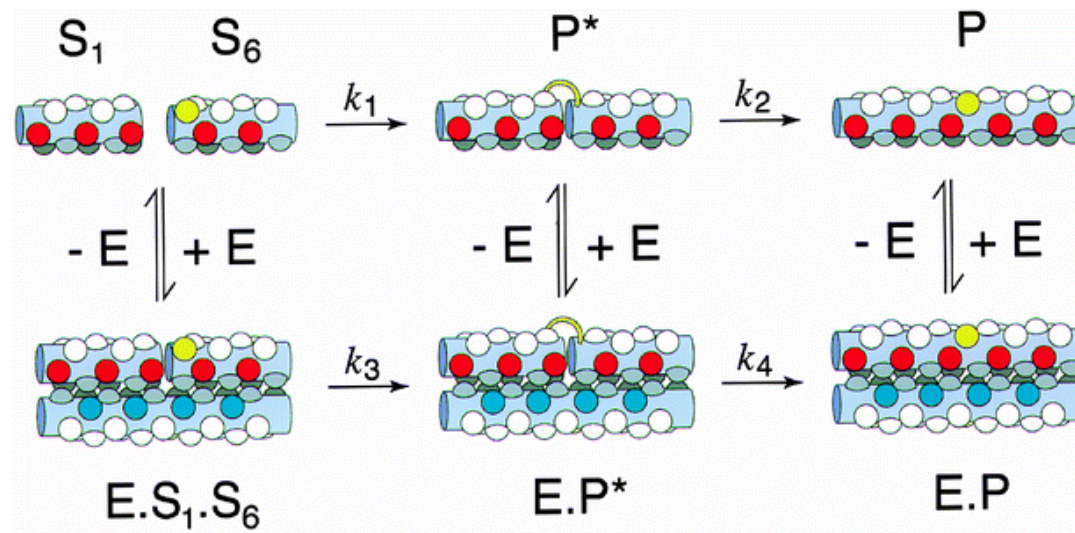


From one type of prebiotic peptide monomer a spectrum of amyloid conformers may be formed (T_1 , T_2 , T_3). By templated conformational replication, the pool of the environmentally fittest type (T_2 , Selection 1) rapidly expands. A change in the environment (e.g., pH, temperature, radiation) induces conformational changes in T_2 (T_{2a} , T_{2b} , T_{2c}). The fittest conformer (T_{2b}) is selected (Selection 2) and undergoes templated conformational replication cycles expanding the (T_{2b}) pool. The environmentally less suitable variants are decomposed and recycled. The environment-induced variations in the amyloid conformations combined with faithful replication of the selected amyloid conformers (variants) and repeated selection cycles allow evolution to occur.

Peptide self-replication



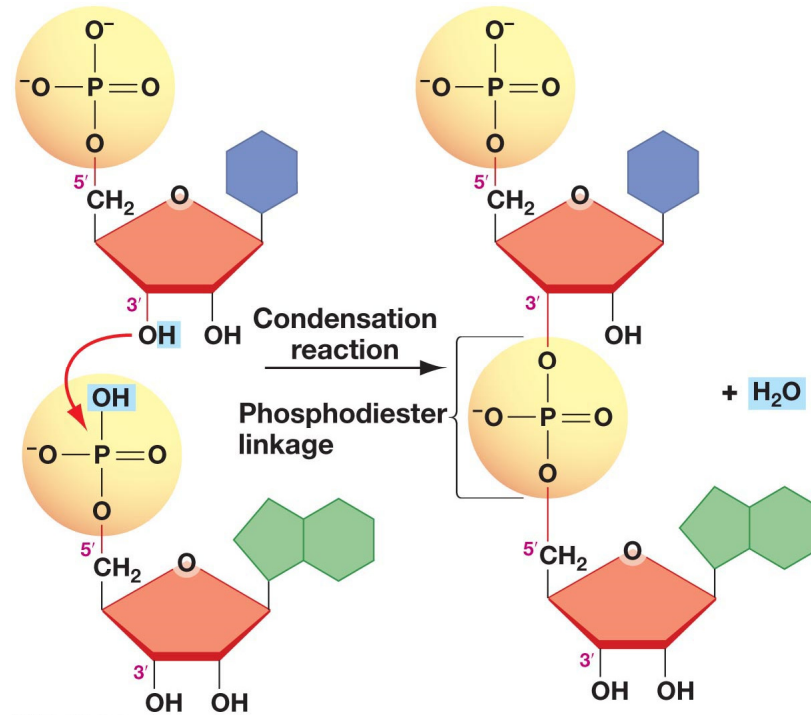
Peptide self-replication



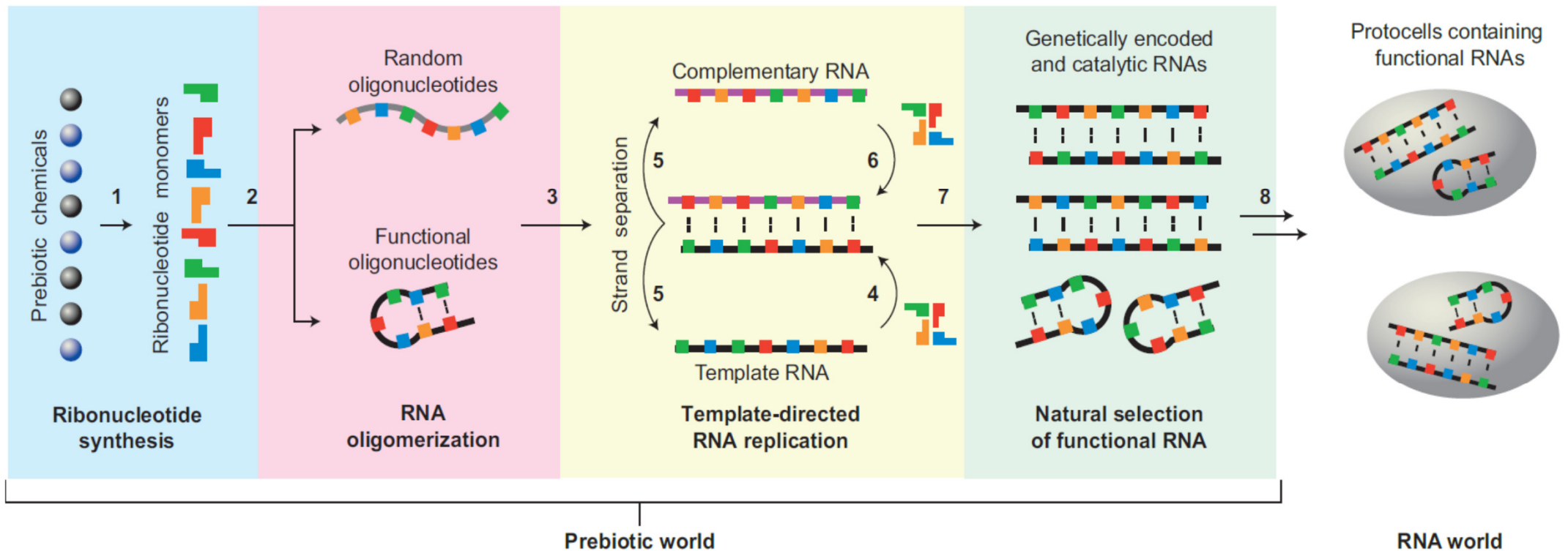
K. Severin, D. H. Lee, A. J. Kennan and M. Reza Ghadiri *Nature* **1997**, *389*, 706-709

Nucleotide polymerization

Regioselective formation of 3'-5' phosphodiester bonds between nucleotides

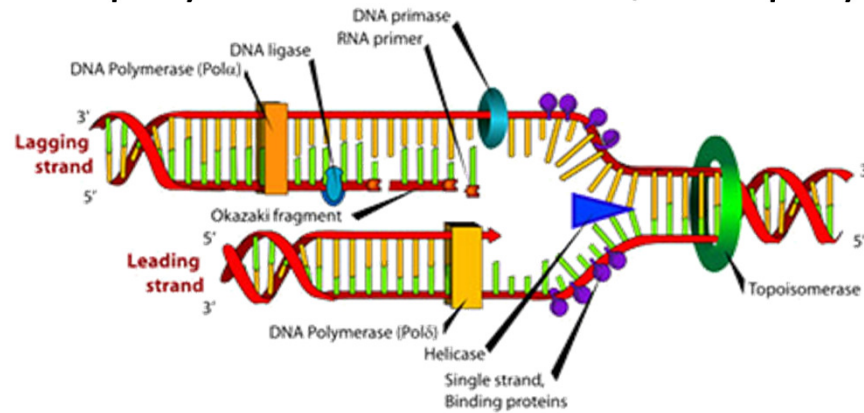


Nucleotide polymerization – sequence control

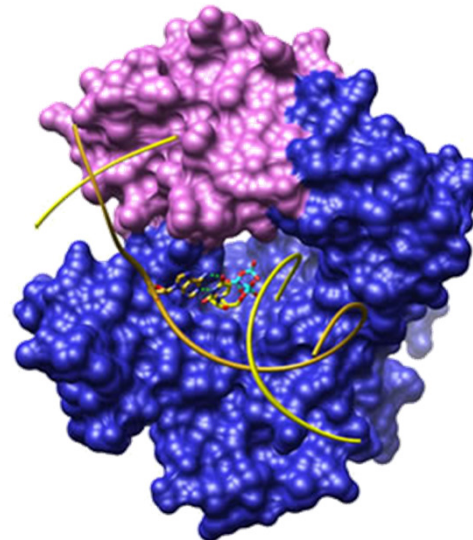
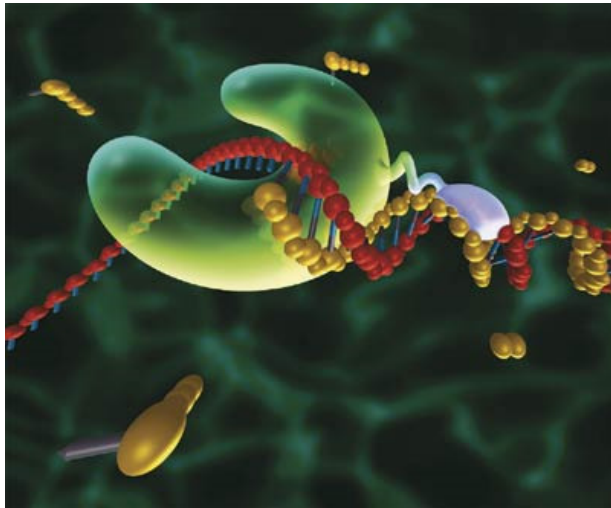


Vital chemical reactions

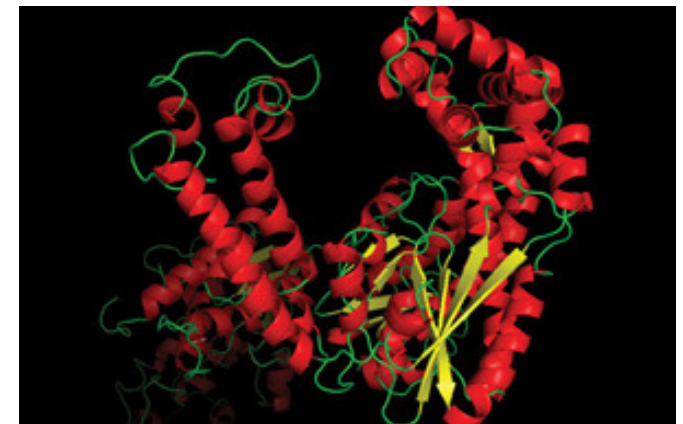
nucleotide polymerization → DNA/RNA polymerases



dxline.info/img/new_ail/dna-polymerase_1.jpg



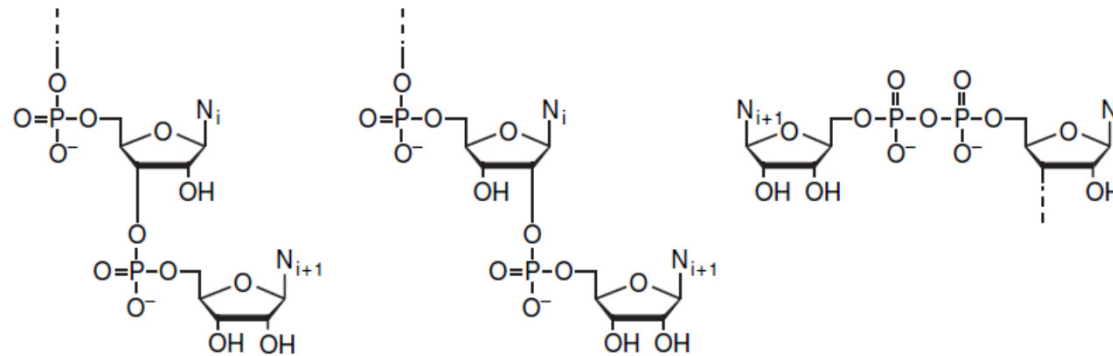
niehs.nih.gov



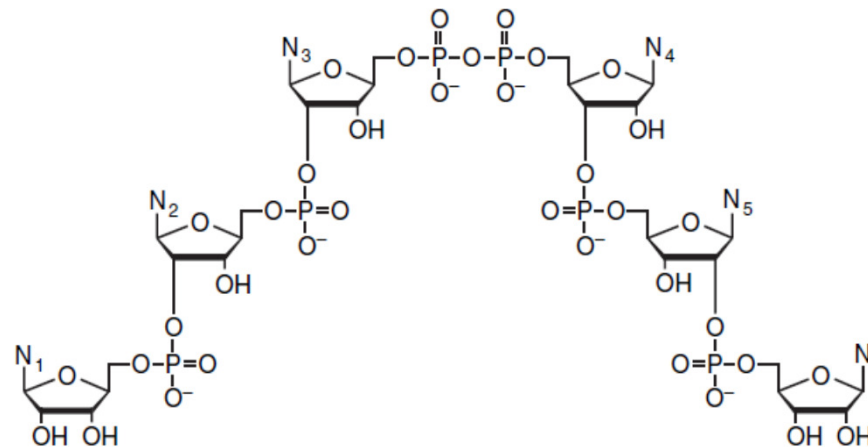
www.neb.com

Products of chemical condensation of nucleotides

A



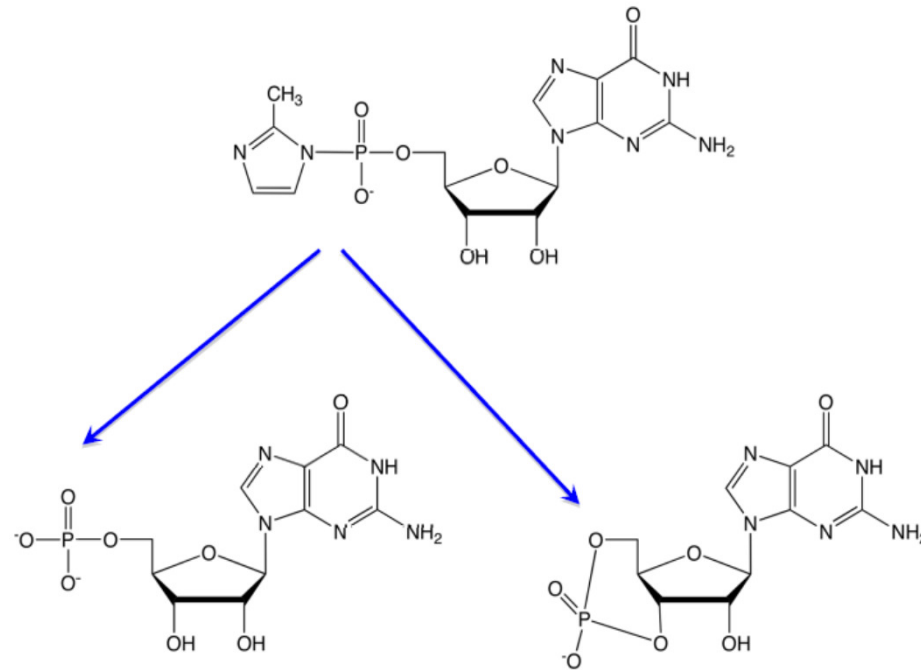
B



(A) Reaction of an activated mononucleotide (N_{i+1}) with an oligonucleotide (N_1-N_i) to form a 3',5'-phosphodiester (left), 2',5'-phosphodiester (middle), or 5',5'-pyrophosphate linkage (right).

(B) Typical oligomeric product resulting from chemical condensation of activated mononucleotides

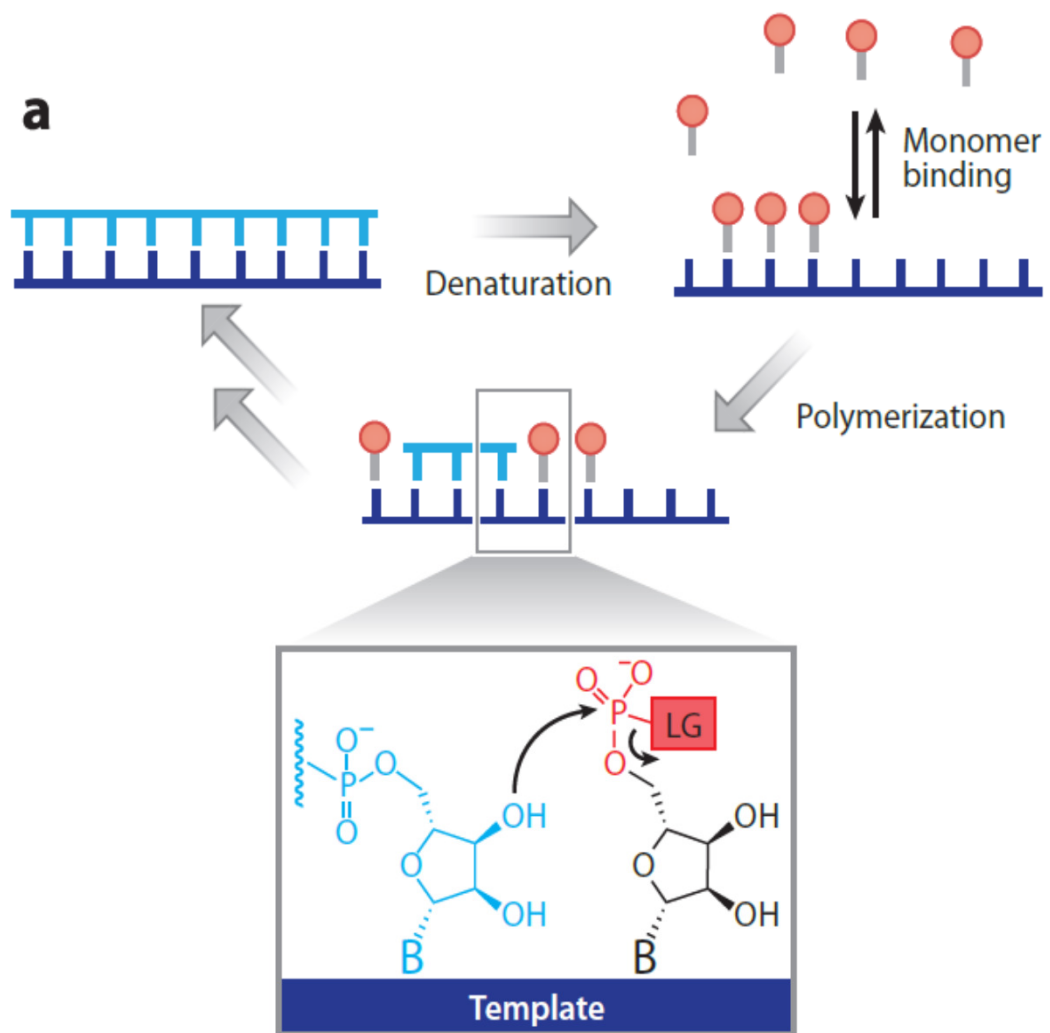
Degradation of activated nucleotides



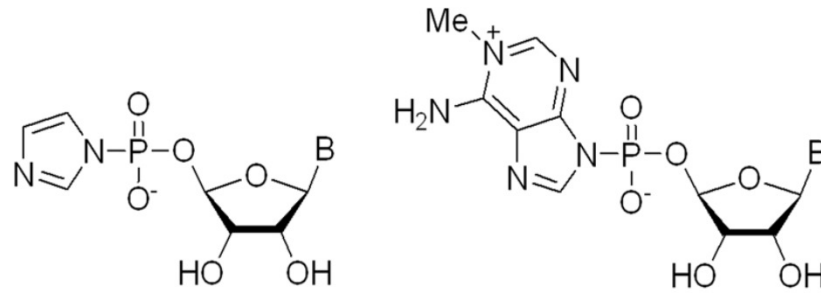
hydrolysis

3',5'-cyclization

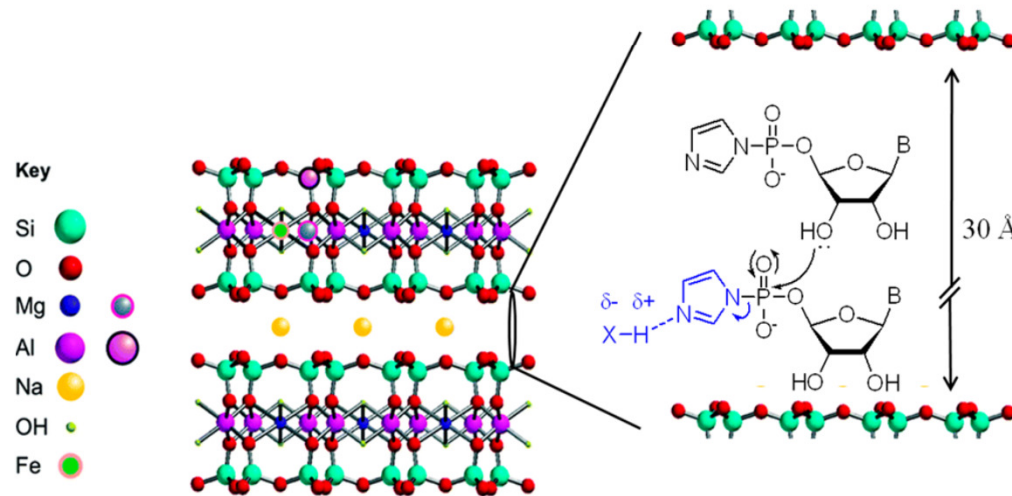
Template-directed synthesis



Montmorillonite



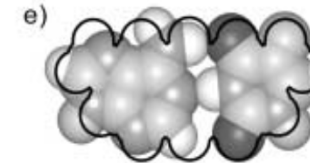
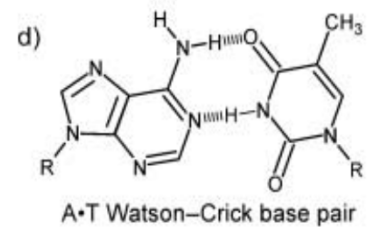
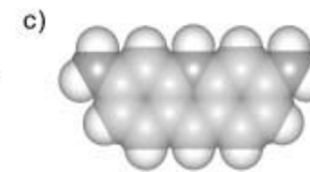
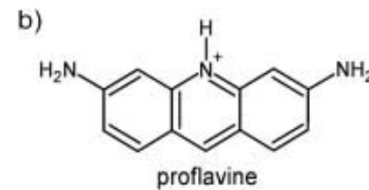
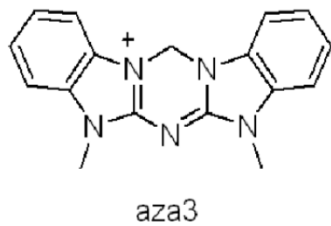
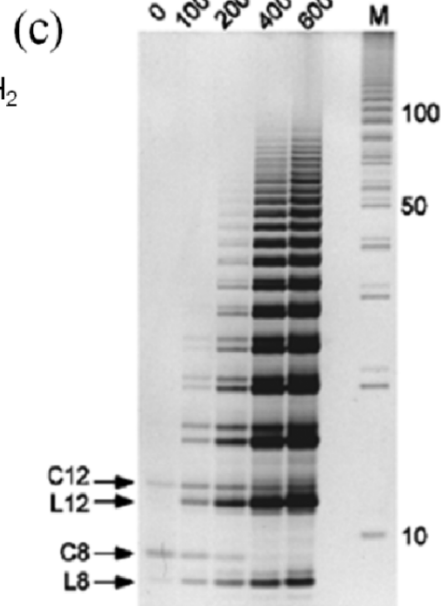
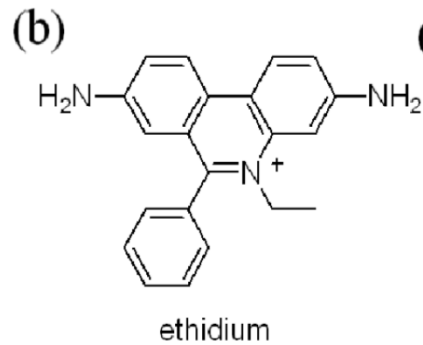
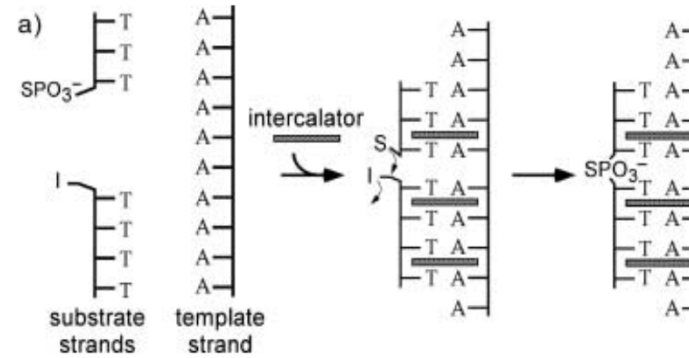
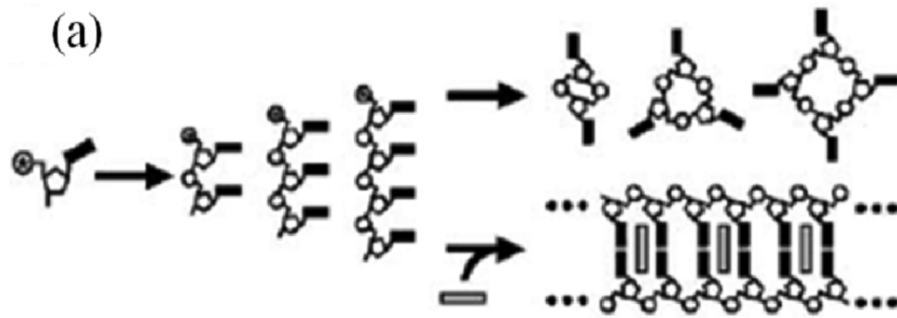
B = adenine, guanine, cytosine or uracil



30-50 units successfully oligomerized

(Top) Structure of ribonucleotide 5'-phosphoimidazolides (left) and ribonucleotide 5'-phosphoro-1-methyladeninium (right). (Bottom) Unit cell of montmorillonite and phosphodiester bond formation within the clay interlayers, as proposed by Ferris and coworkers (right). XH, depicted in blue in the cartoon, is any undifferentiated protic species inside the clay galleries. [Joshi, P. C.; Aldersley, M. F.; Delano, J. W.; Ferris, J. P. *J. Am. Chem. Soc.* **2009**, *131*, 13369](#)

Intercalating agents

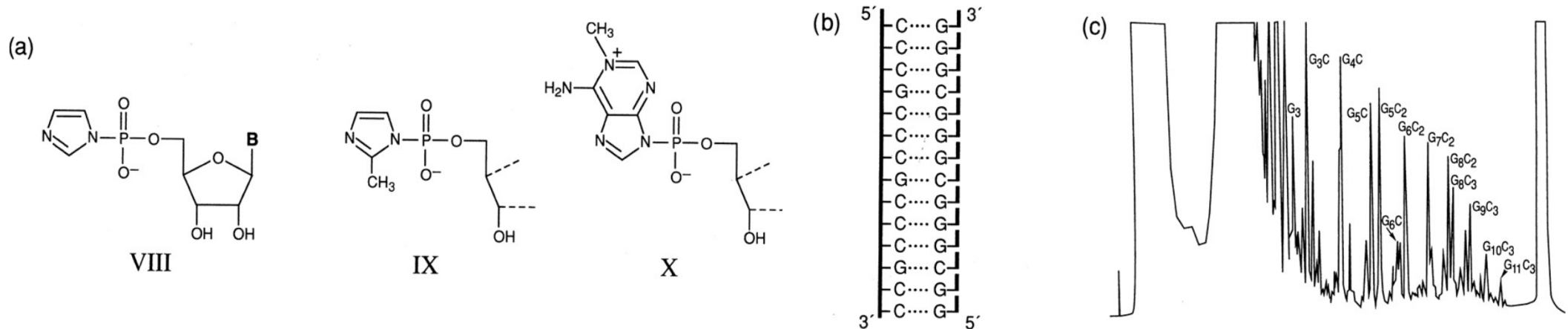


Rate increase by three orders of magnitude vs. ligation without proflavine

N. V. Hud *et al.* *Angew. Chem. Int. Ed.* **2004**, *43*, 2004–2008

Template-directed synthesis

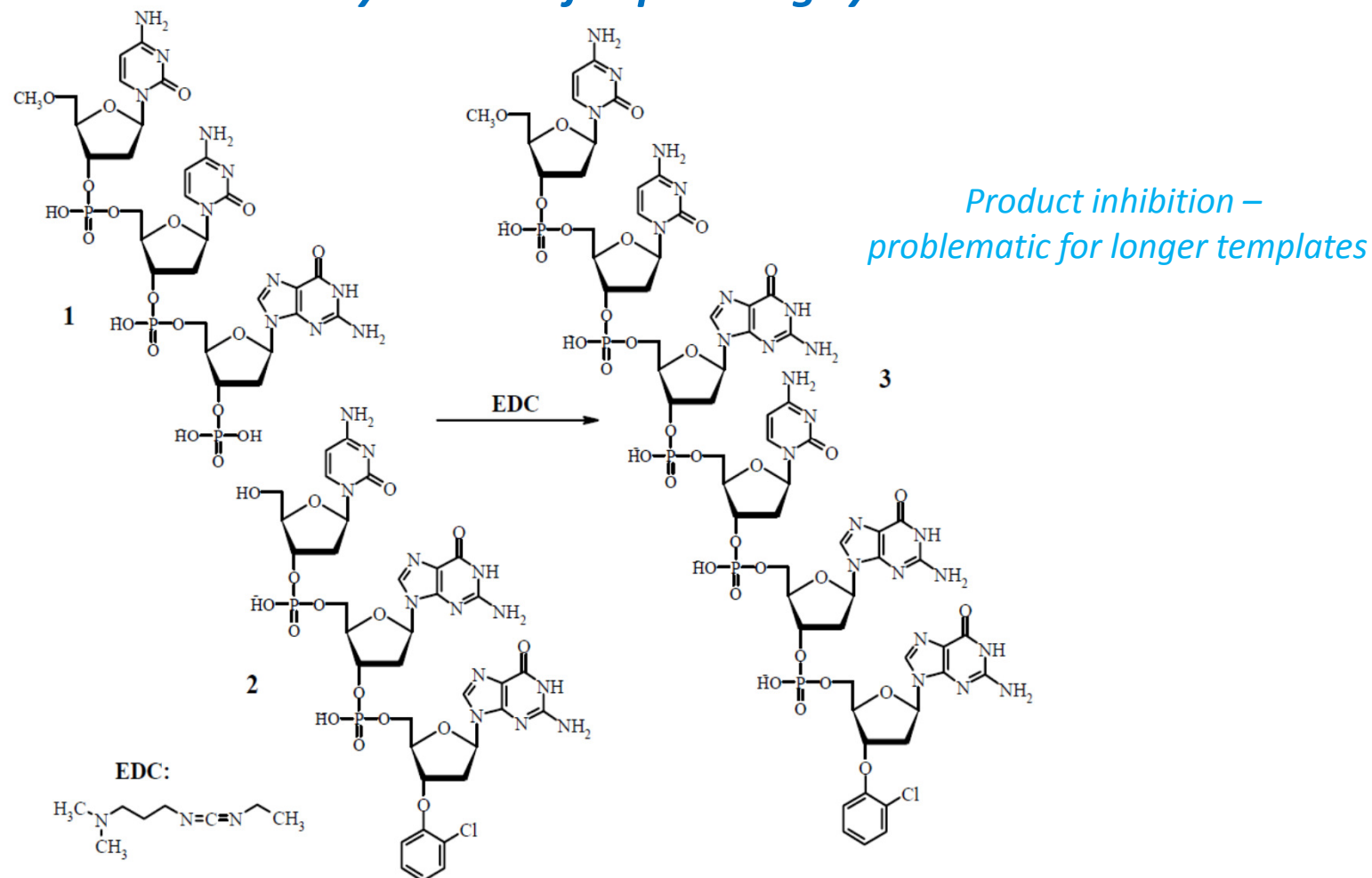
no example demonstrated yet, where single activated nucleotides would form a complementary strand on an RNA (or DNA) template without enzymatic support



Current experiments focus on *primer extension* or *filling abasic sites*— sequence-selective complementary nucleobase addition to a pre-existing strand (or between two pre-existing strands) already hybridized on a template. Here, pre-organization provided by the existing base-pairing network supports selection of the correct nucleoside to be joined.

Complementary approaches are *regioselective ligation reactions* of short oligonucleotides on templates, or *dynamic covalent chemistry*, where nucleobase-containing components would be added sequence-specifically to a pre-existing *empty* backbone on a template

First non-enzymatic self-replicating system

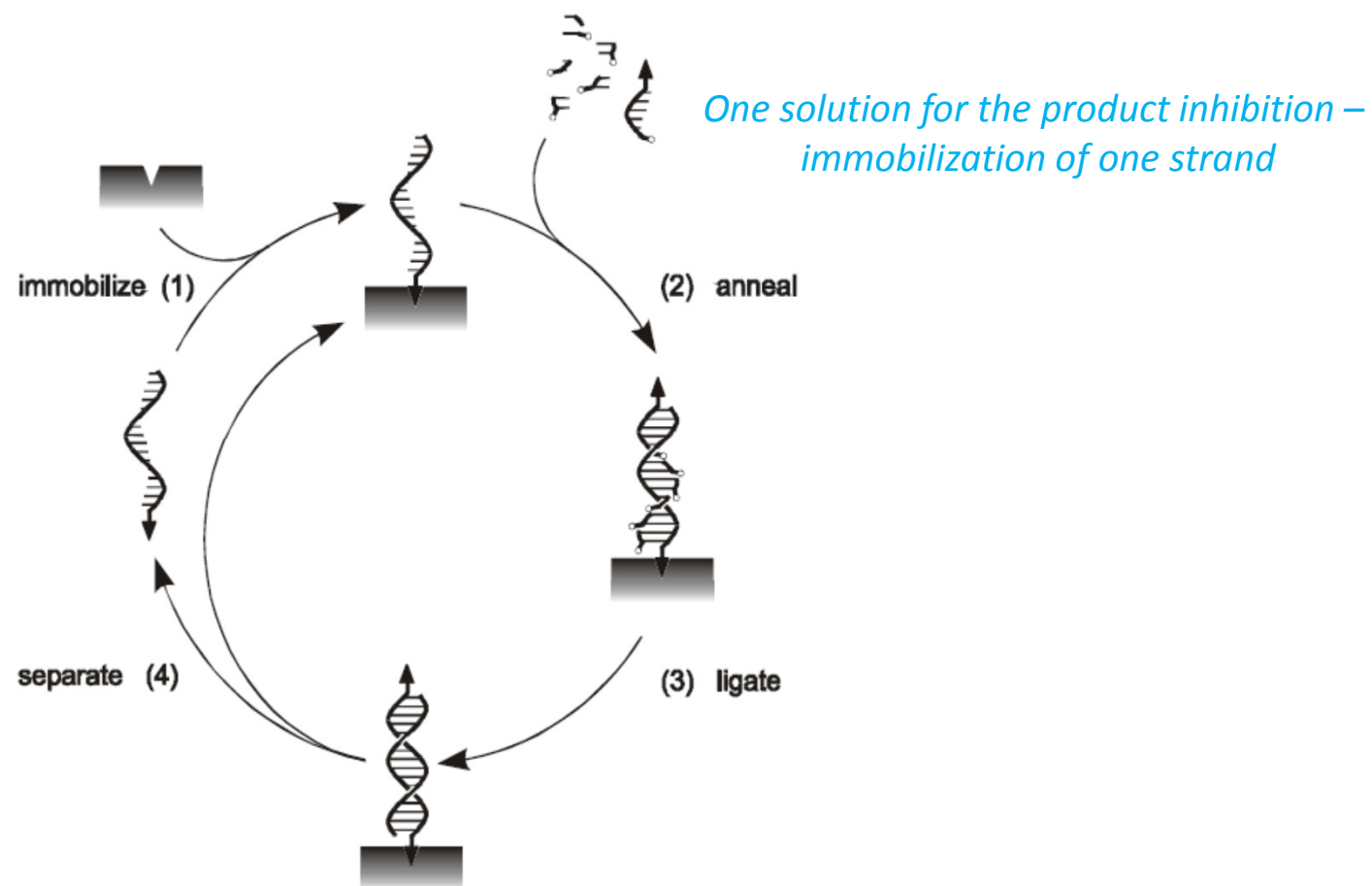


V. Patzke, G. von Kiedrowski *ARKIVOC* **2007** 293-310

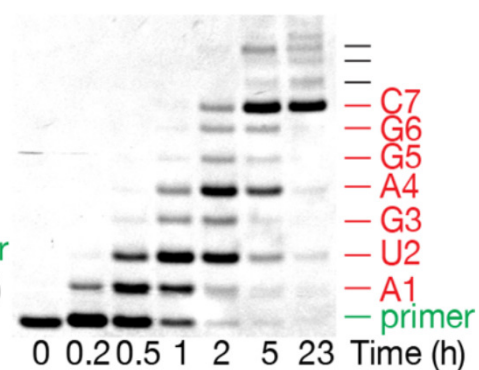
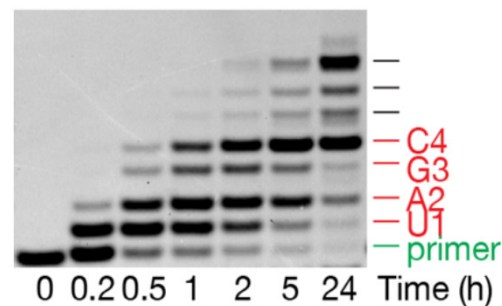
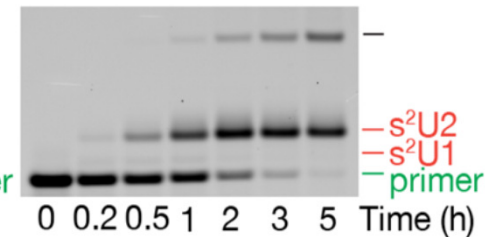
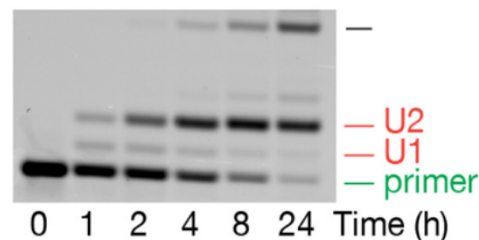
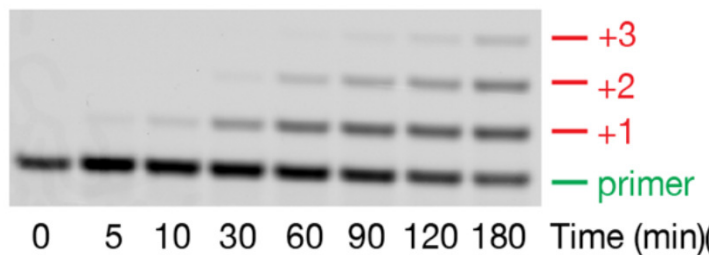
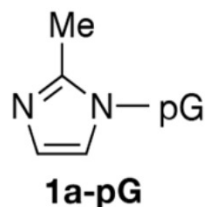
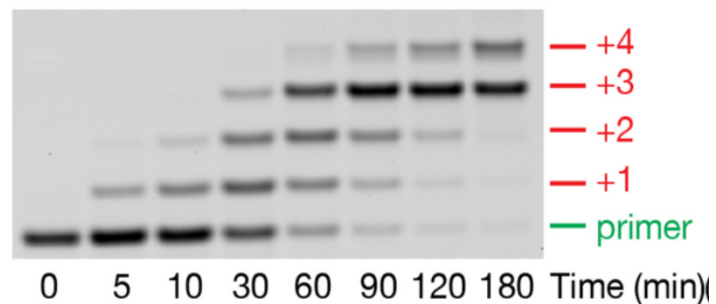
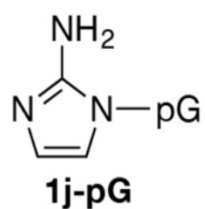
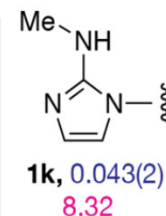
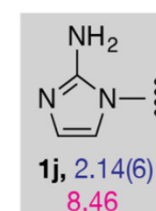
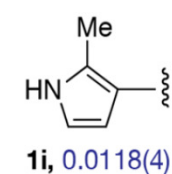
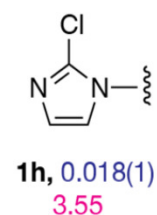
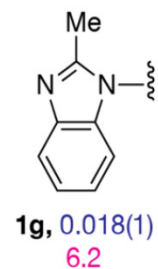
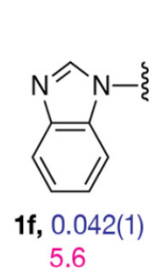
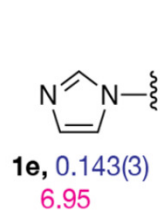
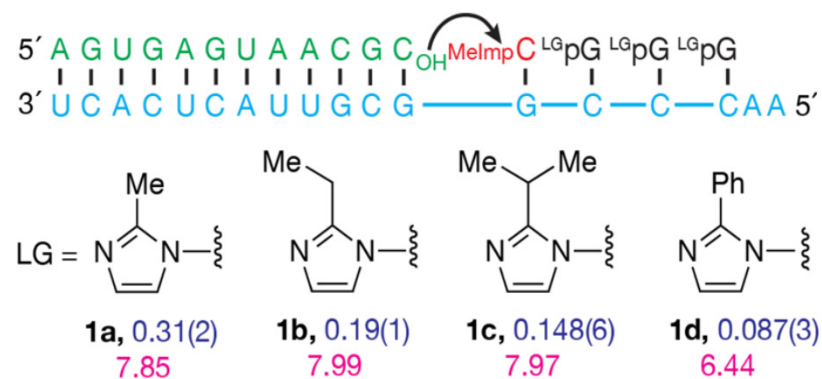
D. Sievers, G. von Kiedrowski *Nature* **1994** 369(6477), 221-224

G. von Kiedrowski *Angewandte Chemie* **1986** 98(10), 932-934

SPREAD – Surface-Promoted Replication and Exponential Amplification of DNA Analogues



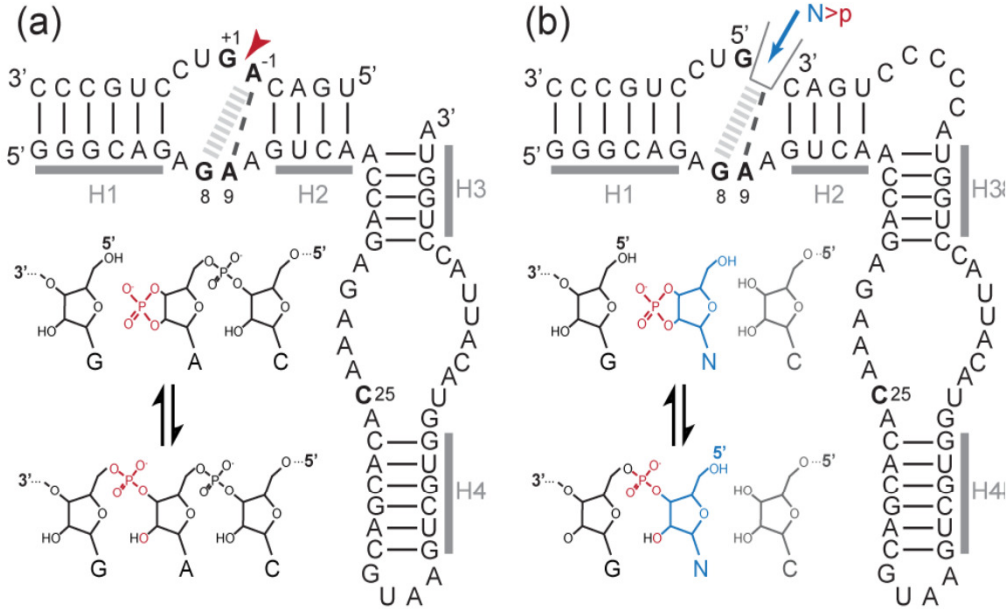
Nonenzymatic primer extension



J. Szostak *et al.* *J. Am. Chem. Soc.* **2017**, *139*, 1810-1813

Ribozyme-catalyzed primer extension

Design of a 5'-nucleotidyl transferase for $N>p$'s.

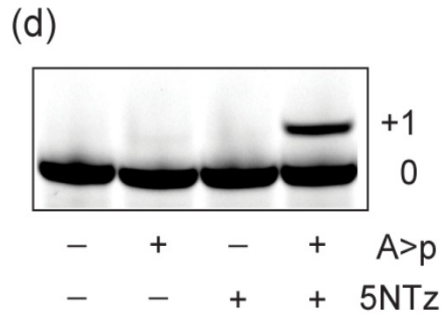
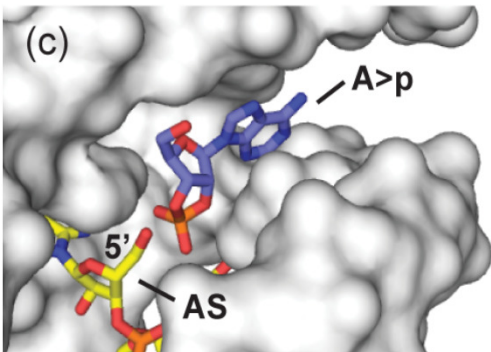


(a) Two-way junction HPz (small hairpin ribozyme), which catalyzes reversible RNA ligation using a 2',3'-cyclic phosphate.

(b) Redesign of HPz into 5NTz (nucleotidyl transferase).

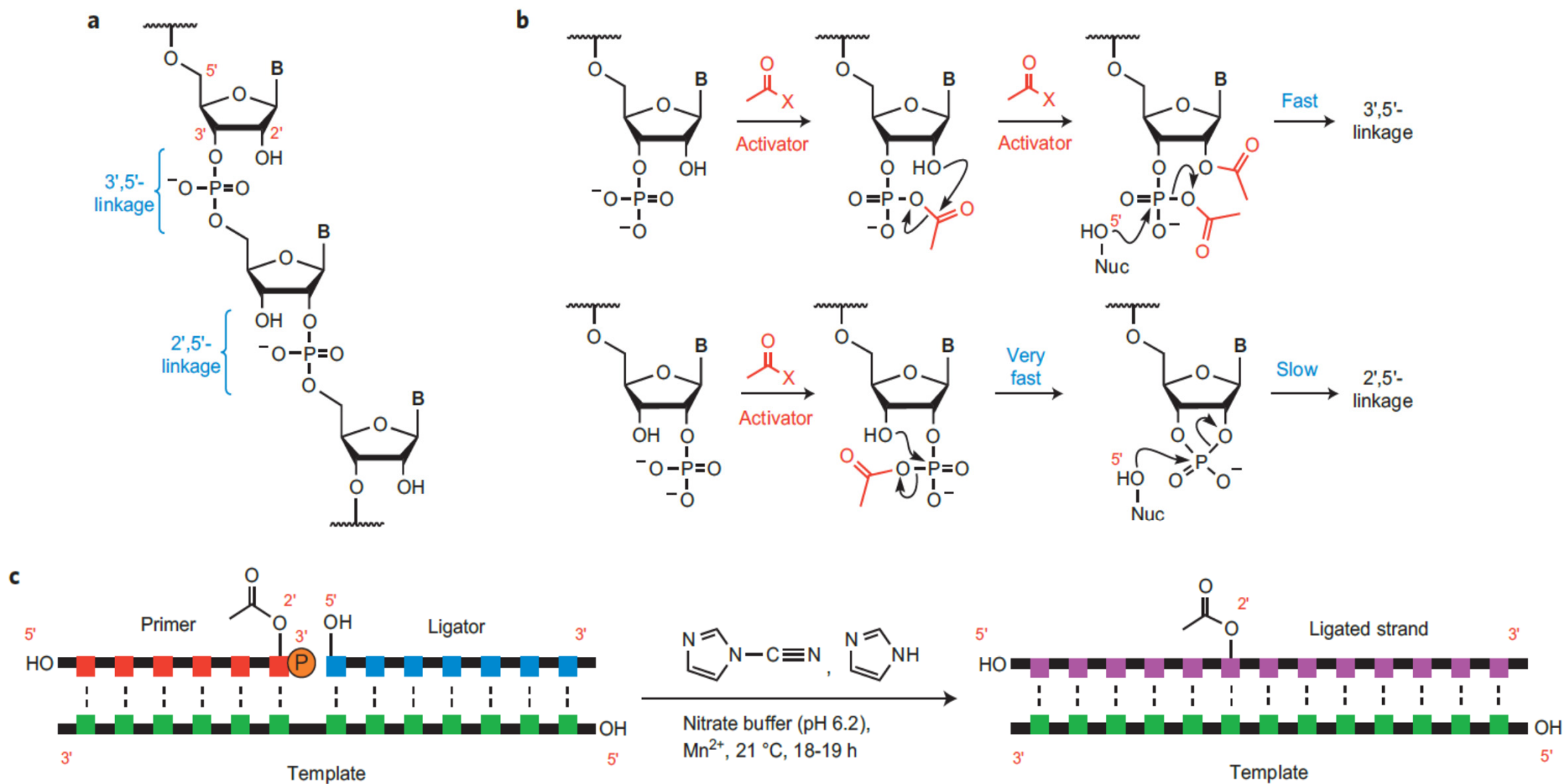
(c) Structural model of the substrate-binding pocket of 5NTz (based on PDB1M5V).

(d) 5NTz catalyzes 5'-adenylation in ice (2 mM $A>p$, 2 μ M 5NTz, 1 μ M 3'-FITC-labeled AS, 72 h in ice at -7 °C).



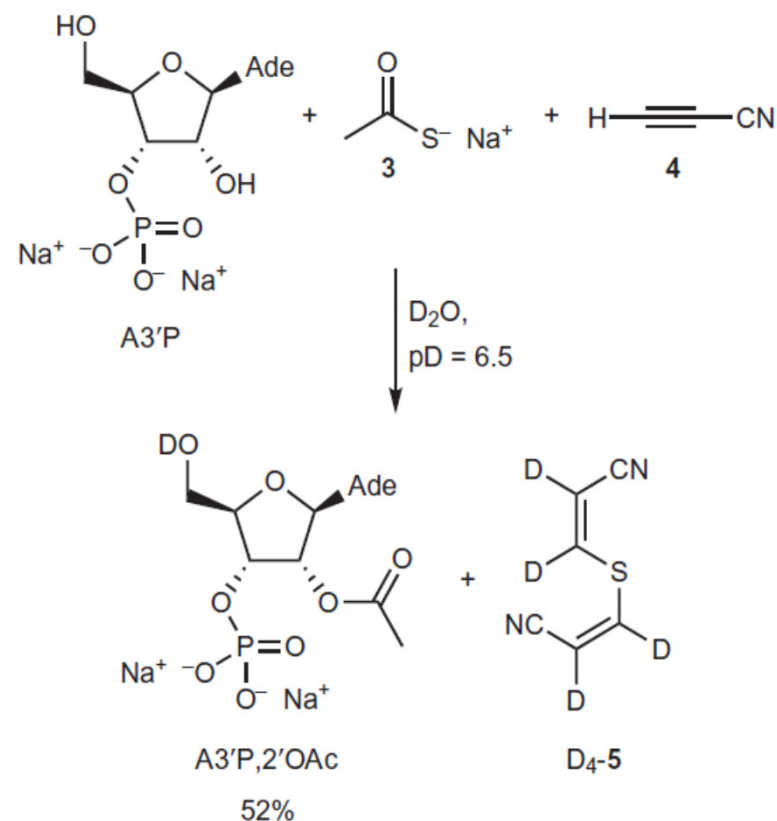
An engineered hairpin ribozyme catalyzes addition of all four $N>p$'s (2',3'-cyclic A-, G-, U-, and CMP) to the 5'-hydroxyl termini of RNA strands (eutectic ice phase formation at -7 °C). 5' addition of 2',3'-cyclic phosphate-activated β -nicotinamide adenine dinucleotide ($NAD>p$), as well as $ACA>p$ RNA trinucleotide, and multiple additions of $GUCCA>p$ RNA pentamers was also observed.

Regioselective ribonucleotide ligation



J. Sutherland *et al.* *Nature Chem.* **2013**, 383-389

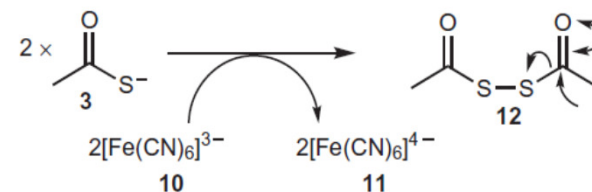
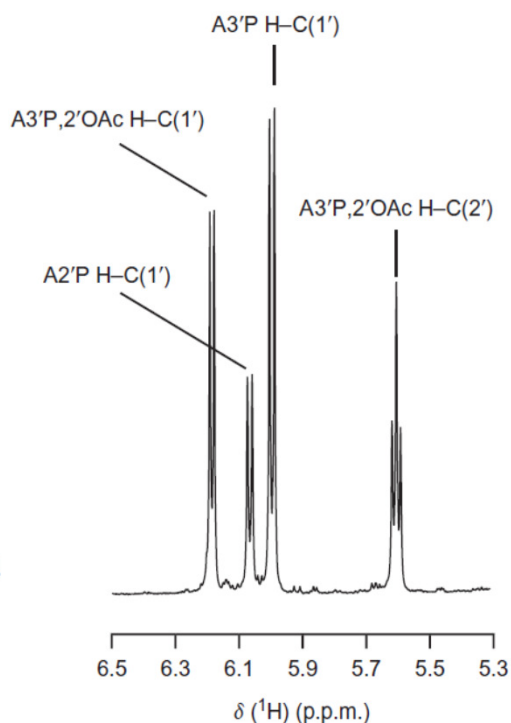
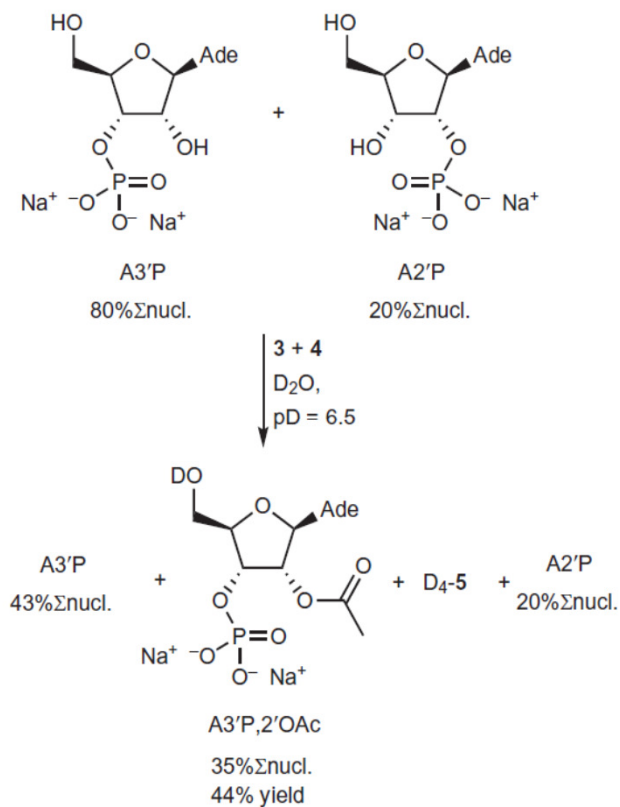
Regioselective ribonucleotide ligation



Treatment of adenosine-3'phosphate (A3'P) (100 mM) with sodium thioacetate **3** (100 mM) and cyanoacetylene **4** (200 mM) in D₂O at neutral pD for 24 hours results in selective acetylation of the 2'-OH group.

J. Sutherland *et al.* *Nature Chem.* **2013**, 383-389

Regioselective ribonucleotide ligation



Additional electrophiles **6–8** shown to drive the acetylation of ribonucleotides with thioacetate **3**.

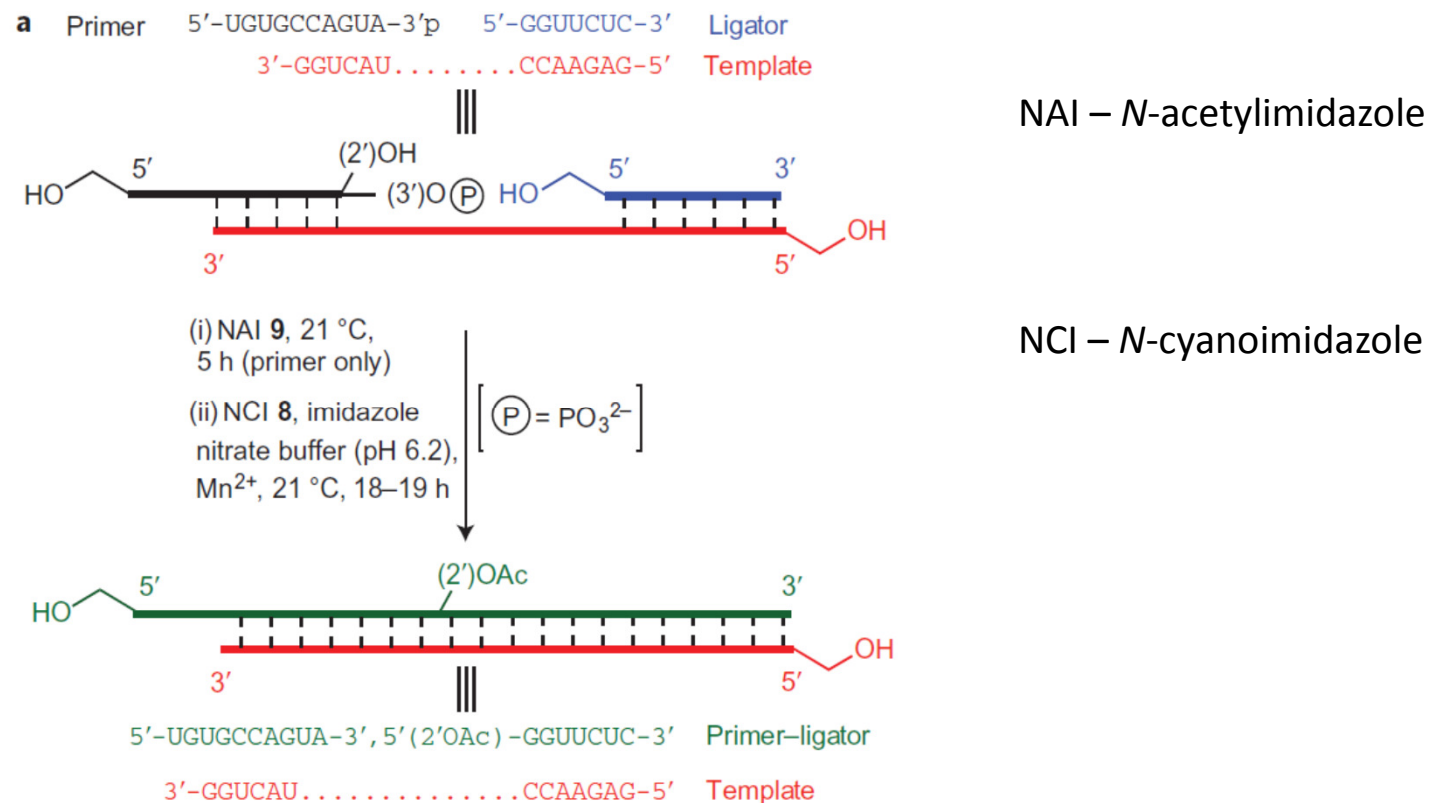
Direct acetylation with **9** is also possible, as is oxidative activation of **3** with ferricyanide **10** to afford ferrocyanide **11** and a dimeric acetylating agent **12**.

Curly arrows indicate electrophilic activation/acetylation steps.

Treatment of **A3'P** (80 mM) and **A2'P** (20 mM) as given before results in the exclusive 2-acetylation of the former nucleotide. Partial ^1H NMR spectrum of the reaction products.

Regioselective ribonucleotide ligation

Chemoselective acetylation of 3'-P-oligoribonucleotides expedites templated ligation

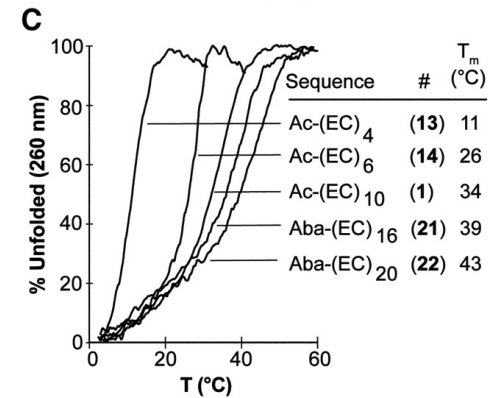
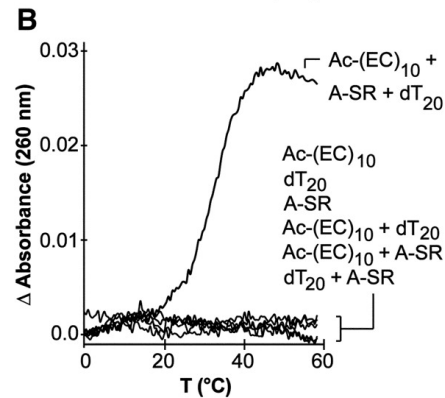
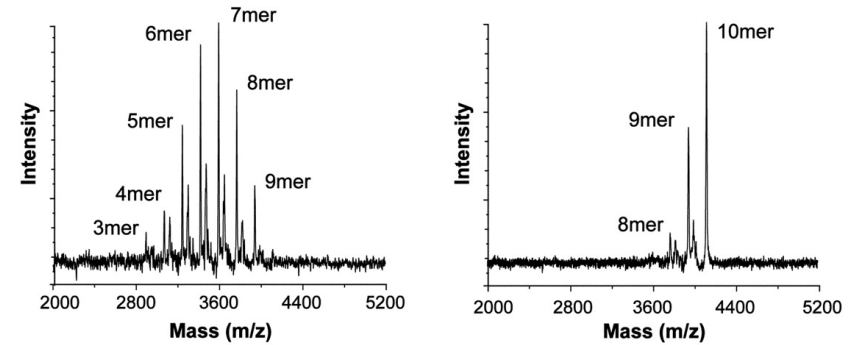
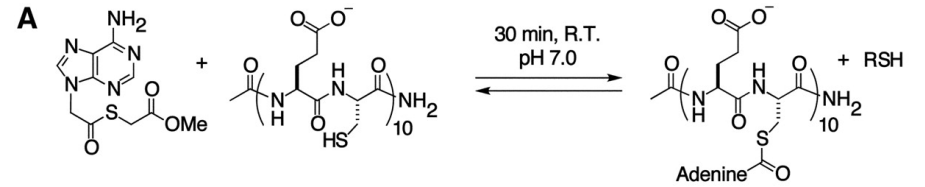
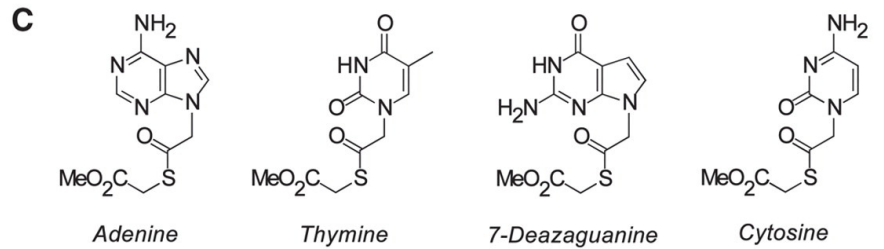
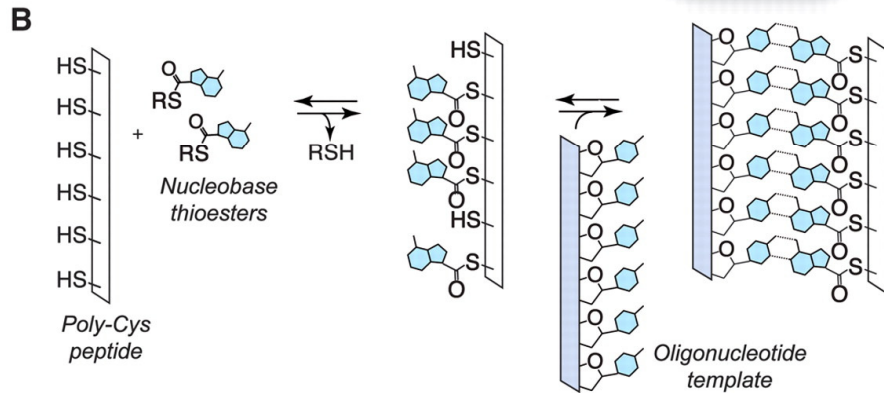
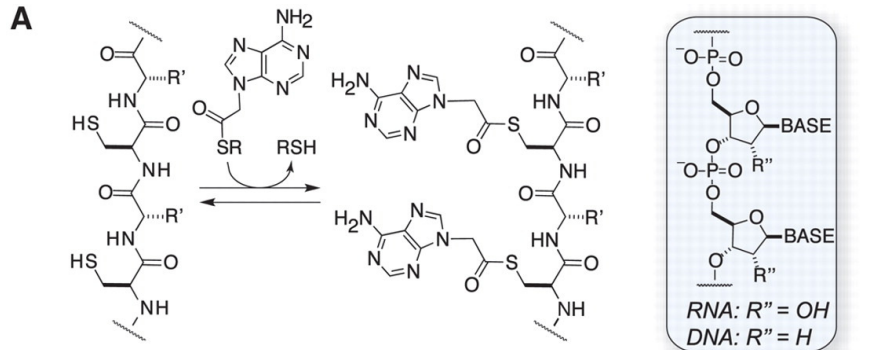


Sequences and reaction conditions employed for acetylation (i) and subsequent templated ligation (ii).

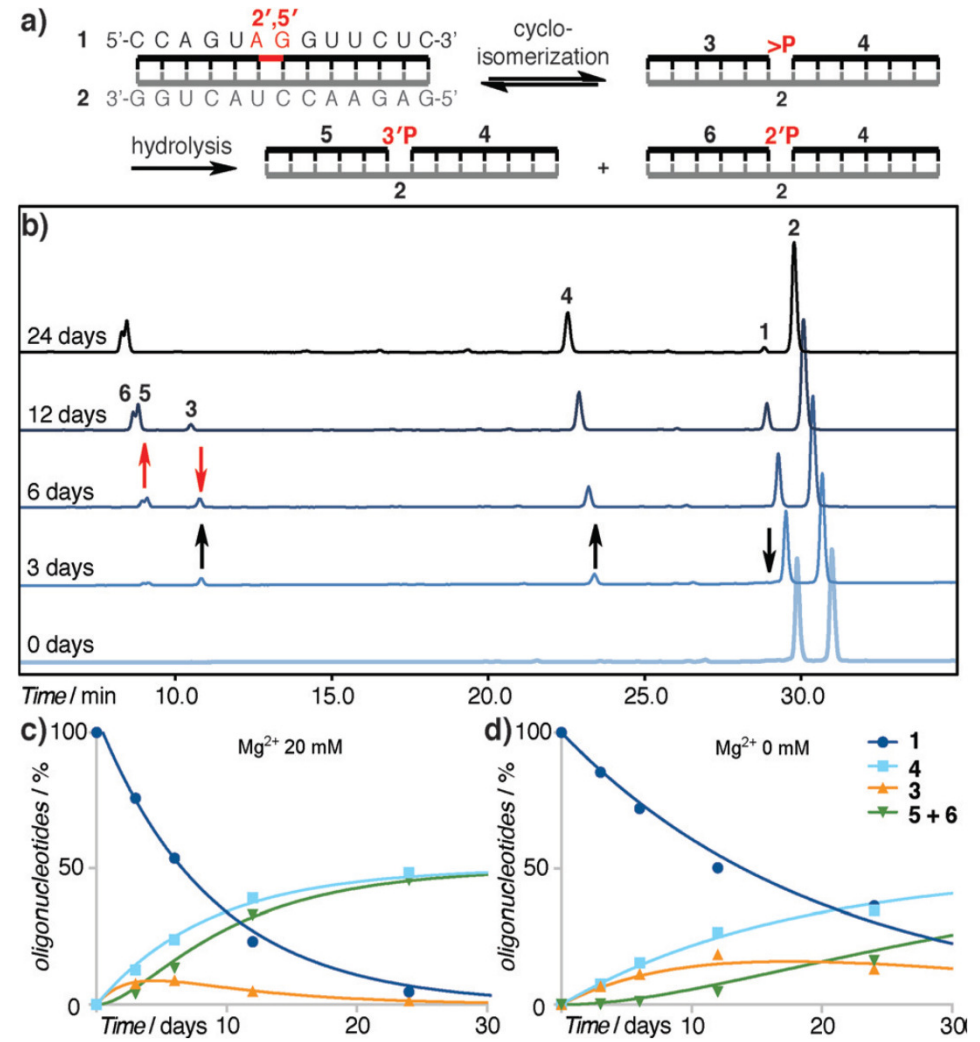
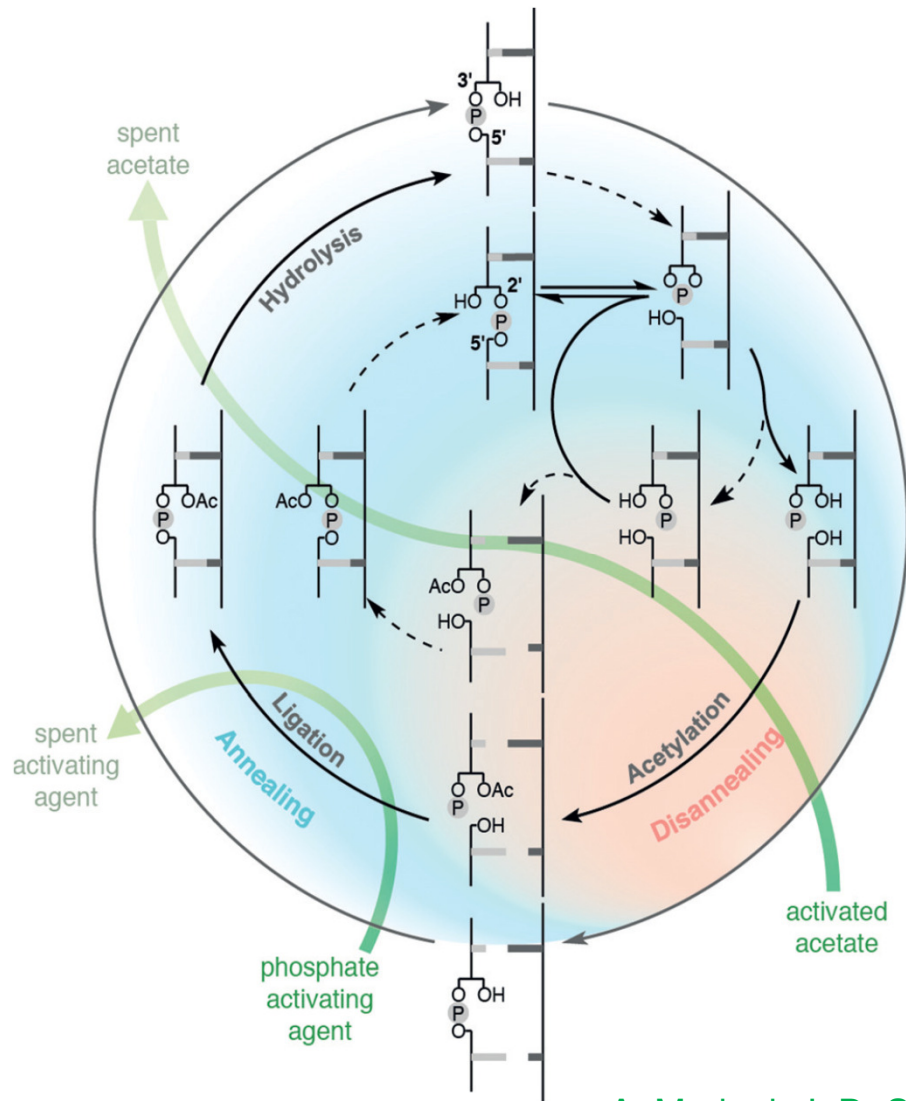
The acetylation mixture contained 80 mM primer and 50 mM NAI; the ligation mixture contained 4 mM primer from the acetylation reaction, 25 mM template, 30 mM ligator, 200 mM imidazole nitrate buffer (pH 6.2), 10 mM MnCl₂ and 100 mM NCI.

J. Sutherland *et al.* *Nature Chem.* **2013**, 383-389

Dynamic oligonucleotide analogue sequence-specific assembly

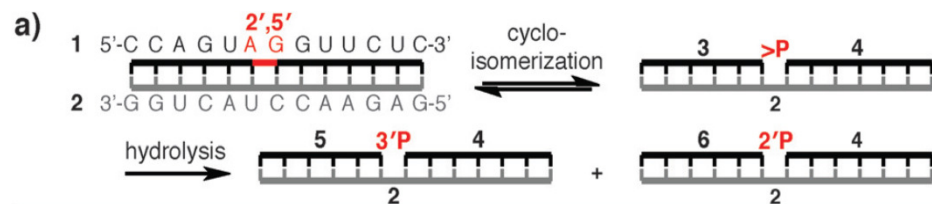


Correction mechanism 2'-5' → 3',5'

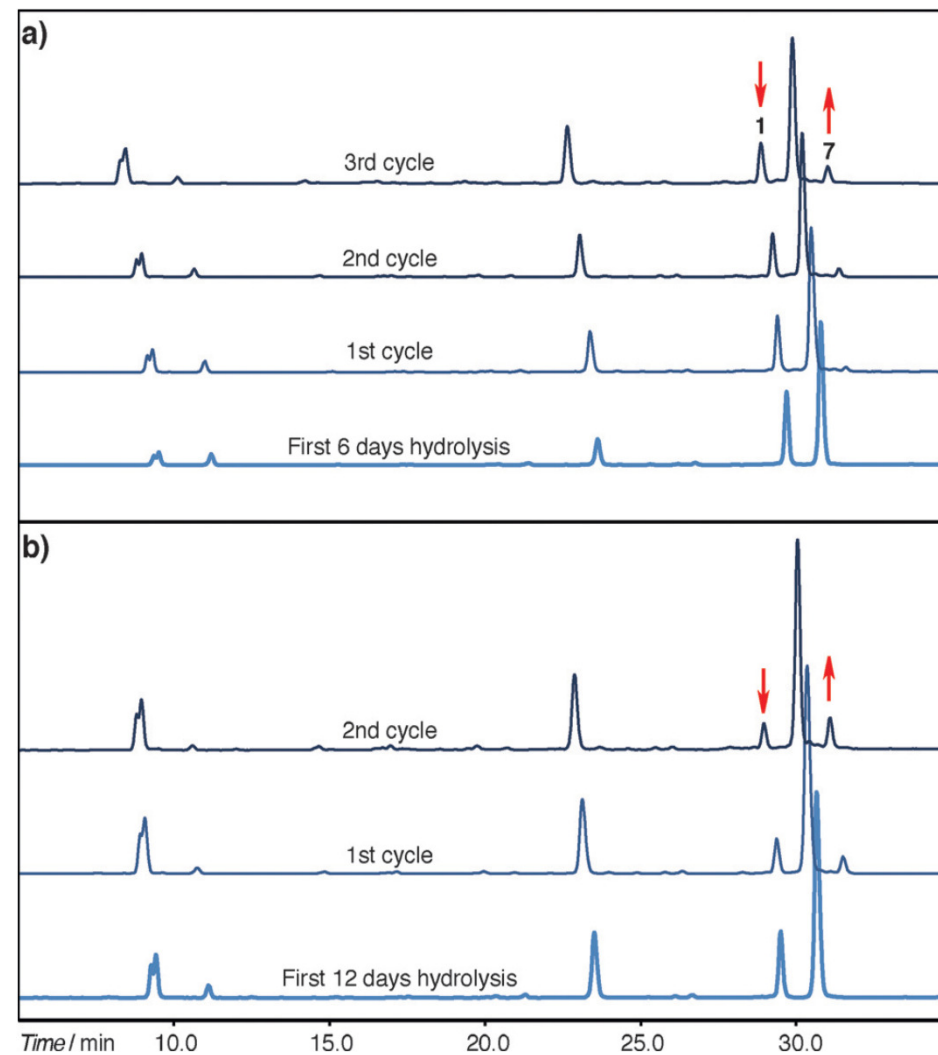
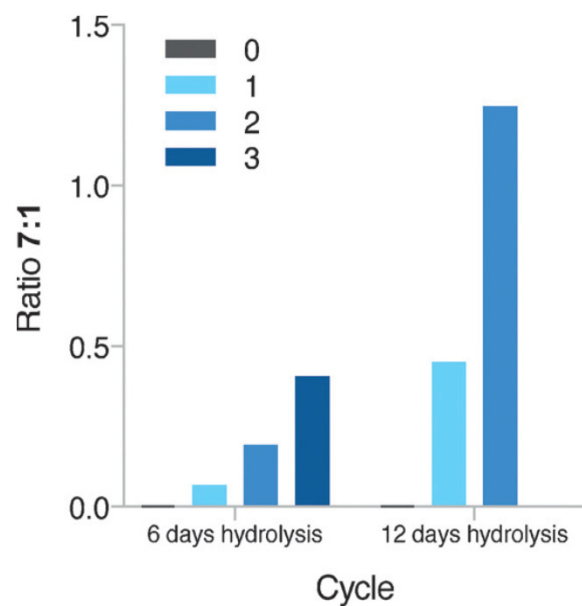


A. Mariani, J. D. Sutherland *Angew. Chem. Int. Ed.* **2017**, *56*, 6563-6566

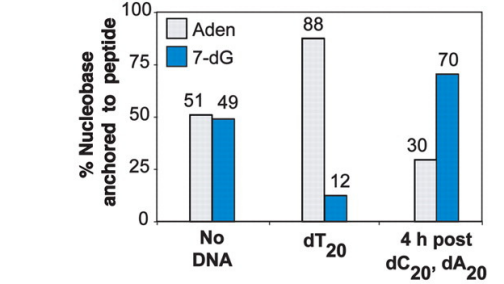
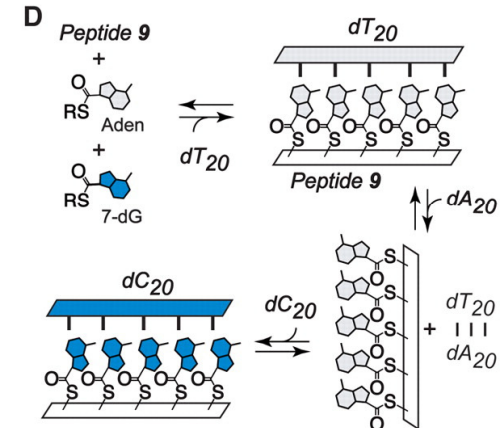
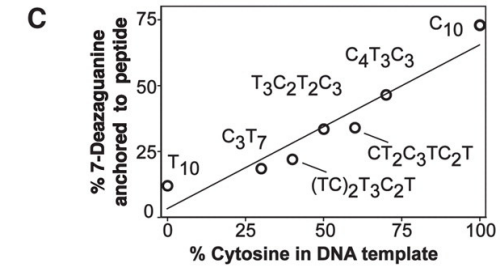
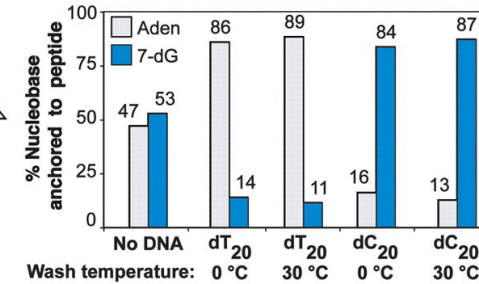
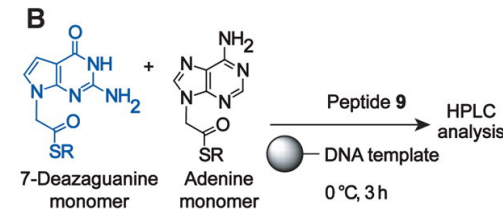
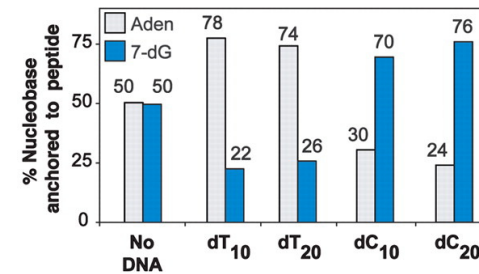
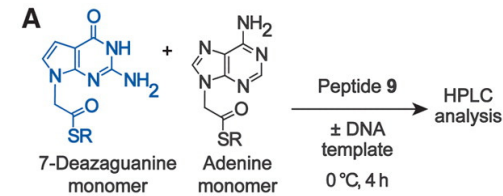
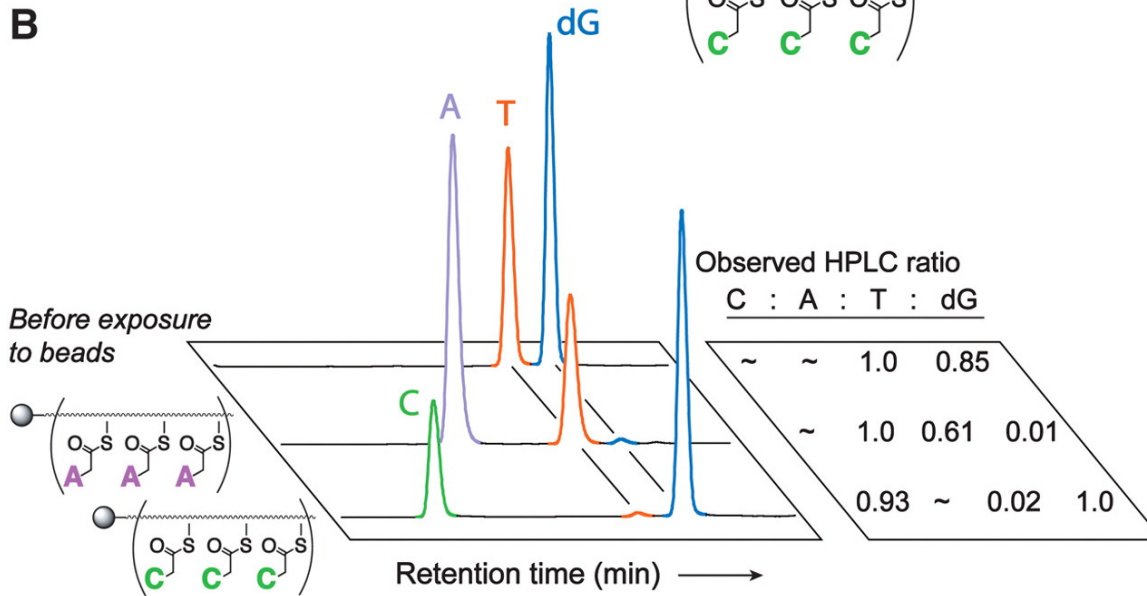
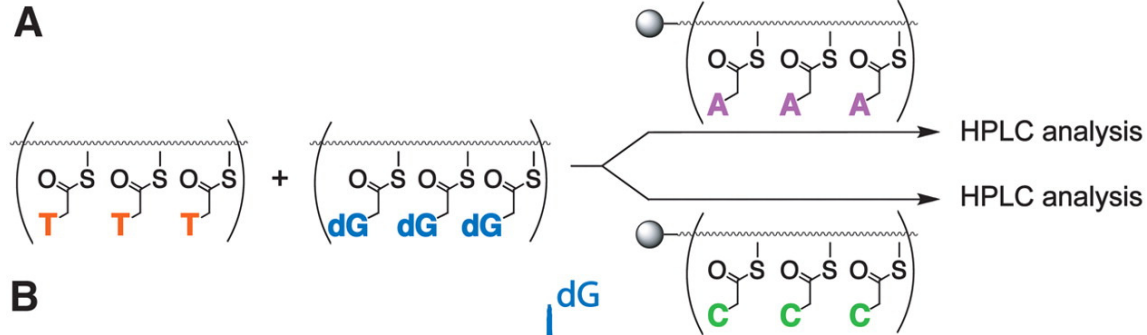
Correction mechanism 2'-5' → 3',5'



1: full 2',5' link
7: full 3',5' link



Dynamic oligonucleotide analogue sequence-specific assembly



M. R. Ghadiri *et al.* *Science* 2009, 325, 73-77